University of Calgary

PRISM Repository **https://prism.ucalgary.ca**

The Vault Open Theses and Dissertations

2017

Defining the Impact of Metabolic Stress and the loss of NOD2 in Epithelial-microbial Interaction

Saxena, Alpana

Saxena, A. (2017). Defining the Impact of Metabolic Stress and the loss of NOD2 in Epithelial-microbial Interaction (Doctoral thesis, University of Calgary, Calgary, Canada). Retrieved from https://prism.ucalgary.ca. doi:10.11575/PRISM/25538

http://hdl.handle.net/11023/4168

Downloaded from PRISM Repository, University of Calgary

UNIVERSITY OF CALGARY

Defining the Impact of Metabolic Stress and the loss of NOD2 in Epithelial-microbial Interaction

by

Alpana Saxena

A THESIS

SUBMITTED TO THE FACULTY OF GRADUATE STUDIES

IN PARTIAL FULFILMENT OF THE REQUIREMENTS FOR THE

DEGREE OF DOCTOR OF PHILOSOPHY

GRADUATE PROGRAM IN GASTROINTESTINAL SCIENCES

CALGARY, ALBERTA

SEPTEMBER, 2017

© Alpana Saxena 2017

Abstract

Reduced ATP levels and irregular mitochondrial structures have been found in gut epithelia in some IBD patients, suggesting that metabolic stress could be an etiologic factor. At the same time, Nucleotide-binding oligomerization domain-containing protein 2 (NOD2) depletion is an important susceptibility trait for IBD. As a result, in our study, we assessed if loss of NOD2 further reduces epithelial barrier integrity under conditions of metabolic stress, instigated by the addition of the oxidative phosphorylation un-coupler, dinitrophenol (DNP). T84 (human colon cell line) cells treated with non-invasive *E. coli* + DNP (16 hrs) showed a significant increase in NOD2 protein. The increase in intracellular bacteria in both wild-type (WT) and NOD2 knock-down cells (NOD2 KD) was dependent on reactive oxygen species (ROS) and resulted in MAPK ERK 1/2 pathway activation; this was determined by adding an antioxidant (mitoTEMPO) or an ERK (U0126) inhibitor. While there was an increase in internalized *E. coli* in cells, no change was seen in the internalization of bead levels or dead *E. coli* suggesting that reduced killing of the bacteria was the primary cause for the increased numbers of bacteria in the NOD2 KD epithelia. This conclusion is reinforced by evidence of attenuated autophagy in NOD2 KD T84 cells.

Neutrophils are potent contributors to IBD. IL-8 is a major neutrophil chemoattractant and signaling molecule; IL-8 levels have been shown to be elevated in IBD patients. As such, we assessed whether metabolic stress induced heightened IL-8 secretion. T84 cells exposed to DNP yielded heightened IL-8 secretion after 16 hrs compared to cells treated with *E. coli* alone in a time-dependent manner. Secretion significantly declined after mitoTEMPO treatment. Bacteria-derived products are necessary for IL-8 secretion; no response was seen to bead co-treatment, but persisted after T84 cells were treated with dead *E. coli*. IL-8 secretion is dependent on endosome

maturation and cytoskeletal rearrangement; administration of chloroquine or cytochalsin D both significantly reduced IL-8 levels. Finally, IL-8 secretion is MyD88 dependent, implicating TLR signaling in the epithelial cell response to metabolic stress in a commensal rich environment.

Taken together, we offer a three-hit hypothesis: lowered barrier function, as a result of metabolic dysfunction is amplified in the absence of NOD2, resulting in increased numbers of live intracellular bacteria. Bacterial presence in the intestinal epithelial cells provokes the release of the neutrophil chemotactic chemokine, IL-8, resulting in inflammation. In NOD2 depleted patients, greater levels of internalized bacteria yield a potent inflammatory effect, given that the antimicrobial effects of both macrophages and Paneth cells are compromised.

Acknowledgements

I would like to thank my supervisor Dr. Derek McKay for accepting me as graduate student in 2012. Since then, he has assisted my development as a researcher throughout my time in his lab.

I would also like to thank my committee members, Dr. Glen Armstrong and Dr. Wallace MacNaughton, for their help and support during my research.

I would like to acknowledge the McKay lab members (past and present) for all of their support throughout my thesis. I would also like to thank my father and my family for their help and support. In particular, I would like to thank my daughter Ankita, and my husband Rajiv for bearing with me during times of stress and worry. Lastly, I want to acknowledge my mother, who is no longer with me, but surely has been looking down upon me and guiding me throughout this journey.

I also want to express my sincere gratitude to the funding agencies that have supported my research endeavours; thank you to the Queen Elizabeth 2 scholarship programme for its generous contribution to my research.

Table of Contents

Abstract……ii
Acknowledgements……..iv
Table of Contents……v
List of Tables……ix
List of Figures…….. x
List of Abbreviations……xiii
CHAPTER 1. INTRODUCTION**…….....1**
1.1 IBD Overview…….....2
1.2 Intestinal Overview……..3
1.2.1 Physiology and Form of the Lower Gastrointestinal (GI) Tract……..…3
1.3 Intestinal Epithelial Barrier……..5
1.3.1 Epithelial Permeability…….....6
1.3.2 Paracellular Permeability……....6
1.3.2a Tight Junctions…….....6
1.3.2b Adherens Junction…….…..8
1.3.3 Transcellular Pathway……10
1.4 Mitochondrial Overview…….13
1.4.1 Mitochondrial Physiology and Function……13
1.4.2 Mitochondria and Reactive Oxygen Species (ROS)……..14
1.4.3 Role of mitochondria in cell signaling……...18
1.4.3a Apoptosis……18
1.5 Evidence for metabolic stress in IBD……..21
1.5.1 Sources of metabolic stress…….22
1.5.1a Microbial Dysbiosis……....22
1.5.1b Invasive Bacteria Induced Metabolic Stress……...22
1.5.1c NSAID-induced Metabolic Stress……...23
1.5.1d Immunosupressive drugs-induced metabolic stress……....23
1.5.1e Phychological Stress causes metabolic stress……..24
1.5.1f Ischemia/Surgery……..25
1.5.1g DNP (2,4 Dinitrophenol) as a Metabolic Stressor……...25

1.6 Pattern Recognition Receptors in the immune Systems……...27
1.7 IBD Associated Polymorphisms…….....28
1.8 NOD2 and IBD…….....29
1.8.1 NOD2 Crystal Structure…….……..30
1.8.2 Expression of NOD2 in Epithelial and Immune cells…….....31
1.8.3 NOD2 Activation and Function……...31
1.8.4 NOD2 and IBD Pathogenesis…….. 36
1.8.5 NOD2 and Autophagy…….....37
1.9 Nuclear factor kappa B (NF-κB) signaling…….…..38
1.10 Mitogen-activated protein kinase (MAPK) signaling…….38
1.11 IL-8…….....39
1.11.1 IL-8 production by intestinal epithelial cells……..40
1.11.2 NOD2 and IL-8 production……....40
1.12 Hypothesis……...41
CHAPTER 2. MATERIALS AND METHODS**……...43**
2.1 Cell lines, Bacteria and Reagents…….....48
2.1.1 Cell Culture……..48
2.1.2 Bacterial Preparation……50
2.1.3 Metabolic Stressor……50
2.2 MTT Assay……51
2.3 Measurement of Transepithelial Resistance (TER)
and *E. coli* Translocation……...51
2.4 Bacterial Internalization (Gentamycin Assay)……..52
2.5 Fluorescence activated cell sorting (FACS)…….....53
2.6 Real time PCR……...54
2.7 Transient Transfection of T84 cells with small Interfering (si) RNA……...57
2.8 Development of a Stable NOD2 knock-down (NOD2 KD) T84 Cell line…....58
2.9 Western Blotting……...59
2.10 Organoid Culture…….....62
2.11 Measurement of ROS……..65

2.12 Enzyme Linked Immunosorbent Assay (ELISA)……65

2.13 Visualization of intracellular *E. coli* or FITC-conjugated latex beads……66

2.14 Statistical analysis and data Presentation……67

CHAPTER 3. RESULTS**……..68**

3.1 Disclosure……..69

3.2 DNP does not affect bacterial growth but reduces mitochondrial function…..70

3.3 Metabolically stressed epithelia display decreased TER and greater translocation and internalization of *E. coli* HB101…….....73

3.4 Internalization of commensal *E. coli* in epithelial monolayer increases NOD2 expression…….....80

3.5 Absence of NOD2 in metabolically stressed T84 epithelium results in increased numbers of viable intracellular bacteria……..84

3.6 Reactive oxygen species (ROS) mediated phosphorylation of ERK1/2 promotes *E. coli* internalization……93

3.7 Absence of NOD2 augments epithelial barrier defect via defective killing of intracellular bacteria……98

3.8 IL-8 production increases in T84 monolayers 16 hrs post-treatment with *E. coli* ± DNP in a time dependent manner…….....104

3.9 Bacteria or bacteria derived products are required for IL-8 production from a metabolically stressed epithelium…….....106

3.10 IL-8 production in DNP + *E. coli* treated epithelia is dependent on TLR signaling……...108

3.11 IL-8 synthesis in DNP + *E. coli* treated T84 epithelium is mediated by MAPK, ERK and ROS…….114

3.12 Absence of NOD2 in DNP + *E. coli* treated T84 epithelium resulted in increased IL-8 production…….117

CHAPTER 4. DISCUSSION**……119**

4.1 Experimental design - pros and cons of the experimental system…….……120

4.2 Discussion (Results)…….…….....124

4.3 Future work…….…...136

4.4. Significance of this Research……139
4.5 Summary Statement……...141
REFRENCES**……146**
Appendix…….....173-175

List of Tables

Table 1: List of materials and reagents used for the experiments……44
Table 2: List of medium used for the experiments……..45
Table 3: Bacterial strains used for the experiments……...…….46
Table 4: Products used for ELISA, immunostaining and
knock-down of protein expression……...……46
Table 5: List of primers used in the experiment……...……..57
Table 6: List of primary and secondary antibodies used
for immunoblotting experiments……...61

List of Figures

Figure 1: Cartoon representation of epithelial junctional complex……..9

Figure 2: Impact of mitochondrial dysfunction on intestinal epithelial cells and intestinal homeostasis……..17

Figure 3: Cartoon representation of Apoptotic pathways……19

Figure 4: Caspase Independent Apoptotic pathways……...20

Figure 5: Structure of 2,4 Dinitrophenol (DNP)……..25

Figure 6: Tripartite structure of NOD2……34

Figure 7: Signalling pathway of NOD2……...35

Figure 8: (a) Representative growth curve of *E. coli* HB101……..71

(b) MTT assay for mitochondrial function……...71

(c) Effect of pharmacological agents used in experiments on growth of *E. coli*……..71

Figure 9: Mitochondrial dysfunction evoked by DNP (2, 4, dinitrophenol) increases epithelial permeability……74

Figure 10: *E. coli* F18 internalization in metabolically stressed T84 monolayers……..76

Figure 11: *E. coli* HB101 internalization in metabolically stressed HT29 and IEC-6 monolayers……77

Figure 12: Immunoblot of caspase-3 cleavage……78

Figure 13: Immunostaining of *E. coli* in DNP ± *E. coli* treated epithelium…….79

Figure 14: Increased NOD2 expression in enterocytes exposed to *E. coli* ± DNP……81

Figure 15: Increased NOD2 expression in HT29 monolayers exposed to *E. coli* ± DNP……82

Figure 16: NOD2 protein expression in T84 monolayers after treatment with muramyl di-peptide (MDP)……..83

Figure 17: Knock-down of NOD2 expression using siRNA or shRNA……..86

Figure 18: Measurement of paracellular permeability in wild-type and NOD2 knock-down epithelium in response to

E. coli HB101 ± DNP treatment…….88
Figure 19: Measurement of intracellular *E. coli* in NOD2 knock-down T84 epithelium treated with *E. coli* HB101 ± DNP……89
Figure 20: Non-steroidal anti-inflammatory drug (NSAID) indomethacin induced mitochondrial dysfunction increases number of viable intracellular *E. coli* in metabolically stressed WT and NOD2 KD epithelium……...91
Figure 21: Measurement of intracellular bacteria in colonic organoid from NOD2$^{-/-}$ and WT mice treated with *E. coli* ± DNP ……...92
Figure 22: Measurement of ROS production in *E. coli* ± DNP treated WT and NOD2 KD T84 epithelium…….…..94
Figure 23: Reactive oxygen species (ROS) mediated phosphorylation of ERK 1/2……..95
Figure 24: Reactive oxygen species (ROS) mediated phosphorylation of ERK1/2 promotes *E. coli* internalization……...96
Figure 25: No significant difference in number of internalized beads in metabolically stressed WT and NOD2 KD T84 epithelium……..99
Figure 26: Reduced killing of internalized *E. coli* in NOD2 KD cells……...100
Figure 27: Reduced autophagy in NOD2 KD cells…….102
Figure 28: Increase in IL-8 production in T84 cell monolayer 16 hrs post-treatment with DNP ± *E. coli*……105
Figure 29: Production of IL-8 from metabolically stressed epithelium is dependent on bacteria or bacteria derived products……..107
Figure 30: IL-8 production in DNP + *E. coli* treated epithelia is dependent on TLR signaling……..110
Figure 31: Disruption of actin cytoskeleton reduces both *E. coli* internalization as well as IL-8 production in DNP co-treated epithelium…….112
Figure 32: Treatment of T84 cell monolayers with different concentrations of LPS for 16 hrs exhibit moderate increase in IL-8 production……113
Figure 33: IL-8 synthesis in DNP + *E. coli* treated epithelium is mediated by MAPK, ERK and ROS…….115

Figure 34: Knock-down of NOD2 (NOD2 KD) from T84 epithelium resulted in increased IL-8 production when treated with DNP + *E. coli*……..118
Summary Figure**……143-144**
Figure 35 (Appendix): Measurement of intracellular *E. coli* in T84 epithelium lacking NOD2 treated with *E. coli* HB101 ± DNP……173
Figure 36 (Appendix): Reduced killing of internalized *E. coli* in NOD2 KD cells……..…174

List of Abbreviations

AP	Activated protein
ADP	Adenosine diphosphate
AIEC	Adherent Invasive *Escherichia coli*
AIF	Apoptosis-Inducing Factor
AMPK	AMP-activated protein kinase
APC	Antigen Presenting Cells
ASA	Aminosalicyclic acid
ATFS1	Activating Transcription Factor associated with stress 1
ATG16L1	gene encoding autophagy related protein 16-1
ATP	Adenosine triphosphate
BSA	Bovine serum albumin
Ca^{2+}	calcium
CAC	Citric acid cycle
CACO-2	Epithelial cell line from colorectal adenocarcinoma
CARD	Caspase recruitment domain
CD	Crohn's Disease
CFU	Colony forming units
Co	Coenzyme
CHOP	CCAAT/enhancer-binding homologous protein; ER stress response protein
CLPP	Caseinolytic peptidase
Cr-EDTA	Cromium-ethylenediaminetetraacetic acid
DAMPS	Damage associated molecular pattern
DIABLO	Direct IAP-Binding protein with Low PI
DAPI	2-(4-Amidinophenyl)-1*H*-indole-6-carboxamidine
dH_20	Distilled water
DMEM	Dulbecco Modified Eagle medium
DNA	Deoxyribonucleic acid
DNBS	Dinitrobenzene sulphonic acid
DNP	2,4-dinitrophenol
Drp1	Dynamin related protein 1
DSS	Dextran sodium sulfate
eIF2α	Eukaryotic transition-initiation factor 2 α (ER stress response protein)
E. coli	*Escherichia coli*
E. coli HB101	*Escherichia coli* HB101
E. coli F18	*Escherichia coli* F18
EEA1	early endosome antigen 1 protein
EGF	Epidermal growth factor
ELISA	Enzyme-linked immunosorbent assay
EPEC	Enteropathogenic *Escherichia coli*
ER	endoplasmic reticulum
ERK	extracellular regulated kinase, a MAPK
ETC	Electron transport chain

F-actin	Filamentous-actin
FAD	Flavin adenine dinucleotide
FACS	Fluorescence activated cell sorting
FBS	Fetal bovine serum
FITC	Fluorescein isothiocyanate
Fyn	Src kinase family member
GI	Gastrointestinal
Grp78	glucose-related peptide 78
GTP	Guanosine triphosphate
GWAS	Genome-wide association studies
HEPES	*N*-2-hydroxethyl-piperazine-*N*'-2-ethanesulfonic acid
hrs	Hours
HRP	Horseradish peroxidase
HT29	Human colon crypt-line epithelial cell line
IBD	Inflammatory Bowel Disease
IFN-γ	Interferon gamma
IEC	Intestinal epithelial cell
IEC-6	Rat small intestine epithelial
IFN-γ	Interferon-γ
Ig	Immunoglobulin
IL	Interleukin
IMM	Inner mitochondrial membrane
IRE1	inositol-requiring transmembrane kinase-endoribonuclease; ER stress response protein
JAM	Junctional adhesion molecule
KD	Knock-down
LAMP1	Lysosomal-associated membrane protein 1
LB	Luria Bertani
LC3 II	Microtubule-associated protein 1A/1B-light chain 3
LDH	Lactate dehydrogenase
LPS	Lipopolysaccharide
LRR	Leucine rich repeat
MAPK	Mitogen-activated protein kinase
MβCD	Methyl-β-cyclodextrin
MCT	Monocarboxylate transporter
mCU	Mitochondrial Ca^{2+} uniporter
MDCK	Madin-Darby Canine Kidney Epithelial Cell
MDP	Muramyl di-peptide
mitoTEMPO	Mitochondria-targeted antioxidant
mRNA	Messenger ribonucleic acid
mtDNA	Mitochondrial DNA
mtUPR	mitochondrial unfolded protein response
MTT	3-(4,5-dimethyl-thiazol-2-yl)-2,5-diphenyltetrazoliumbromide salt
MZ	Monozygotic

NAD^+	Nicotinamide adenine dinucleotide
NFκB	Nuclear factor κB
NOD	Nucleotide-binding oligomerization domain
NOD2	Nucleotide-binding oligomerization domain-containing protein 2
NOD2KD	Nucleotide-binding oligomerization domain-containing protein
KD	Knock-down
NSAID	Non-steroidal anti-inflammatory drugs
$O2^-$	Superoxide
OD	Optical density
OXPHOS	Oxidative phosphorylation
OM	Outer mitochondrial membrane
PI3K	phosphoinositide-3-kinase
PAMP	Pathogen associated molecular patterns
PBS	Phosphate buffered saline
PCR	Polymerase chain reaction
PDGF	Platelet derived growth factors
p-ERK	Phosphorylated Extracellular Signal-Regulated Kinase
P-gp	P-glycoprotein
PI-3K	Phosphatidylinositol-3 kinase
PINK1	PTEN-induced putative kinase 1
p-IKK	Phosphorylated-IKK
p-IκBα	Phosphorylated- IκB-α
PMA	Phorbol 12-myristate 13-acetate
PMF	Proton motive force
PPAR	Peroxisome proliferators-activated receptor
PPS	Plasminogen/plasmin system
PRR	Pattern recognition receptors
PTP	Permeability transition pore
PVDF	Polyvinylidene difluoride
Q-PCR	quantitative polymerase chain reaction
REGIIIγ	Regenerating islet-derived protein IIIγ
ROS	Reactive oxygen species
RNA	Ribonucleic acid
RNS	Reactive Nitrogen Species
SCFA	Short-chain fatty acids
SDS	Sodium dodecyl sulfate
SEM	Standard error of the mean
siRNA	small interfering RNA
shRNA	Short hairpin RNA
SMAC	Second Mitochondria-derived Activator of Caspases
SMCT	Sodium-coupled monocarboxylate transporter
T84	Human colon crypt-line epithelial cell line
TAD	Transcriptionally active domain
TBST	Tris-biffered saline/0.1% Tween-20
TEM	Transmission electron microscope

TER	Transepithelial electrical resistance
Th-1	T-helper 1
THP1	Human monocytic cell line derived from an monocytic leukemia patient
TJ	Tight junctions
TLR	Toll-like receptors
TNBS	Trinitrobenzene sulphonic acid
TNF	Tumor necrosis factor
TxA	Toxin A
TxB	Toxin B
U0126	pharmacological inhibitor of ERK
Ubc	Ubiquitin-like conjugating enzyme
UC	Ulcerative colitis
VDAC	Voltage Dependent Anion Channel
VEGF	Vascular Endothelial Growth Factor
WT	wild-type
WT T84	wild-type T84
XBP1	X-box binding protein; ER stress response protein
ZO	Zonula occluding

CHAPTER 1 – Introduction

1.1 IBD Overview

Inflammatory bowel disease (IBD) is an idiopathic disease, which is comprised of two main types of chronic intestinal disorders: Crohn's disease (CD) and ulcerative colitis (UC). This multi-factorial disease is caused by disruption of host-microbe interactions in a genetically susceptible host, which results in an immunological imbalance and thus inflammation and loss of cellular homeostasis.(1, 2) Inflammation in Crohn's disease is often transmural, and can affect any part of the gastrointestinal tract but most commonly occurs in the terminal ileum or the perianal region in a non-continuous fashion. In contrast, ulcerative colitis is characterized by inflammation that is usually confined to the mucosa and is limited to the colon: it begins in the rectum and spreads proximally in a continuous fashion and frequently involves the peri-appendiceal region.(1, 2) IBD affects approximately 1.4 million Americans with peak onset time in individuals of 15 to 30 years of age with the annual health cost exceeding 1.7 billion USD.(3) One in every 150 Canadians suffers from IBD, with approximately 233,000 Canadians living with IBD. Of this number, 129,000 suffer from Crohn's disease while 104,000 are treated for ulcerative colitis.(4) The rate of incidence of IBD in Canada has been rising since 2002 and every year, approximately 10,200 new cases of IBD are diagnosed.(4) Current medications enable patients to manage IBD symptoms for short periods of time; however, IBD still has an enormous impact on both patient and caregiver quality of life.(5-7)

IBD places a significant burden on the Canadian economy via healthcare costs; in 2012 the direct medical cost to IBD was estimated to be $ 1.2 billion annually (approximately $12,000 per IBD patient).(4) Advances in treating IBD have been made but to date, neither has a precise cause been determined, nor a cure been found.(8, 9) Therefore, understanding the causes and pathogenesis of IBD is essential to develop targeted and more effective therapeutics. Previous

research has shown that decreased epithelial barrier function can contribute to inflammation, a major symptom of IBD. (10-12)

1.2 Intestinal Overview

1.2.1 Physiology and Form of the Lower Gastrointestinal (GI) Tract

The GI tract is a complex structure that begins with the mouth and concludes at the anus. After large-scale mechanical digestion in the mouth and stomach, macromolecules move into the small intestine. The small intestine starts from the pylorus and ends at the ileocaecal valve, and can be divided into three segments: the duodenum, jejunum and the ileum. The large intestine begins at the caecum and ends at the anus. The large intestine is divided into the ascending colon (proximal colon), the transverse colon and the descending (distal) colon. Both small and large intestines constitute a continuous tube which is lined inside by a single layer of epithelial cells.(13) The epithelium extends the intestinal surface area by arranging themselves into finger like projections into the lumen called villi, which aid in the digestion and absorption of nutrients and electrolytes. Villi are absent, in the caecum and colon. The surface area of both the small and large intestine in human is renewed every 3-5 days through the activity of multipotent stem cells present in crypts; these stem cells give rise to different kinds of mature cells. Most of the newly differentiated cells are absorptive enterocytes; however, this category also contains Paneth cells, goblet cells, tuft cells and neuroendocrine cells. Newly formed cells move upwards from the base of the crypt, with the sole exception of Paneth cells in the small intestine, which shift downward.(13, 14)

Peyer's patches are elevated areas within the small intestine that contain M cells, which provide the underlying lymphoid follicles with a veritable antigen sampling system. M cells are

specialized epithelial cells with particular receptors that enable the transcytosis of antigens and live bacteria from the lumen.(15) The antigens pass through the cell and are released to antigen presenting cells (APCs). The mechanism has yet to be precisely elucidated; however, dendritic cells and T cells work synergistically to activate and prod naïve B-cells to become IgA^+ plasma cells. These cells secrete dimeric IgA throughout the small intestine, and to a limited extent, in the general lamina propria.(16) IgA is transported to the lumen by the epithelial polymeric IgA receptor (polyIgR).(17) IgA has the ability to block toxins and pathogens from adhering to the epithelial surface; for example, mouse models have shown that IgA is essential for blocking the effects of cholera toxin exposure to the lumen.(18, 19)

Absorptive epithelial cells are covered with mini-protrusions known as microvilli, which have nutrient transporters and digestive enzymes embedded in their apical surface.(20) Goblet cells are mucus-producing cells, making up 25% of all epithelial cells in the distal colon but only 10% in the upper small intestine of human. Mucus is composed of mucin-glycoprotein and acts as a physical barrier for microbes. Mucosal thickness is at its zenith in the colon, where both an epithelial surface-attached layer of mucus, and an outer, loose layer exist.(21) Paneth cells also uniquely localize to the small intestine. They secrete anti-microbial peptides such as lysozymes, defensins, and regenerating islet-derived protein IIIγ (REGIIIγ) in response to interleukin (IL)-22 or toll like receptor (TLR) signaling.(22, 23)

Taken together, the mucosa is comprised of the epithelium, the lamina propria, a thin layer of connective tissue that underlies the epithelium and is host to many lymphocytes, blood vessels, lacteals, and nerve endings, and the muscularis mucosae, a lean layer of muscle underneath the lamina propria. The submucosa follows the muscularis mucosae, and holds an interface of parasympathetic nerves. The main role of these nerves is to control vascular and

epithelial transport, with one function being regulation of ion transport. The submucosa, in turn, is lined by a thick, circular, muscle layer known as the muscularis externa. The muscularis externa is responsible for gut motility and is encircled by longitudinal muscle. The muscularis externa promotes contraction of the gut along its diameter, while longitudinal muscle compresses the tube. The myenteric plexus enervates and intercedes with both muscle layers and enables the propulsion of intestinal contents. Finally, the last layer of the GI tract is the serosa, a dense fibrous covering which partitions the peritoneal cavity from the intestines.(24)

1.3 Intestinal Epithelial Barrier

Intestinal barrier function can be defined as, "the ability to control uptake and maintain the delicate balance between absorbing essential nutrients while preventing the entry of, and responding to, harmful contents across the mucosa."(25) The intestinal epithelium is an endoderm-derived single layer of cells that has a defined cell polarity, with apical and basal sides.(26, 27) The epithelium forms an interface between the contents of the gut, the intestinal microbiome, as well as the lymphoid tissues associated with the gastrointestinal system. Intestinal epithelial cells function as a barrier against the excessive entry of bacteria and other antigens from the intestinal lumen into the circulation in conjunction with their responsibility of nutrient absorption.(1) In the absence of any injury to the epithelium, luminal material crosses the epithelium via microfold (M) cells, dendritic cells or passes through the tight junctions (TJ) in between the enterocytes, which are regulated by the tight junction proteins. Examples of the aforementioned proteins include claudins, occludin and JAM (Junctional Adhesion Molecules).

(Figure 1) This paracellular space allows the movement of water, nutrients and neutrophils into the lumen in a very regulated manner. Conversely, a transcellular pathway defines passage of luminal material directly through enterocytes.(28, 29)

1.3.1 Epithelial Permeability

The intestinal microbiome consists of a diverse population of microorganisms. Most of these are commensal organisms that have colonized the gut and live as part of a symbiotic relationship with the host organism. They provide the host many benefits, an example being the synthesis of butyrate, which is a key energy source for enterocytes.(30, 31) Maintaining the barrier function of the intestinal epithelium is crucial in the regulation of intestinal homeostasis.(2) An increase in intestinal epithelial permeability is associated with IBD.(32) An increase in epithelial permeability can result in the translocation of commensal bacteria either through the transcellular pathway or by the paracellular pathway to the mucosa that results in local inflammation. In more severe cases, when bacteria enter the blood circulation, the result can be sepsis and subsequent death.(33)

1.3.2 Paracellular pathway

(1.3.2a) Tight Junctions

Tight junctions (TJ) consist of claudins and occludin. Claudins are 20-70 kDa integral membrane proteins with cytoplasmic N and C terminal domains and two extracellular loops.(34) The C terminal end of claudins binds to the PDZ domain of the peripheral membrane protein zonula occludens (ZO-1, ZO-2 or ZO-3), which in turn, are connected to the dense, peri-junctional ring of actin and myosin.(35) PDZ's name is derived from first letter of the three

proteins in which this motif was discovered (PSD-95 (post synaptic density-95), Dig (the *Drosophila* disc large protein) and ZO1(the zonula occludens 1)).(36) At the same time, the extracellular loops of claudins are involved in the formation of ion-selective channels through interactions with homophilic and/or heterophilic TJ proteins. In humans, members of claudin family are expressed in a tissue specific manner.(37) Claudin 2, in particular, is a pore forming claudin and *in vitro* studies have shown that its expression increases tight junction permeability in MDCK (Madin-Darby Canine Kidney) epithelial cells as assessed by the reduction of TER (transepithelial resistance).(38) *In vivo* studies also suggest that claudin plays an important role in regulating intestinal barrier function, as claudin $1^{-/-}$ mice die within 1 day of birth.(39) This is consistent with research showing that tight junctions play an important role in determining mucosal permeability through size and charge selectivity.(40, 41)

Occludin was the first TJ protein to be identified.(42) It has two extracellular loops and its N and C terminal domains lies in the cytoplasm. The C terminal domain interacts with the PDZ domain of ZO-1 that links to actin cytoskeleton.(43) The role of occludin in barrier function is less understood as occludin$^{-/-}$ mice show no difference in TJ organization, paracellular transport and barrier function compared to wild-type mice.(44, 45) However, some studies suggest a role for occludin in cellular adhesion.(46) Phosphorylation of occludin is essential for its localization to the tight junctional complex.(47, 48) It has been shown in an *in vitro* study that PKCη (protein kinase C isoenzyme), a kinase expressed mainly in intestinal epithelium is responsible for occludin phosphorylation at threonine residues, T403 and T404. The authors of that study further stated that the inhibition of PKCη mediated phosphorylation of occludin disrupts its localization at the TJ resulting in a decrease in barrier function.(49)

Junctional Adhesion Molecule (50), a member of the immunoglobulin subfamily is another tight junction protein.(51) They are expressed in many isoforms, of which JAM-A is expressed mainly in endothelial and epithelial cells.(52) JAMs interact with an adjacent cell via homotypic interaction and intracellularly through PDZ domain with ZO-1. It helps in the formation and assembly of the TJ.(53) It has been shown in a study that knock-down of JAM-A using siRNA in SK-C015 epithelial cells results in increased permeability.(52) Consistent with these findings Laukoetter et al. showed that JAM-$A^{-/-}$ mice exhibit increased DSS (dextran sodium sulfate)-induced mucosal permeability compared to DSS-treated wild-type control mice as measured by TER and FITC-dextran flux.(52) Measurement of TER allows us to quantify the tightness of tight junctional dynamics and paracellular flux (transport capacities).(54)

(1.3.2b) Adherens junctions

Adherens junctions and desmosomes play important roles in establishing proper assembly of tight junctions. They provide strong bonds between neighbouring cells and thus ensure cellular proximity. The adherens junction also helps in epithelial polarization and differentiation and are composed of cadherins (transmembrane proteins).(55) These proteins contain a single transmembrane domain, a cytoplasmic domain and an ectodomain.(56) E-cadherin forms Ca^{2+} dependent homotypic interactions with the molecules present on the adjacent epithelial cells.(57) The cytoplasmic domain of E-cadherin interacts directly with p-120 catenin or β-catenin. Finally, the β-catenin anchors to the actin cytoskeleton via α-catenin.(58, 59) Absence of adherens junctions results in defective epithelial cell polarization and differentiation as well as premature apoptosis.(55) (Figure A) Microbial pathogens such as enteropathogenic *Escherichia coli* (EPEC) and several pro-inflammatory cytokines like IFN-γ (interferon gamma) can contribute to the loss of tight junction proteins that ultimately results in a leaky epithelium.(60, 61)

Figure 1: Cartoon representation of epithelial junctional complex

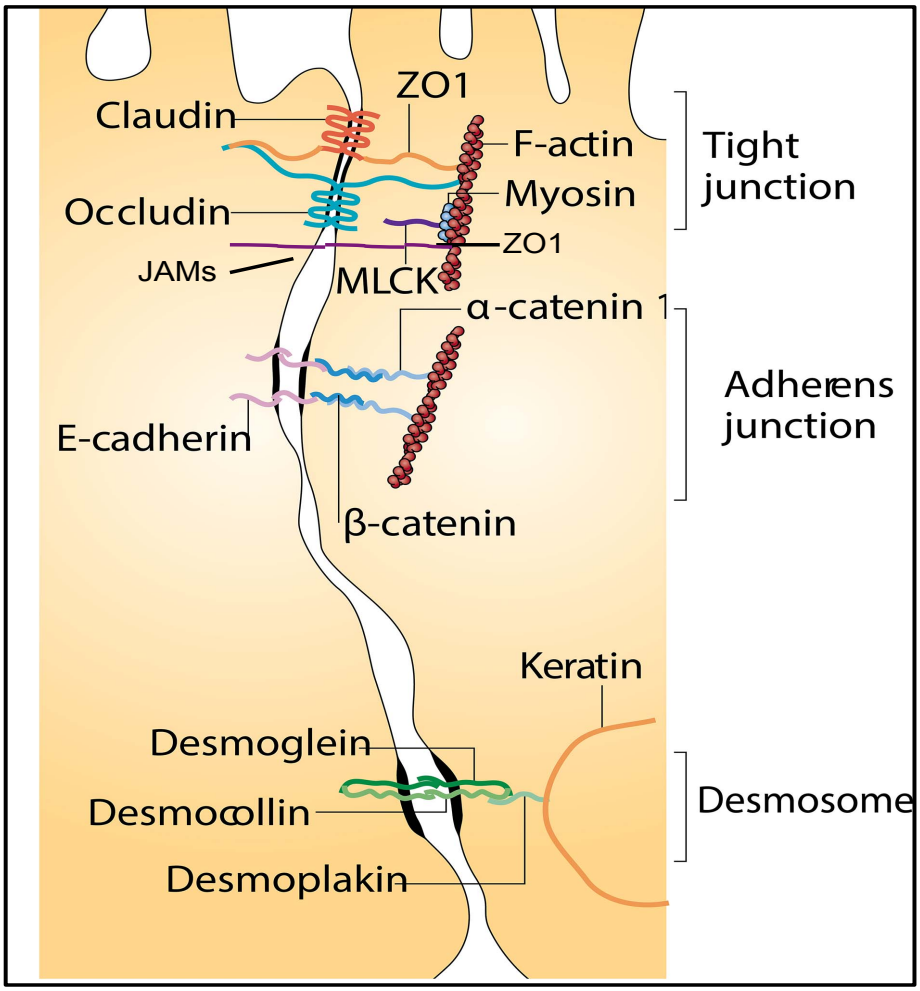

(Adapted from Turner R: Nature Reviews Immunology, 2009 (20))

Figure 1: Several transmembrane proteins such as claudins, occludin, and junctional adhesion molecules make up the tight junction. These proteins are linked to cytosolic plaque proteins of the zonula occluden (ZO) family which are in turn, tied to the actinomyosin ring of epithelial cells. Adherens junctions are formed by E-cadherin which are connected to F-actin via α-catenin 1, ß-catenin and p120 (not shown) (20)

1.3.3 Transcellular pathway

It has been shown that pro-inflammatory cytokines such as IFNγ, tumour necrosis factor-α (TNFα) and IL-6 can also enhance the transcellular passage of proteins across the epithelium.(62) Menard *et al.* provided evidence in support of the transcellular transport of celiac disease associated gliadin peptides through intestinal epithelium.(63) Microbial pathogens can enter into non-phagocytic cells, including epithelial cells by negotiating the apical cell membrane to enter and the basolateral cell membrane to exit, thereby avoiding destruction.(64) One way microbial pathogens can enter the cell is by expressing surface proteins which bind to eukaryotic surface receptors, instigating the formation of a vacuole, and subsequent cytoskeleton rearrangement, and membrane extension.(64) Indeed, *Yersinia pseudouberculosis* and *Listeria monocytogenes* utilize this method to enter the epithelial cells. Other pathogens such as *Shigella* and *Salmonella* can enter epithelial cells by injecting effectors through the type III secretory system (TTSS).(64) TTSS modulates actin cytoskeleton rearrangement, prompting the formation of filopodia and lamellipodia which facilitate the entry of bacteria inside epithelial cells. Following internalization, bacteria can either remain inside the vacuole, where they replicate by resisting late endosome maturation into lysosomes, or escape from the internalized vacuole and replicate in the cytosol.(64) *Salmonella typhimurium* infects the intestinal epithelium and lamina propria of the intestinal mucosae and causes frequent diarrhea.(65) *S. typhimurium* enter the epithelial cells through a TTSS facilitated invasion to the apical side of the epithelial cell.(66) Work by Müller *et al* with a streptomycin mouse model of *S. typhimurium* diarrhea revealed that the bacterium uses the type III secretion system-2 (TTSS-2) for transepithelial trafficking and is released into the lamina propria through the basolateral side of the epithelium via exocytosis.(67)

It has been shown that *Campylobacter jejuni* can induce transcytosis of non-invasive *E. coli* across a monolayer of Caco-2 (epithelial cell line from colorectal adenocarcinoma) cells.(68) It is not yet known whether the metabolic stress-induced bacterial internalization occurs through either clathrin-dependent endocytosis or through lipid-rafts/caveolin mediation. For one piece of the puzzle, Kalischuk *et al.* have shown that *Campylobacter jejuni* induced transcytosis of non-invasive *E. coli* HB101 is lipid raft dependent. Treatment of the T84 human colonic epithelial cell monolayer with MβCD (methyl-β-cyclodextrin), a cholesterol-depleting agent, reduces *Campylobacter jejuni* induced *E. coli* HB101 transytosis.(69) A study by *Clark et al.* showed dose-dependent, IFNγ mediated translocation of commensal *E. coli* C25 across the T84 monolayer.(70) T84 cells pre-treated with 1.0 IU/ml IFNγ for 48 hrs exhibited a significant increase in bacterial translocation compared to an untreated control monolayer. However, at this concentration of IFNγ, no significant changes in TER or tight junctional proteins such as claudin and occludin were witnessed in treated monolayers compared to the control.(70) Similar results were seen in Caco-2 monolayers treated with IFNγ up to 100 IU/ml. Administration of filipin and methyl-ß-cyclodextrin (MCD), compounds that sequester membrane cholesterol and disrupt lipid rafts to Caco-2 cells before IFNγ and *E. coli* treatment, resulted in significantly attenuated *E. coli* C25 internalization.(70) McKay *et al.* have shown IFNγ-induced transcytosis of non-invasive *E. coli* HB101 in T84 cells (human colonic adenocarcinoma cell line) in an ERK-dependent manner.(71)

Clathrin mediated endocytosis is also known as receptor mediated endocytosis, which is the best-known form of pinocytosis. This process involves a triskelion shaped scaffold protein called clathrin. The process of clathrin-coated vesicle formation occurs in five stages.(72) The macromolecule first binds to cell surface receptors which accumulate at clathrin coated pits.

These clathrin coated pits bud-off from the membrane and form clathrin-coated vesicles. The budding process is dependent on the activity of the enzyme dynamin. These clathrin-coated vesicles are later fused with early endosomes in which cargo sorting takes place. Later cargo can either go to lysosomes or be recycled back to the plasma membrane.(72) The best studied example of clathrin-mediated endocytosis is the uptake of cholesterol by mammalian cells.(73) However, this pathway can also be used by bacteria or viruses to gain entry to the cell. (74)

Cells also use another, clathrin-independent method to endocytose fluids or molecules - caveolae/raft dependent endocytosis. The morphological appearance of caveolae is cell dependent.(75) In this process, membrane-bound molecules are taken up in small invaginations of the plasma membrane of approximately 50-80 nm in diameter known as caveolae. Caveolae contain cholesterol and sphingolipid-rich lipid rafts as well as the protein caveolin (Cav). Three members of the Cav family have been identified: Cav-1, Cav-2, and Cav-3. Cav-1(21kDa) is an essential membrane protein.(76) Briefly, during caveolae endocytosis, dynamin, a GTPase directly interacts with Cav-1. In response to ligand binding, the actin cytoskeleton is disrupted, which prompts the recruitment of dynamin II to the site of internalization. Dynamin oligomerization then results in conformational changes and the appearance of a collar like structure at the neck of the caveolae, which enables the formation of a free transport vesicle. This vesicle can fuse with early endosomes, late endosomes, endolysosomes and lysosomes. Many viruses have been shown to exploit this pathway to gain entry to the cell.(77) It has been reported that because of the small size of caveolae, bacterial uptake requires the fusion of several caveolae and the formation of a bigger endocytic microdomain.(78)

1.4 Mitochondria Overview

Mitochondria are eubacteria-derived, dynamic organelles and are typically found either in the cell as individual organelles or in large, interconnected, tubular structures.(79, 80) Mitochondria are comprised of more than 1000 proteins, depending on the species, and their intracellular location.(81-83) The majority of mitochondrial proteins are nuclear coded, but mitochondria also have a small amount of their own DNA, better known as mitochondrial DNA (mtDNA). mtDNA is circular, consisting of ~16,500 base pairs (bp), and is organized into 37 genes. Indeed, mtDNA, much like bacterial DNA, lacks histones and is organized like a nucleoid.(84) Replication of mtDNA is independent of the cell cycle.(85) These genes either code for proteins that form subunits of complex I, III, and IV present in the respiratory complex, or code for the 22 tRNAs and 2 rRNAs required for the translation of these proteins. The majority of the proteins necessary for mitochondrial biosynthetic and oxidative functions are coded by the nucleus.(86, 87)

1.4.1 Mitochondrial Physiology and Function

Mitochondria consist of two membranes: an outer membrane, which is permeable to small molecules and ions, and an inner membrane that is impermeable or selectively permeable via carriers and channels to most small molecules and ions. The electron transport chain (ETC) generates an electrochemical gradient across the mitochondria inner membrane that is comprised of both a membrane potential and a H^+ gradient. These gradients are collectively known as the proton motive force (pmf) and drive ATP synthesis by ATPase. In order to maintain the pmf, the inner membrane must maintain its impermeability under normal aerobic conditions. However, in response to stress, the permeability of the inner membrane increases via the formation of voltage

dependent non-specific pores in the inner membrane known as the mitochondrial permeability transition pore (PTP). These PTPs allow for the diffusion of all molecules less than 1.5 kDa in size, which results in the loss of ionic homeostasis, matrix swelling and rupture of the outer membrane.(88)

1.4.2 Mitochondria and Reactive Oxygen Species (ROS)

Pyruvate produced through glycolysis in the cytosol enters the mitochondria where it goes through the Krebs cycle and the ETC to produce 30 molecules of adenosine triphosphate (ATP) per molecule of glucose oxidized. NADH and FADH formed during the citric acid cycle are the main sources of electrons. In this two-step process, high-energy electrons pass along a series of electron transporters embedded in the inner membrane of the mitochondria. The energy generated during this electron transfer in the ETC allows for the pumping of protons (H^+ from water) into the intermembrane space that generates an electrochemical proton gradient. The backflow of H^+ allows the generation of ATP from adenosine diphosphate (ADP) and free inorganic phosphate (P_i) by ATP synthase.(89) The electrochemical proton gradient is necessary for both ATP production, and Ca^{2+} buffering. The accumulation of protons on the inner membrane space creates a negative potential and enables the entry of Ca^{2+} from the cytosol to the mitochondrial matrix via the mitochondrial Ca^{2+} uniporter (mCU) present in the inner mitochondrial membrane.(90, 91)

Many factors including reduced nutrients, toxins and certain medications can disturb epithelial mitochondrial function that can give way to increased permeability and decreased barrier function.(92, 93) Rodenburg *et al*. reported that rats fed fructo-oligosaccharides display increased epithelial permeability in the large intestine. They also showed that decreased

epithelial barrier function is independent of tight junction defects; however, intestinal epithelial cells isolated from the colon displayed increased expression of OXPHOS (oxidative phosphorylation) complex genes, suggesting mitochondrial distress, a hallmark indicator that disturbed ATP homeostasis is happening.(94)

Disruption of the ETC can lead to the production of ROS such as superoxide ($O2^{-}$), hydrogen peroxide (H_2O_2) and if nitric oxide is available, peroxynitrite ($ONOO^{-}$).(89) Electrons leaking from complex I and complex III of the ETC are acquired by O_2. ROS ($O2^{-}$) is generated by the addition of one extra electron to molecular oxygen.(95) ROS can also be produced by the enzymic activity of xanthine oxidase (XO), as well as NADPH oxidase, which catalyzes one electron reduction of molecular oxygen.(96) Xanthine oxidase is highly expressed in endothelium and intestinal epithelial cells.(96) When ROS concentration is at physiological levels, ROS functions as a signaling molecule, and is involved in various processes that include cell growth, cell adhesion and differentiation, in addition to apoptosis and senescence.(97) However, increased ROS levels can also be pathological.(97, 98) Mitochondrial dysfunction can lead to increased production of ROS and reactive nitrogen species.(93). In turn, ROS can trigger an inflammatory response, and increased ROS has been reported in IBD.(99, 100) Decreased levels of endogenous antioxidants such as glutathione peroxidase or α-tocopherol have also been reported in IBD patients.(101, 102) Intestinal epithelial cells (IECs) isolated from murine models of colitis also exhibit increased levels of ROS.(103, 104) A study by Wang *et al* showed that 2,4 dinitrophenol (DNP) induced mitochondrial dysfunction in T84 or HT29 epithelial cell monolayers and resulted in increased bacterial (*E. coli* HB101) internalization and translocation in conjunction with increased ROS.(105) Co-treatment with the mitochondria directed antioxidants, mitoTEMPO or MitoQ, significantly reduced DNP-induced bacterial internalization

and translocation. This result was recapitulated in a mouse model of DSS-induced colitis, where both the severity of colitis, as well as FITC-dextran flux (a measure of barrier permeability) was decreased by systemic delivery of mitoTEMPO.(105)

(The role of the mitochondria in maintaining intestinal barrier function is illustrated in Figure 2.)

Figure 2: Impact of mitochondrial dysfunction on intestinal epithelial cells and intestinal homeostasis

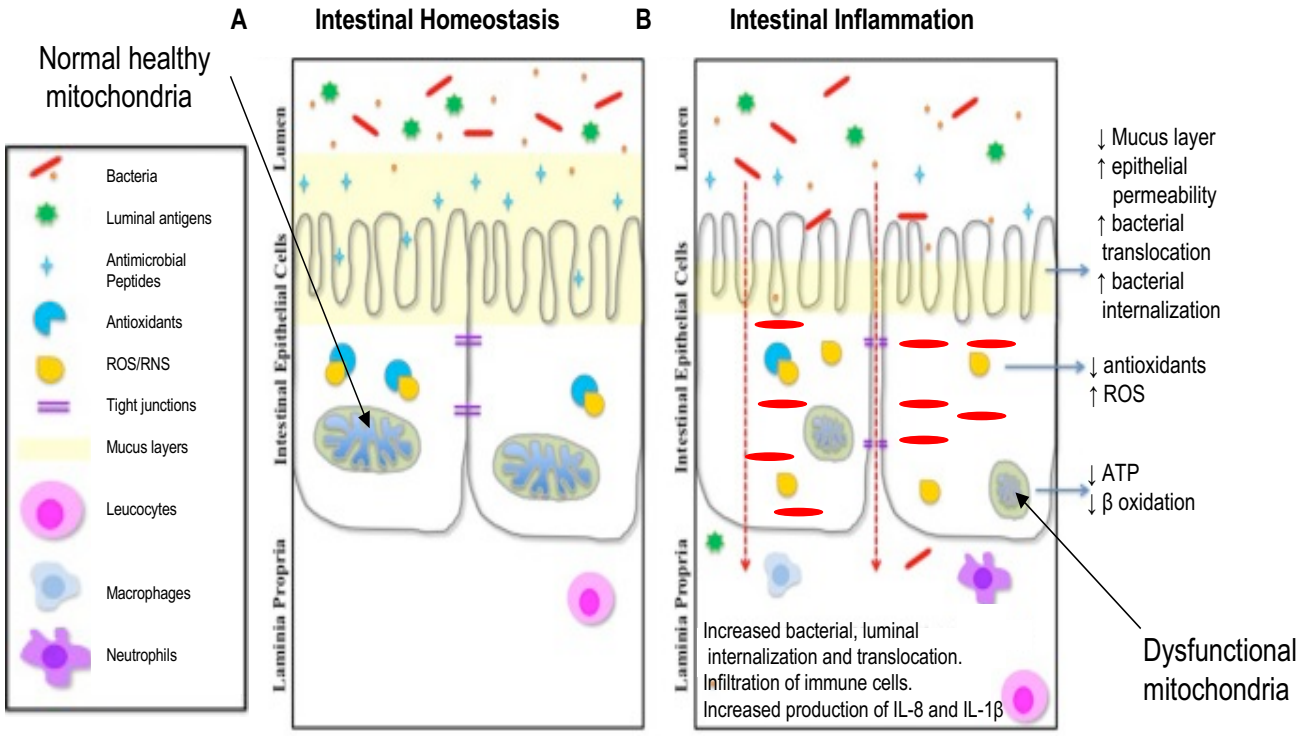

(Adapted from Novak, E. A. and Mollen K. P., Mitochondrial dysfunction in Inflammatory Bowel Disease, 2015 (106))

Figure 2: Mitochondrial dysfunction influences epithelial homeostasis and instigates increased epithelial permeability, bacterial internalization and translocation leading to inflammation. Increased ROS production, reduced ATP production, decreased ß oxidation of short chain fatty acids as well as reduced antioxidant levels are hallmarks of dysfunctional mitochondria which are known to complement reduced barrier function.(106)

1.4.3 Role of mitochondria in cell signaling:

Besides energy production, mitochondria regulate apoptosis.(107) Mitochondria, in response to either intracellular perturbation of homeostasis or extracellular stimuli, can promote apoptosis (programmed cell-death). (Figure 3) (108)

1.4.3a: Apoptosis:

Destructive stimuli can lead to attenuated mitochondrial transmembrane potential ($\Delta\Psi m$), allowing the release of several mitochondrial proteins such as cytochrome c, serine protease HTRA2 (HtrA Serine Peptidase 2)), or SMAC (Second Mitochondria-derived Activator of Caspases), also known as DIABLO (Direct IAP-Binding protein with Low PI) into the cytosol. If released, all of the aforementioned mitochondrial proteins can activate caspases and trigger programmed cell death.(109) However, the release of apoptosis-inducing factor (AIF), an NADH oxidoreductase into the cytoplasm, results in caspase-independent cell death. (Figure 4) (109-111)

Figure 3: Cartoon representation of Apoptotic pathways

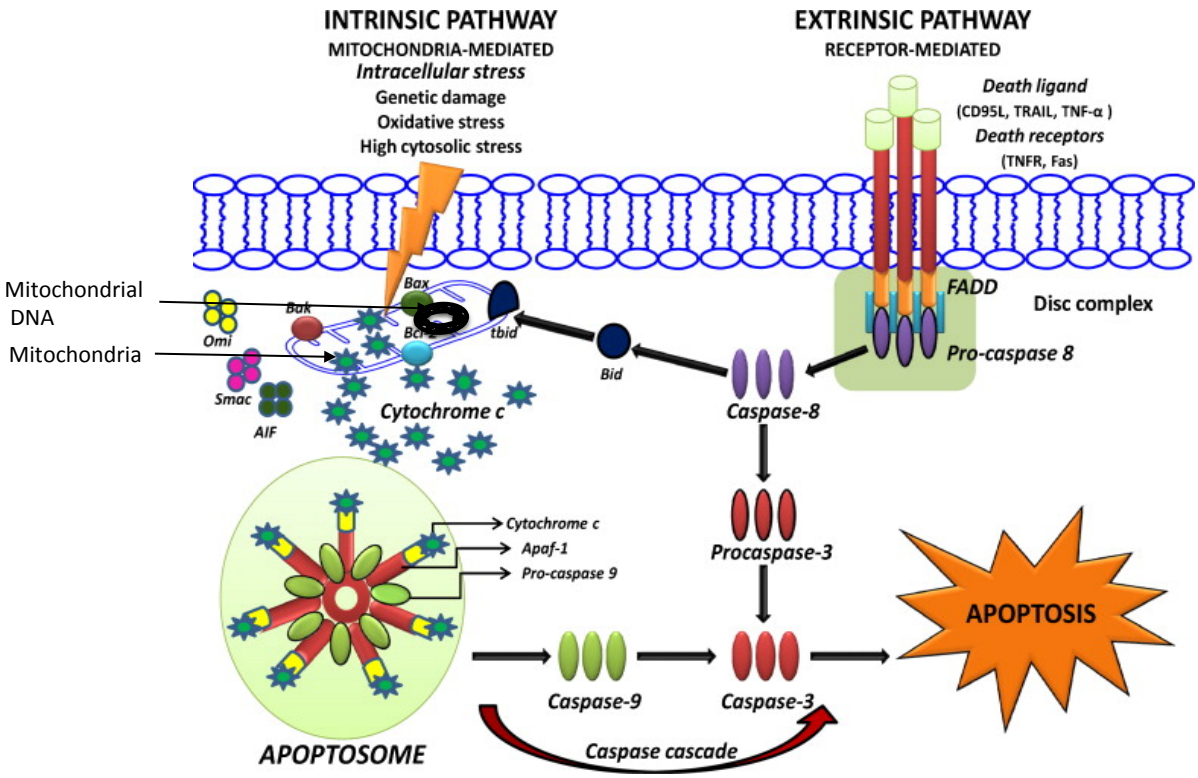

(Adapted from Beesoo *et al.*, Mutation Research/Fundamentals and Molecular Mechanism of Mutagenesis, 2014 (112))

Figure 3: Extrinsic (receptor mediated) and intrinsic (mitochondria-mediated) are the two main pathways of apoptosis. These pathways require specific signals to initiate the energy dependent cascade of molecular events. Each pathway has its own specific initiator caspase (e.g. caspases 8, 9), which in turn activates the executioner caspase-3. Caspase-3 is one of the most important executioner caspases; however, other executioner caspases like 6 and 7 also exist in the cytosol. The execution pathway results into cell shrinkage, chromatin condensation, and ultimate formation of apoptotic bodies which are phagocytosed by macrophages or nearby parenchymal cells or neoplastic cells.(112, 113)

Figure 4: Caspase independent Apoptotic pathways

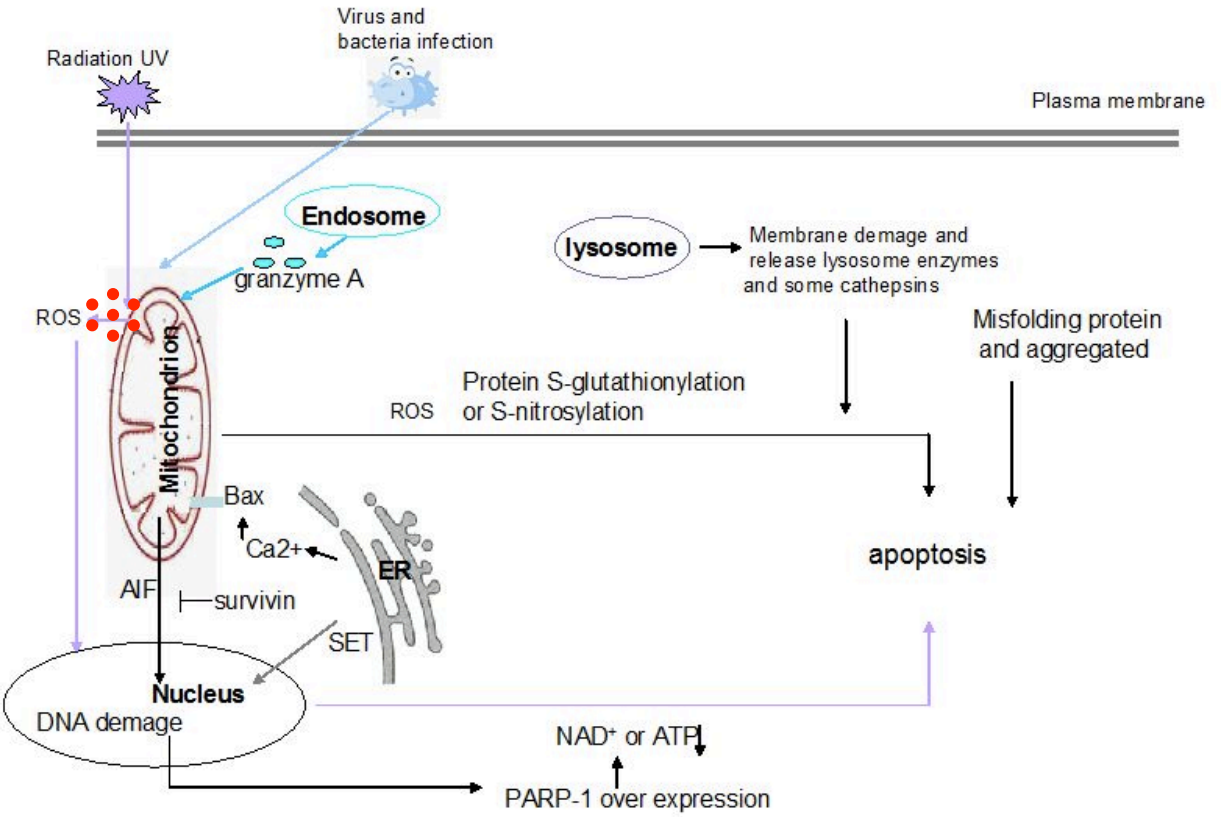

(Adapted from Hongmei Zhao: Intech, 2012 (114)

Figure 4: This figure shows caspase independent pathways of apoptosis. Mitochondrial damage is the centerpoint of this pathway, which can lead to increased production of ROS, and, in turn, ROS may be the main factor to induce the caspase independent apoptosis. However, ROS can also be involved in caspase-dependent apoptosis. Release of apoptosis-inducing factor (AIF) may also be dependent on ROS as it can mediate the poly (ADP-ribose) polymerase-1 (PARP-1) activation which is required for the release of AIF from the mitochondria.(114)

1.5 Evidence for metabolic stress in IBD

Roediger stated that ulcerative colitis could be an energy deficient disease.(115) He showed that colonocytes isolated from the distal colon of patients exhibit impaired oxidation of n-butyrate to CO_2 and ketone bodies compared to colonocytes isolated from control patients. Santhanam *et al.* showed that colonic biopsies from ulcerative colitis patients display reduced activity of the mitochondrial acetoacetyl coenzyme A (CoA) thiolase compared to controls; acetoacetyl CoA thiolase is responsible for catalyzing the last step in butyrate oxidation.(116) Another study by Santhanam *et al.* further demonstrated that colonic biopsies obtained from ulcerative colitis patients show reduced complex II activity within the ETC compared to controls. (50) This finding was recapitulated in model systems; mitochondrial preparations from colonocytes isolated from DSS-treated mice also exhibited decreased complex II and complex IV activity.(50)

Microscopic examination of biopsies of IBD patients show swollen mitochondria with irregular cristae.(117, 118) Reduced ATP levels have been reported in the colon of some patients with Crohn's disease.(119) Biopsies of individuals with IBD show more susceptibility to capric acid, an uncoupler of oxidative phosphorylation.(120) Additionally, it has been shown in various studies that there is reduced expression of mitochondrial-associated enzymes required for ATP production and antioxidant production.(116, 121, 122)

It has been shown that an inflammatory response can lead to metabolic stress, thus creating a positive–feedback loop. A study informed that TNF-α and IFN-γ, mediators in Crohn's disease (123), can upregulate O_2^- expression in colonic epithelial cells.(124) Additionally, exposure of mouse astrocytes to pro-inflammatory cytokines has also been noted to induce ROS production.(125)

1.5.1 Sources of metabolic stress:

1.5.1a Microbial Dysbiosis

Microbial dysbiosis could be the source of metabolic stress. Many studies have shown that the microbiota of IBD patients differ from healthy subjects by the under representation of the bacterial phylum Firmicutes. This phylum consists of microorganisms that produce the short chain fatty acid butyrate, which is the energy source for colonocytes and has anti-inflammatory effects.(126-128) Impaired butyrate oxidation has also been shown to be associated with IBD.(115, 116)

1.5.1b Invasive Bacteria Induce Metabolic Stress

Mitochondrial damage and reduction in ATP production has been observed following infection with pathogens. *Clostridium difficile* toxin A can localize to the mitochondria of intestinal epithelial cells and result in irregular morphology of mitochondria and a reduction in ATP production.(129) Similar results have been reported when murine epithelial cells are treated with *Citrobacter rodentium*.(130) *C. rodentium* uses type 3 secretion systems (TTSS) to inject effector proteins into host epithelial cells. The mitochondrial associated protein (Map) is one effector protein that contains a mitochondrial target sequence (MTS) and co-localizes with mitochondria to disrupt mitochondrial membrane potential. Map is involved in epithelial barrier dysfunction, as polarized Caco-2 cells (human colon-derived cancer cell line) treated with *C. rodentium* show a drop in TER in a TTSS dependent manner. Additionally Map also contributes to the colonization of *C. rodentium* to its murine hosts.(130) Caco-2 cells show dissociation of proteins from the tight junction in conjunction with the reduction of the ATP production when infected with the rotavirus.(131) Additionally, alterations in mitochondrial structure have been observed when T84 epithelial cells are infected with *E. coli* (strain C25).(132)

1.5.1c NSAID-induced Metabolic Stress

It has been shown that several medications can also provoke metabolic stress. Non-steroidal anti-inflammatory drugs (NSAID) are often used as pain relievers. NSAIDs work by inhibition of cyclooxygenase (COX) activity, and subsequently, reduce prostaglandin synthesis. NSAID gastropathy and enteropathy (i.e. NSAID-directed damaged of the stomach and intestines, respectively) are considered to be different conditions; the former is directly associated with lowered prostaglandin levels, while the latter is hypothesized to be an outcome of three different factors.(133-136) Bjarnson *et al* proposed a 'three hit' hypothesis arguing that NSAIDs solubilize phospholids present on the epithelial surface, and cause damage to epithelial mitochondria. Damaged mitochondria, in turn, yield reduced ATP levels and instigate calcium evacuation and ROS generation, thereby increasing paracellular permeability. Compromise of mucosal integrity results in entry of toxins and commensal bacteria, instigating inflammation.(137) Previous work done by the McKay lab has shown that indomethacin use, in particular, can have deleterious consequences – it perturbs mitochondrial activity and induces ROS production. This can lead to increased permeability of model epithelia which results in increased translocation of commensal *E. coli* as shown by Schoultz *et al*.(138) They also demonstrated that the increase in the translocation of commensal *E. coli* was reduced by vitamin C, an antioxidant, further implicating ROS in barrier dysfunction.(138)

1.5.1d Immunosuppressive drugs-induced metabolic stress

FK506, a *Streptomyces tsukubaensis* derived macrolide antibiotic (Tacrolimus^{TM}) is commonly used as an immunosuppressant. FK506 functions by inhibiting both the cell mediated and humoral immune response by binding immunophilin and subsequently blocking the calcineurin-dependent NFAT pathway as well as calcineurin-independent JNK and p38

pathways. (139, 140) In addition to its immunosuppressive function, FK506 is also known to cause mitochondrial dysfunction and enhanced intestinal permeability.(141) Madsen *et al* demonstrated that rats given FK506 show enhanced permeability in the jenjum, while rats given higher doses also showed decreased ileal barrier function.(141) Importantly, enterocytes isolated from both gut regions of FK506-treated rats showed reduced mitochondrial activity.(141) Cyclosporin-A is another immunosuppressive drug utilized in autoimmune disease treatment that has been associated with nephrotoxicity.(142, 143) Glomeruli isolated from cyclosporin-A treated mice have enhanced mitochondrial ROS production, while a study from Hornedo *et al.* confirmed these results in LLC-PK1 (procrine kidney cells).(144, 145) Also observed was an increase in oxidized cardiolipin (the lipid component of the mitochondrial inner membrane) concentration and attenuated mitochondrial potential.(145)

Finally, another prominent immunosuppressive known to have palpable effects on mitochondrial function is thiopurine 6-thioguanine (6-TG).(146) Although a potent anti-cancer and anti-inflammatory molecule, 60% of IBD patients treated with the compound later develop nodular regenerative hepatic hyperplasia.(147, 148) Mechanistically, 6-TG instigates mitochondrial damage by assimilation into mitochondrial DNA (mtDNA) and rapid oxidation.(149) Indeed, HCT116 (human colorectal carcinoma) epithelial cells grown in a culture medium containing 6-TG for up to 10 days showed irreversible accumulation of 6-TG in mtDNA and a concurrent decline in ATP output.(149)

1.5.1e Psychological Stress causes Metabolic Stress

Psychological stress has been implicated in relapses suffered by patients with IBD. A study in which IBD patients were exposed to a cold–pain stress test resulted in swollen mitochondria with ruptured cristae and reduced ATP production and greater epithelial

damage.(150) Soderholm *et al.* showed that rats exposed to psychological stress had altered mitochondrial structure; stressed animals showed enlarged mitochondria and elevated numbers of phagosomes.(151)

1.5.1f Ischemia/Surgery

Ischemia, or the deprivation of oxygen, is another source of metabolic stress. Reduction in oxygen levels results in the interruption of oxidative phosphorylation and decreases ATP production. Disruption in the oxygen metabolism in the mitochondria can also lead to low oxygen levels.(152) Local ischemia due to surgery (50-70% of CD patients undergo surgery) can cause metabolic stress as represented by dilated mitochondria in epithelial cells after surgery.(153) Swollen mitochondria with deranged cristae has also been observed in rat enterocytes post-surgery.(154)

1.5.1g DNP (2,4 Dinitrophenol) as a Metabolic Stressor

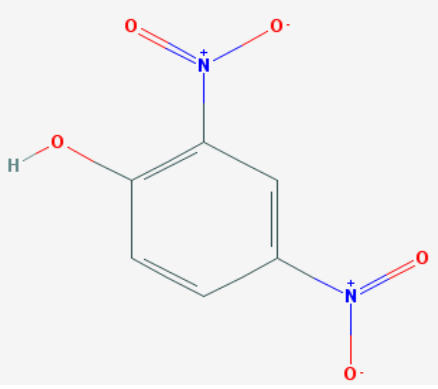

Figure 5: Structure of 2,4 Dinitrophenol (DNP)
(downloaded on 21-06-17 from PubChem, https://pubchem.ncbi.nlm.nih.gov/compound/2_4-dinitrophenol#section=Top)

DNP (2,4–dinitrophenol) is an H^+ ionophore and functions by uncoupling oxidative phosphorylation. It is a lipophilic acid and permeates the membrane because of its neutral protonated condition. DNP can bind to the protons in the inter-membrane space and reverse the

flow of the protons to the mitochondrial matrix resulting in the loss of the proton gradient and disruption of ATP-synthase activity.(155) It has been chosen as a metabolic stressor in many experiments because of its specific effect on the mitochondria. Previous studies have showed a significant decrease in TER, and increased translocation and internalization of bacteria in T84 epithelial cell monolayers treated with DNP (0.1 mM) and *E. coli* HB101 (non-pathogenic, non-invasive, non-toxigenic bacteria) relative to cells treated with *E. coli* or DNP alone over a 24 hr period. Additionally, exposure of T84 cells to DNP + *E. coli* HB101 increased the transepithelial influx of HRP (horseradish peroxidase). Finally, a decrease in the barrier function in these model epithelia is not a result of increased apoptosis.(118, 156) Interestingly Lewis *et al*. showed that T84 epithelia after 6 hrs of treatment with DNP exhibit swollen mitochondria with smaller cristae compared to non-treated epithelia. Additionally, DNP + *E. coli* treated cells displayed increased numbers of pseudopodia compared to *E. coli* only treated cells.(157) Nazli *et al.* also showed that DNP induced internalization of bacteria required an intact enterocyte cytoskeleton, as disruption of the actin cytoskeleton through pharmacological agents reduced bacterial internalization.(158)

Previous studies done in the McKay lab have shown that metabolically stressed model epithelia exhibit increased translocation of commensal bacteria; however, upon butyrate treatment, this barrier effect was not observed.(152) In another study, Nazli *et al.* showed that when DNP was delivered directly into the distal ileum of rats, it resulted in mitochondrial damage, increased bacteria levels in the tissue, and increased epithelial permeability compared to control rats given only phosphate-buffered saline (PBS). Here, epithelial permeability was defined as increased ion conductance and HRP flux. Additionally, 6-to-24 hrs after DNP

exposure, increased numbers of mononuclear and granulocytic immune cells were seen in the mucosa of the treated rats.(118)

1.6 Pattern Recognition Receptors in the Immune Systems

The two main arms of the vertebrate immune system are the innate and the adaptive immune systems. The innate immune system functions by detecting conserved pathogen-derived motifs known as pathogen associated molecular patterns (PAMP) or host-derived markers of cell stress or damage called damage associated molecular pattern (DAMPS), and responds by clearing these insults. To achieve this, innate immunity utilizes germline-encoded pattern recognition receptors (PRR). The majority of PRRs are signaling receptors and are divided into various classes such as Toll-like receptors (TLRs), retinoic acid-inducible gene-1 (RIG)-like receptors (RLRs), and nucleotide-binding oligomerization domain (NOD) like receptors (NLRs).(159-161)

The NLRs are a family of cytosolic PRRs and represent a second line of defense against pathogens that invade the cell. They share a common domain organization: a C-terminal leucine-rich repeat (LRR) domain which is involved in ligand sensing (except NLRP10), a central nucleotide-binding and oligomerization domain (NACHT) that is important for oligomerization, and activation and an N-terminal effector domain involved in the signal transduction to downstream targets through protein-protein interaction, such as NF-κB or caspase-1-triggered inflammasome cascades.(Figure: 6) (159-161)

NLRs can be grouped into two sub-families based on the amino terminal domains. The NLRC subfamily is characterized by the presence of the caspase activating and recruiting domain (162); examples include NOD1 (Nucleotide Binding Oligomerization Domain

Containing 1), NOD2 (Nucleotide Binding Oligomerization Domain Containing 2), NLRC4 (NOD like Receptor family CARD domain-containing protein 4) as well as uncharacterized but similar domains e.g. NLRX1 (NLR family member X1), NLRC3 (NLR Family CARD Domain Containing 3) and NLRC5 (NLR Family CARD Domain Containing 5). The second NLRP sub-family typically has pyrin domains present at the NH2-terminal with 14 members currently reported.(163-165)

1.7 IBD Associated Polymorphisms:

IBD is considered to be the result of an inappropriate and continuing inflammatory response to commensal microbes in a genetically susceptible host. Genome-wide association studies (GWAS) in IBD have successfully provided insights into the disease's pathobiology by highlighting some key molecular pathways. GWAS have identified over 200 non-overlapping genetic risk loci associated with IBD, 2/3 of which are shared between Crohn's disease and ulcerative colitis.(2, 166, 167) At the same time, 30 Crohn's disease-specific loci and 23 ulcerative colitis- specific loci have been identified. Similar genes are implicated in childhood-onset and adult-onset IBD suggesting that similar genetic predispositions and pathophysiological pathways are involved in disease progression.(2) In a study conducted in Germany, it was shown that the development of ulcerative colitis in monozygotic twins is 10-15% compared to 30-35% in Crohn's disease: this suggests that genetic polymorphism plays a bigger role in Crohn's disease compared to ulcerative colitis.(168, 169) Additionally, genes and genetic loci implicated in IBD revealed the involvement of many pathways that work to maintain cellular homeostasis such as: barrier function, epithelial restitution, microbial defense, innate immune regulation,

ROS generation, autophagy, regulation of adaptive immunity and endoplasmic reticulum (ER) stress.(2)

The intestinal mucosa exists in a functional equilibrium with the luminal milieu dominated, in the colon, by microbes and their products. During normal mucosal physiology this homeostasis is maintained; however, its perturbation leads to the pathophysiology of IBD.(170) IEC (intestinal epithelial cells) are key players in both barrier function and signal transduction of conditions in the gut lumen. Abnormal intestinal permeability has been associated with IBD: genes within several IBD-associated loci such as *CDH1* (gene codes for E-cadherin), *GNA12* (gene codes for G protein G_{α}) and *PTPN2* (tyrosine phosphatase) are involved in maintaining barrier integrity. Thus, mutations in the genes involved in epithelial barrier function predispose individuals to IBD.(171-174) Other important genes associated with IBD pathogenesis are *NOD2,* a gene associated with the intracellular sensing of muramyl dipeptide (MDP), which modulates both the innate and adaptive immune response, and *ATG16L1* and *IRGM,* genes that are involved in autophagy.(175-178) Autophagy is a process involved with the degradation and recycling of cytosolic contents and organelles, as well as resistance against infection and the removal of intracellular microbes.(2)

1.8 NOD2 and IBD:

NOD2 was the first gene found to be associated with Crohn's disease.(2) NOD2 is encoded by the *NOD2/Card15* gene that is located on chromosome 16q12 in humans. The three main variants (loss of function mutations) commonly found to be associated with the *NOD2* gene and are thus identified as the risk factors for Crohn's disease include: a frameshift mutation at position 1007(1007 fs) resulting in the partial translation of the LRR (leucine rich repeat) and

early termination; a glycine to arginine conversion at amino acid residue 908 (G908R); and arginine to tryptophan conversion at amino acid residue 702(R702W). Most Crohn's disease-associated mutations are clustered in or near the LRR domain of NOD2 that results in improper ligand sensing.(179-181) Homozygosity of either of the alleles increases the risk of Crohn's disease by ~40-fold; however, not all individuals who are homozygous for these mutations develop the disease, and those do typically remain asymptomatic for the first 10-15 years of their lives. This reaffirms that both genetic and environmental factors are involved in the development of the disease.(179)

1.8.1 NOD2 Crystal Structure:

Maekawa *et al.* recently introduced the crystal structure of the NOD2 when bound to ADP (inactive form) without the CARD domain.(182) They described the ADP bound NOD2 as being folded into a hook-shaped structure. The NOD domain is divided into the nucleotide-binding domain (NBD), the helical domain 1 (HD1), the winged helix domain (WHD) and helical domain 2 (HD2).(165) The LRR domain consists of ten leucine rich repeats that comprise a horse-shoe like structure arranged in a single curvature. α-helices constitute the convex surface while the β-strands form the concave surface of the LRR region of NOD2. They further showed that the ADP bound to the winged helix subdomain of NOD domain links the NBD and HD 1 subdomains while the adenosine moiety of ADP is embedded in the cavity between NBD and HD 1, enabling the subdomains to lie in a closely packed structure. At the same time, the sub-domain interaction of the NOD domain also assists in the establishment of a closed and inactive conformation. It was also shown that inter-domain interactions exist between the NOD domain and the LRR domain, and that the potential ligand-binding site likely lies on the concave

surface of the LRR domain on a hydrophobic pocket capable of binding peptide from MDP or glycan.

1.8.2 Expression of NOD2 in Epithelial and Immune cells:

Olga *et al.* reported that under non-stimulatory or basal conditions, NOD2 is expressed in myelomonocytic cells, dendritic cells, Paneth cells and, to a lesser extent, T lymphocytes.(183) However, NOD2 expression can also be up-regulated in epithelial cell lines such as SUM159, MCF-7 (breast cancer cell lines) and FHC (normal fetal colon cell line) upon stimulation with TNFα. This induction is mediated through activation of the nuclear factor kappa-light-chain-enhancer of activated B cells (NF-κB) transcriptional factor.(183) Additionally, Uehera *et al.* showed through immunostaining and flow cytometry analyses that HT-29, T84 and Caco-2 epithelial cells express NOD2.(184)

1.8.3 NOD2 Activation and Function:

The NOD2 is the intracellular sensor of MDP, a product of peptidoglycan present in both gram-positive and gram-negative bacteria. MDP consists of *N*-acetyl muramic acid-$_{L}$-Ala-$_{D}$-Glu.(185, 186) The exact mechanism of NOD2 activation is still unknown. However, it has been proposed by Tanabe *et al.* and Hsu *et al.* that under steady conditions NOD2 exists in the cytosol in an inactive conformation through the auto-inhibition of the NOD domain through the LRRs; when MDP is present, this inhibition is disrupted.(187, 188) After ligand recognition, NOD2 undergoes a conformational change and subsequently, the NOD domain is oligomerized which leads to the exposure of the CARD domain and recruitment of receptor-interacting serine/threonine-protein kinase 2 (RIP2) through CARD-CARD interactions.(189, 190) Upon

activation, RIP2 switches on the downstream NF-κB and mitogen-activated protein kinase (MAPK) signaling cascade. RIP2 also activates the IκB kinase (IKK) complex either alone or together with transforming growth factor β activated kinase 1 (TAKI) and induces the phosphorylation, ubiquitination, and degradation of IκB and results in the nuclear localization of NF-κB.(Figure 7) This transcription factor is involved in the induction of pro-inflammatory cytokine and chemokine production.(191, 192) RIP2 and TAKI are also involved in the activation of the MAPK pathway; however, the exact mechanism is yet to be elucidated.(193, 194) It has been shown in *in vitro* studies that many pathogenic bacteria such as *Streptococcus pneumoniae, Staphylococcus aureus, Shigella flexneri, Mycobacterium tuberculosis* and *Salmonella typhimurium* can activate NOD2.(185, 195-198) (Figure: 7)

Additionally, NOD2 signaling is also required for the regulation of commensal microbiota as shown by Petnicki *et al.* They demonstrated that NOD2-and RICK-deficient mice exhibit an increased load of commensal resident bacteria in the terminal ileum and that NOD2-deficient mice also have a decreased ability to kill bacteria in intestinal crypts isolated from the ileum.(199) It has been suggested that the impaired bacterial killing might be associated with the decreased production of α-defensin by Paneth cells within the ileal crypt of NOD2 deficient mice.(199, 200) NOD2 signaling controls the numbers and composition of the commensal microbiota. It has been shown that NOD2 expression in the intestine of germ-free mice can be restored after reconstitution with commensal bacteria such as *Lactobacillus plantarum* or non-pathogenic *E. coli* suggesting that the commensal microbiota positively regulate NOD2-RICK signaling.(199)

Barnich *et al.* showed that NOD2 is expressed by various intestinal cell lines and that in response to MDP stimulation, wild-type NOD2 localizes to the plasma membrane, while the

mutant NOD2 3020insC, which is associated with Crohn's disease, remains confined to the cytosol and vesicular compartments.(201) They further found that the wild-type NOD2 co-localizes with E-cadherin, a transmembrane protein and a membrane marker, in response to MDP. The 33 amino acids present at the COOH-terminal domain of NOD2 are critical for its plasma membrane localization in response to MDP. At the same time, NOD2 recruitment to the plasma membrane was discovered to be essential for MDP induced activation of NF-κB, because mutant NOD2 that failed to be recruited to the plasma membrane displayed little to no activation of NF-κB in response to MDP.(201)

Figure 6: Tripartite structure of NOD2

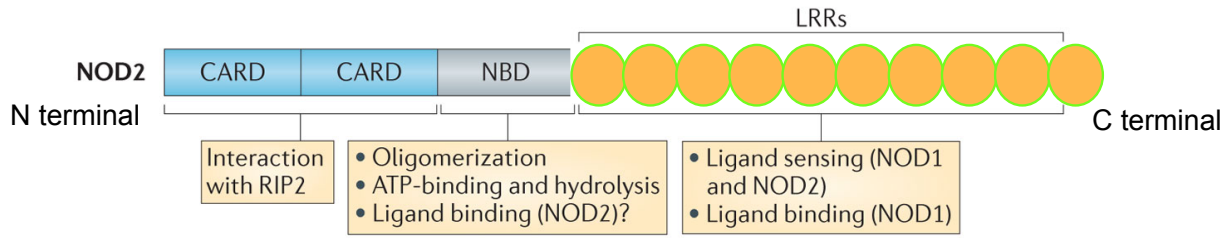

(Adapted from Philpott *et al:* Nature Reviews Immunology,2014 (202))

Figure 6: NOD2 contains two N-terminal CARDs (caspase activation and recruitment domain) that interact with the CARD of RIP2 (receptor-interacting protein 2). NOD2 contains a central nucleotide-binding domain (NBD), which binds to ATP and mediates NOD oligomerization, and carboxy-terminal leucine-rich repeats (LRRs), which are involved in ligand sensing.(202)

Figure 7: Signalling pathway of NOD2

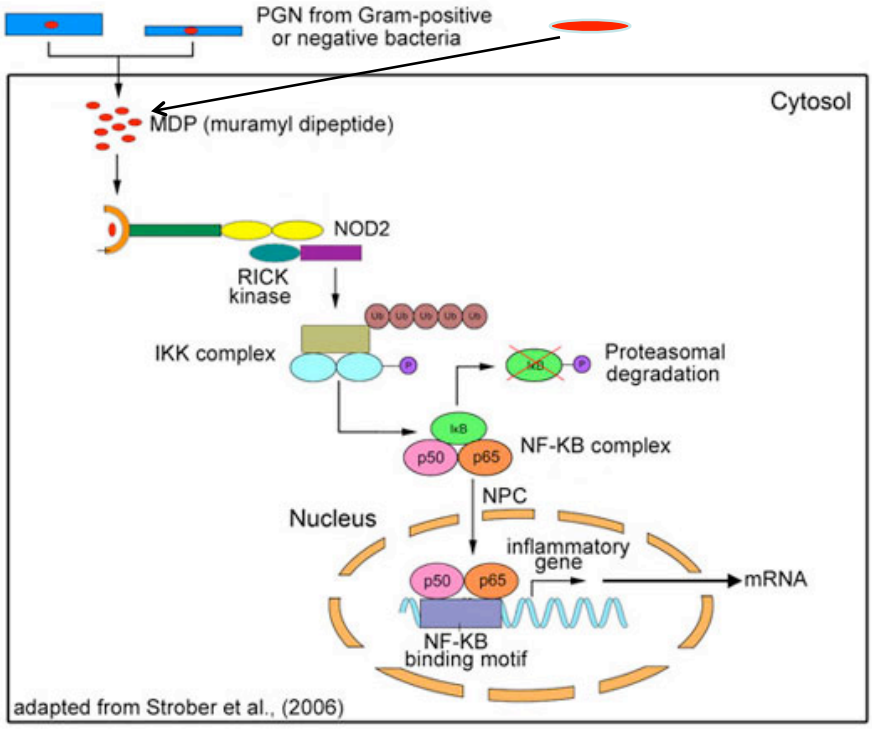

(Adapted from Strober *et al:* Nature Reviews Immunology,2006 (203)

Figure 7: After recognizing its ligand, MDP, NOD2 undergoes a conformational change and interacts with RICK kinase (also known as RIP2 kinase) through CARD-CARD interaction. After its activation, RICK kinase sequentially activates NF-κB signaling.

1.8.4 NOD2 and IBD Pathogenesis

Couturier-Maillard *et al.* investigated the role of NOD2 mediated dysbiosis in affecting susceptibility to Crohn's disease and colitis-associated cancer (CAC). They showed that dysbiosis induced by NOD2 deficiency is transferrable and contributes to Crohn's disease and CAC development in mice. Mutant and dysbiosis-exposed mice underwent fecal transplants from $NOD2^{-/-}$ and $NOD2^{+/+}$ mice. Transplants of feces from $NOD2^{+/+}$ mice induced a recovery of the commensal microbiota and rescued knockout and exposed mice from DSS-induced colitis risk; recipients of $NOD2^{-/-}$ transplants showed opposite results, as well as a loss of critical mucin-producing epithelial cells and greater morbidity. (204)

Peptidoglycan, a component of the bacterial cell wall, can be recognized extracellularly, by TLR2, while NOD2 senses this component intracellularly; recognition by either receptor/sensor leads to the activation of NF-κB. NOD2 negatively regulates TLR2 mediated TH1 response as shown by Watanabe *et al.,* who reported that splenocytes isolated from $NOD2^{-/-}$ mice show increased production of TH1 cytokines compared to wild-type mice.(205) Additionally, they also found that $CD11b^{+}$ antigen presenting cells (APCs) isolated from $NOD2^{-/-}$ mouse spleen produce significantly greater amounts of IL-12 and NF-κB activation with regard to c-Rel when compared with wild-type splenic $CD11b^{+}$ APCs.(205)

To determine if NOD2 plays any functional role in intestinal inflammation, Corridoni *et al*. administered MDP, DSS, or a combination of the two to SAMP1/YitFc mice (derived from brother and sister breeding of AKR mice).(206) SAMP1/YitFc mice lack *NOD2* mutations, but spontaneously develop Crohn's disease-like ileitis by the time they are 20 weeks old without the need for treatment with any chemical and immunological agent or genetic alterations. Through *in vivo* studies, they showed that spontaneous or DSS-induced colitis in SAMP1/YitFc mice cannot

be rescued by the administration of MDP compared to parental AKR control strain mice. This result is suggestive of defective NOD2 signaling, as it has been shown that MDP administration can protect wild-type mice from DSS-or TNBS-(2,4,6-trinitrobenzenesulfonic acid) induced colitis.(206, 207)

Corridoni *et al.* further demonstrated that bone marrow-derived macrophages (BMDM) isolated from pre-inflamed SAMP1 mice produce decreased amounts of cytokine compared to age-matched, AKR control mice in response to MDP treatment, further implicating abnormal NOD2 signaling. Finally, it has also been shown that BMDM from SAMP1 mice have an increased bacterial load through defective clearance, which is another effector function of NOD2, as compared to AKR control mice BMDMs.(206)

1.8.5 NOD2 and Autophagy

Many studies have demonstrated a link between NOD2-mediated bacterial sensing and the induction of autophagy. Autophagy is a highly conserved self-degradation system which involves the elimination of misfolded protein and damaged organelles to maintain cellular homeostasis.(208) The process of autophagy starts with the formation of an isolation membrane also known as a phagophore, that is followed by the transport and maturation of the autophagosome which ultimately fuses with the lysosome to degrade their cargo and recycle biomolecules to the cytoplasm.(209) Besides the aforementioned function, autophagy is also very important for host defense against bacterial, viral and parasitic pathogens.(210) MDP induces autophagy in fibroblasts, epithelial cells, monocytes, macrophages and dendritic cells in a NOD2-dependent fashion.(211-213) Besides ligand-induced autophagy, the entry of live bacteria can also be sensed by NOD2, which activates autophagy.(211-213) NOD2-dependent

induction of autophagy requires an interaction between NOD2 and ATG16L1 (an autophagy protein).(213) Polymorphisms in ATG16L1 are associated with an increased risk of developing Crohn's disease.(211, 212)

1.9 Nuclear factor kappa B (NF-κB) signaling

NF-κB is a dimeric transcription factor and a major regulator of innate and adaptive immunity as well as the inflammatory response. There are five subunits: NF-κB1 (p50 and its precursor p105), NF-κB2 (p52 and its precursor p100), and c-REL, REL A (p65), and REL B. Typically, NF-κB is bound to inhibitory (IκB) proteins and remains in the cytoplasm. However, phosphorylation of IκB leads to the inhibitors' ubiquitination and subsequently, its rapid degradation by the proteasome. This frees NF-κB and allows it to move to the nucleus and bind to DNA. This is a crucial process for NF-κB activation.(214)

1.10 Mitogen-activated protein kinase (MAPK) signaling

A number of instrumental cellular processes that include proliferation, differentiation, motility, stress response, apoptosis and survival involve the function of MAPKs. These MAPKs translate extracellular signals into intracellular signaling cascades. This protein group consists of a highly conserved family of serine/threonine kinases. Notable MAPKs include the extracellular signal-regulated kinase 1 and 2 (Erk1/2 or p44/42), the c-Jun N-terminal kinases 1-3 (JNK1-3), stress activated protein kinases (SAPK1A, 1B, 1C), the p38 isoforms (p38α, β, γ, and δ), and Erk5.(215) It has been shown that stimuli capable of instigating ROS production can induce MAPK signaling, such as ERK and JNK signaling pathways.(216, 217) As one example, Ruffels *et al.* showed that neuroblastoma cells (SH-SY5Y cells) treated with exogenous H_2O_2, to mimic

ROS, led to activation of MAPK pathways.(218) At the same time, this MAPK signaling activation can be prevented by the use of antioxidants.(216, 217)

Epidermal growth factor (EGF) and platelet derived growth factors (PDGF) are major drivers of the ERK pathway and function by activating the small GTP-binding proteins Ras and Raf.(219) It has been further shown by Verbon *et al*. that ROS can activate growth factor receptors even in the absence of their ligand. (220) Studies have also shown that MAPK, and ERK can regulate endocytosis.(221, 222) Interestingly, a study by Smyth *et al*. demonstrated that pharmacological inhibition of ERK activity reduced IFNγ-induced bacterial internalization into the T84 epithelial cell line.(223)

1.11 IL-8:

Interleukin-8 (IL-8, or CXCL8) is a chemokine produced by macrophages, IECs, endothelial cells, and other cell types.(224) It uniquely targets neutrophils, provoking their migration, release of lysosomal enzymes, generation of superoxide and hydrogen peroxide, and increases the expression of adhesion molecules on neutrophils. IL-8 is a member of the CXC family, indicating that the first two cysteine residues in the amino terminal portion of the protein are separated by one amino acid. IL-8 has a glutamic acid-leucine-arginine sequence (the ELR motif) prior to its cysteine residues, which has been associated with chemotactic activity for neutrophils.(224, 225) CXCR1 and CXRC2 are two G-protein coupled receptors (GPCR) through which IL-8 signaling can occur.(226) Binding of IL-8 to CXCR1 on a neutrophil activates G-protein coupled signaling and production of second messengers that leads to neutrophil migration, the release of effectors through exocytosis, and an oxidative burst to kill phagocytosed bacteria.(226)

1.11.1 IL-8 production by intestinal epithelial cells

The production of IL-8, a major human cytokine, is induced in intestinal epithelial cells after stimulation by bacteria. It is secreted basolaterally.(227) An increase in IL-8 secretion from T84 cells is also triggered by TNF-α stimulation.(228) Biopsies of the proximal and distal regions of the colonic mucosa from patients with ulcerative colitis show a ~10-fold increase of IL-8 production over control subjects suggesting an immunoregulatory role of IL-8 in the pathogenesis of IBD.(229) It has been suggested that bacterially stimulated, epithelial-derived IL-8 is sufficient to elicit neutrophil recruitment into the lamina propria but additional chemotactic and/or activating signals are still required to complete transepithelial migration and fully activate the recruited neutrophils.(230) The above studies illustrate bidirectional communication between epithelial cells and mucosal immune and inflammatory cells. A study by Akhtar *et al.* showed that intestinal epithelial cells (T84, HT29 or Caco-2) treated with *E. coli* DNA exhibit increased IL-8 mRNA as well as a time- and dose-dependent increase in IL-8 secretion via an ERK 1/2 dependent pathway.(231)

1.11.2 NOD2 and IL-8 production:

Additionally, NOD2 has been linked with IL-8 production: a recent study by Isabella *et al.* demonstrated that conjunctival cells treated with *S. aureus* show up-regulation of IL-8 production.(232) They further reported that this increase is a result of increased production of PGE_2 through the increased expression of COX2 (cyclooxygenase-2). Increased expression of NOD2 is responsible for the up-regulation of expression of COX2 via a JNK (c-Jun NH(2)-terminal kinase) dependent pathway.(232)

Based on this background information:

1. Epithelial mitochondrial dysfunction occurs in IBD;
2. Epithelia under metabolic stress exhibit increased internalization and transcellular transcytosis of non-pathogenic, non-invasive bacteria;
3. Increased reactive oxygen species (ROS) is present in IBD and murine models of colitis;
4. The IBD susceptibility trait of loss of function mutation in NOD2 is a cause of inflammation;
5. NOD2 and the autophagy protein ATG16L1 are expressed in transporting enterocytes;
6. NOD2 senses intracellular bacteria and is also involved in xenophagy;
7. Modulation of endocytosis through the activity of ERK (MAPK);
8. Production of IL-8 from epithelial cells in response to bacterial infection;

I made the following hypotheses.

1.12 Hypothesis:

Overall Hypothesis: The absence of NOD2 will leave the enterocyte more vulnerable to metabolic stress and result in increased internalization and translocation of *E. coli*.

To test this hypothesis, experiments were conducted under the following aims:

Aim 1: To determine the expression of NOD2 in human colon cancer-derived epithelial cell lines and assess its inducibility via treatment with MDP, *E. coli*, and DNP (alone or in combination).

Aim 2: To assess whether the absence of NOD2 affects the impact of metabolic stress (DNP treatment) on the epithelium as measured by (i) intracellular *E. coli* and (ii) IL-8 production.

Aim 3: To determine if an exaggerated response of the epithelium to *E. coli* ± DNP as a consequence of reduced NOD2 expression is due to ROS production.

Aim 4: To determine if epithelial ROS results in ERK1/2 phosphorylation that promotes internalization of non-pathogenic *E. coli.*

Aim 5: To determine if increased numbers of intracellular bacteria in NOD2 knock-down (48) cells is due to increased uptake or decreased killing of bacteria.

Hypothesis: The metabolically stressed T84 monolayer will have increased permeability and subsequently, increased internalization and translocation of luminal antigens (likely bacteria) which will result in increased interleukin 8 (IL-8) production.

To test this hypothesis, experiments were conducted under the following aims:

Aim 1: To determine if bacteria or bacterial products are necessary for increased IL-8 production in a metabolically stressed epithelium and whether this is a time and dose dependent process.

Aim 2: To determine if TLRs (233) are involved in the IL-8 production.

Aim 3: To determine if ROS are involved in IL-8 production.

Aim 4: To determine if IL-8 production by T84 cells treated with *E. coli* HB101 ± DNP is NF-κB or ERK dependent.

In order to address these aims, I used an *in vitro* model utilizing the T84 cell line (colon-derived crypt like T84 cell line). Additionally, to test the validity of my data from epithelial cells lines in a more representative system, I also used organoids grown from the colon of wild-type and $NOD2^{-/-}$ mice. The aforementioned questions were answered in these cells post-exposure to an uncoupler of oxidative phosphorylation (i.e. DNP) and a non-invasive, non-pathogenic, laboratory strain of *E. coli* HB101.

CHAPTER 2 - Materials & Methods

A list of materials and reagents utilized, including media for cell culture and specific bacterial strains, as well as other items used to create a cell culture model of metabolic stress are detailed in the tables 1-4.

Table 1: List of materials and reagents used for the experiments

Reagent Name	Supplier	Catalog No	Final Conc	Reference
2,4-dinitrophenol (DNP)	Sigma-Aldrich, St. Louis, MO, USA	D198501	0.1 mM	(118)
3-(4,5-dimethyl-thiazol-2-yl)-2,5-diphenyltetrazoliumbromide salt (MTT)	Sigma-Aldrich	398-93-1	100 μM	(156)
4',6-diamidino-2-phenylindole (DAPI)	Molecular Probes, Eugene, OR, USA	D1306	1:500 in PBS	N/A
DCFDA, kit for ROS measurement	Abcam	ab11385		N/A
FITC-dextran (4 kDa)	Sigma-Aldrich	FD4	100 μg/ml	(223)
Gentamycin	Sigma-Aldrich	G1272	200 μg/ml	(158)
GFP control lentiviral particles (copGFP Control Lentiviral Particles)	Santa Cruz Biotechnology, Dallas, Texas, USA	sc-108084	1×10^5 particles	N/A
HEPES	Sigma-Aldrich	H3537	N/A	N/A
Indomethacin	Sigma-Aldrich	17378	1 μM	(138)
IntestiCult™ Organoid Growth Medium (Mouse)	Stem Cell Technologies Vancouver, BC, Canada	06005	N/A	(234)
L-glutamine	Sigma-Aldrich	G7513	1.2 mM	(235)
Lipofectamine	Invitrogen, Carlsbad, California, USA	13778	N/A	N/A
Luria Bertani (LB) agar	EMD Chemicals Inc, Billerica, Massachusetts, USA	1.10283.0500	N/A	N/A
Luria Bertani (LB) broth	BD Biosciences,	244620	N/A	N/A

	Missisauga, ON, Canada			
Matrigel	Corning, Tewksbury, MA, USA	354248	N/A	(234)
mitoTEMPO	Santa Cruz Biotechnology	sc-221945	10 μM	(105)
muramyl di-peptide (MDP)	Invivogen	tlrl-mdp	1-2 μg/ml	N/A
$NaHCO_3$ (sodium bicarbonate)	Life Technologies, Carlsbad, California, USA	27080-094	1.9%	(235)
Paraformaldehyde	Sigma-Aldrich	P6147-500G	4%	(223)
Penicillin-streptomycin	Sigma –Aldrich	P-0781	2%	(235)
PMA (phorbol-12-myristate-13-acetate)	Sigma-Aldrich	16561-29-8	0.1 μM	(156)
Polybrene	Santa Cruz Biotechnology	sc-134220	5μg/ml	N/A
Puromycin dihydrochloride	Santa Cruz Biotechnology	sc-108071	2.5 μg/ml	N/A
Sodium pyruvate	Sigma-Aldrich	S8636	1 mM	N/A
TMB (3,3',5,5'tetramethylbenzidine)	Sigma-Aldrich	T0440	N/A	N/A
Triton X-100	Sigma-Aldrich	X-100	0.1%	(158)
Trypan blue	Lonza, Allendale, NJ, USA	17-942E	N/A	N/A
TrypLE	Invitrogen	12605-036	N/A	N/A
Tween 20 (Polyoxyethylenes orbitan monolaurate)	Sigma-Aldrich	P1379-1L	N/A	N/A

Table 2: List of Medium used for the experiments

Reagent Name	Supplier	Catalog No	Reference
Opti-MEM	Life Technologies	31985-070	(223)
DMEM (Dulbecco's modified Eagle's Medium)	Sigma-Aldrich	D5796	(157)

DMEM-F12 (Dulbecco's modified Eagle's Medium/Ham's F-12 medium)	Sigma-Aldrich	D6421	(235)
DMEM/F-12 Phenol free (Dulbecco's Modified Eagle Medium/Nutrient Mixture F-12)	Sigma-Aldrich	D6434	(156)
RPMI 1640	Sigma-Aldrich	R8758	(156)
HI FBS	Gibco	12484-028	(235)
ADF (Advanced DMEM/F-12)	Thermo Fisher Scientific, Waltham, MA, USA	12634010	(234)

Table 3: Bacterial strains used for the experiments

Bacteria	Source	Conc	Reference
E. coli F18	Dr. Philip Sherman University of Toronto, ON	1 x 10^6 cfu/ml	(157)
E. coli HB101	Dr. Philip Sherman University of Toronto, ON	1 x 10^6 cfu/ml	(118)

Table 4: Products used for ELISA, immunostaining and knock-down of protein expression

Product Name	Supplier	Catalog No	Final Conc	Reference
anti-*E. coli* antibody	Abcam, Toronto, ON, Canada	ab30522	1:200	N/A
BLOCK-iT fluorescent oligo	Thermo Fisher Scientific	2013	N/A	N/A
Chloroquine	Sigma-Aldrich	C-6628	10 μM	(231)
Cytochalsin D	Sigma-Aldrich	C-8273	0.2 μM	(158)
FITC conjugated latex beads (1 μm)	Molecular Probes	F8823	3 x 10^6	N/A
FITC labeled heat killed *E. coli* (K 12) particles	Molecular Probes	E2861	3 x 10^6	N/A
Fluorosave	EMD Millipore Billerica Massachusetts, USA	34578920ML	N/A	N/A

IL-8 (human), Duo ELISA kit	R & D Systems Minneapolis, MN, USA	DY208	N/A	N/A
Lipopolysaccharide (LPS)	Sigma-Aldrich	L4005	N/A	N/A
MyD88 inhibitor	Novus Biologics, Littleton, CO, USA	NBP2-29328	100 μM	N/A
NOD2 shRNA (h) Lentiviral Particles	Santa Cruz Biotechnology	sc-43937-V	1×10^5 particles	N/A
NOD2 siRNA	Santa Cruz Biotechnology	sc-43937-V	120-240 pM	N/A
scramble siRNA	Santa Cruz Biotechnology Inc	sc-4420	120-240 pM	N/A
TNFα Human (Tumor necrosis factor alpha)	Cederlane, Burlington, ON, Canada,	CL103	40 ng/ml	(231)
U0126	Sigma-Aldrich	U0126	25 μM	(118)

2.1 Cell lines, Bacteria and Reagents

2.1.1 Cell Culture

The immortalized T84 cell line was obtained as a gift from Dr. Kim E. Barret (UC San Diego) and was maintained according to guidelines provided by ATCC (American Type Culture Condition). T84 medium was prepared in 1:1 Dulbecco's modified Eagle's Medium/Ham's F-12 medium (Sigma-Aldrich, Canada) supplemented with penicillin-streptomycin (2%), 1.5% HEPES, 1.9% $NaHCO_3$, 1.2 mM L-glutamine, 1mM sodium pyruvate (Sigma-Aldrich) and 10% fetal bovine serum (FBS: PAA Laboratories, VWR International, Edmonton, AB, Canada). T84 cells are colon cancer-derived, crypt-like epithelial cells.(236) Cells were grown in T75/T175 flasks in 25 ml/35 ml T84 medium at 37^0C and 5% CO_2 and medium was changed every 2-3 days. Once the cells had grown to confluence (~5-6 days) the cells were passaged by adding 8-12 ml Trypsin-EDTA (0.25% from Life Technologies, Carlsbad, California, USA) into the flask and incubating at 37^0 C for ~40 min. Once the cells lift from the flask surface, the trypsin was neutralized by adding 12-15 ml of T84 medium, and the cells were dissociated into single cell suspension by gentle pipetting up and down. Then cells were transferred into a 50 ml falcon tube and were centrifuged at 372 x g at 4^0 C for 5 min. After centrifugation, the supernatant was discarded and cells were re-suspended in 10-15 ml medium and cell viability assessed through Trypan blue exclusion (Sigma–Aldrich), and 0.5 x 10^6 cells/well for 12-well plate or 1 x 10^6 cells/well for 6-well plate were seeded. Once the cells reached ~70% confluency (assessed by phase contrast microscopy) the desired treatment was applied.

To grow the cells on the transwells, 1 x 10^6 cells/ml were seeded on each transwell filter support of pore size 3.0 μm (Costar Inc., Cambridge, MA) while 1.5 ml of medium was added to the basolateral side of the well. Cells were allowed to grow, changing the medium every 2-3 days

until the transepithelial resistance (TER) was ≥ 750Ω/cm^2 and at this point the desired experiment was performed.(118) The T84 cells used in the experiments were from passages 60-100.

Another human cancerous colonic epithelial cell line, HT-29 (ATCC, Manassa, VA) was grown in T75/T175 flasks in HT-29 medium at 37^0 C at 5% CO_2. Culture medium was changed every 2-3 days and the cells were passaged once a week. To prepare HT-29 medium: DMEM medium was supplemented with 5% FBS, 1% pencillin-streptomycin, 0.1% L-glutamine and 0.5% sodium bicarbonate. One million HT-29 cells were seeded on a 6-well plate and once the cells attained ~70% confluency the desired experiment was performed.

The IEC-6 (rat non-transformed small intestinal epithelial cells) cell line was obtained from ATCC, and was maintained in DMEM medium supplemented with 2 mM L-glutamine, 0.1 IU/ml insulin and 5% FBS in a T75/T175 flask and culture medium was changed every 2-3 days. Once confluent, the cells were trypsinized and 1 x 10^6 cells/well were seeded into a 6-well plate. Once the cells were ~70% confluent they were considered suitable for experimentation.

The THP-1 cell line is a human monocytic cell line derived from a one year old male leukemia patient.(237) This cell line was obtained from ATCC, and was maintained in RPMI-1640 medium (Sigma-Aldrich) supplemented with 10% FBS and 2% pencillin-streptomycin and 36 μM HEPES at 37^0 C and 5% CO_2 (THP-1medium). The THP-1 cells (2.5 x 10^5 cells/well) were seeded in a 12-well plate. To induce the differentiation of THP-1 cells into a macrophage–like phenotype they were treated with 0.1 μM phorbol-12-myristate-13-acetate (PMA; Sigma-Aldrich) for 3 days and then medium was replaced with fresh THP-1 medium and the cells allowed to rest two more days before any treatment. The resulting differentiated cells were called monocyte–derived macrophages.

2.1.2 Bacterial Preparation

Escherichia coli strains HB101 and F18 were obtained from Dr. Philip Sherman, University of Toronto, Toronto, ON and used in all experiments. *Escherichia coli* HB101 (*E. coli* HB101) is a gram-negative, rod shaped bacteria. This is a common laboratory strain which is the hybrid of *E. coli* K12 and *E. coli* B and is resistant to streptomycin. It is a noninvasive, nonpathogenic strain that has a rapid growth rate, doubling every 20-30 min. *Escherichia coli* F18 (*E. coli* F18) is a human fecal commensal strain. *E. coli* HB101 and *E. coli* F18 were cultured by streaking on Luria Bertani (LB) (EMD Chemicals Inc, Massachusetts, USA) agar plates and a single colony was picked and inoculated in 10 ml of LB broth (BD Biosciences, Missisauga, ON) in a 50 ml tube and was grown at 37^0C for 15 hrs in an orbital shaker incubator (Forma Scientific, Marietta, OH, USA). After that, broth was centrifuged at 1258 x g for 20 min and the supernatant was discarded. The bacteria were re-suspended in 10 ml of antibiotic free T84 medium and optical density (138) of the bacteria suspension and the antibiotic free T84 medium (blank) was measured at 595 nm using a Victor3V spectrophotometer (PerkinElmer, Waltham, MA). Measurement of optical density (OD) was used to determine the bacterial count and 1.0 OD unit was equal to 1 x 10^{10} colony forming units (cfu). In our laboratory, this method is validated every 4 months by growing the particular OD bacterial suspension dilutions on agar plates at 37^0C for 24 hrs. After that bacterial colonies are counted and cfu is determined. Finally, the bacteria were diluted in T84 medium to 1 x 10^6 colony cfu/ml.

2.1.3 Metabolic Stressor

In this study, 2,4-dinitrophenol (DNP: Sigma-Aldrich) was utilized as the metabolic stressor. A 10 mM DNP solution was prepared by performing a 1:10 dilution of a 100 mM DNP solution (made with the addition of 0.1841 g DNP into 10 ml of 100% ethanol) into 70% ethanol.

Further adding 10 µl of the 10 mM solution into 1 ml of media resulted in a 0.1 mM DNP concentration.(118) Additionally, the nonsteroidal anti-inflammatory drug (NSAID), indomethacin (1 µM; Sigma-Aldrich) was also used as a metabolic stressor.(138)

2.2 MTT Assay

The 3-(4,5-dimethyl-thiazol-2-yl)-2,5-diphenyltetrazoliumbromide salt (MTT: Sigma Aldrich) assay was used to examine mitochondrial activity. The T84 cells ($1x10^5$ cells/well) were seeded into a 96 well plate and cultured for 48 hrs. Then cells were exposed for 16 hrs to DNP (0.1 mM). After that cells were washed with phenol-free RMPI medium, supplemented with 10% FBS and 36 µM HEPES and 100 µl of MTT (0.5 mg/ml) was added to each well. Cells were incubated for 4 hrs at 37^0C. Afterwards the MTT reagent was carefully removed and 50 µl acidic isopropanol (0.04N HCL in absolute isopropanol) was added into each well to dissolve the purple formazan crystals formed by the reduction of MTT. Absorbance was then measured at 595 nm using the Wallac 1420 Victor2 spectrophotometer. Data are presented as OD units.

2.3 Measurement of Transepithelial Resistance (TER) and *E. coli* Translocation

Paracellular permeability was measured by assessing TER across filter-grown epithelial cell monolayers. One million cells were seeded into a semi-permeable-transwell-support filters (pore size 3.0 µm, Costar Inc) and TER was measured using an external voltmeter connected to chop-stick electrodes (Millicell-ERS; Millipore, Bedford, MA). Once the TER reached a consistent TER $\geq$ 750 Ω/cm^2 (typically $\geq$1000 Ω/cm^2) the monolayer was treated apically with DNP (0.1 mM) ± *E. coli* HB101 (1×10^6 cfu/ml) for 16 hrs in antibiotic free medium. TER was recorded before the experiment began and 16 hrs post-treatment, and data expressed as a percentage of pretreatment TER values using the formula:

$$\Delta \text{ TER} = \frac{(T_2 - T_1)}{T_1} \times 100\%$$

Where T_2 is TER after treatment, T_1 is TER before treatment

Bacterial translocation was assessed in parallel to TER measurement. To measure bacterial translocation 10 µl of basolateral medium was collected 16 hrs post-treatment. Quantification of translocated bacteria was done by serial dilution in PBS and culture on LB-agar plates at 37^0 for 24 hrs.(118) To measure the flux of FITC-dextran (4 kDa, Sigma-Aldrich) 100 µg/ml was added to the apical surface of the epithelial monolayer in a transwell ± DNP, samples (100 µl) were collected from the basolateral compartment 6 hrs later and fluorescence measured on a Wallac 1420 Victor2 spectrophotometer. Data are presented as arbitrary units.(223)

2.4 Bacterial Internalization

Gentamycin Assay:

T84 cells were grown in 6 or 12 well plates and once they reached ~ 70% confluency were treated with *E. coli* HB101 (1 x 10^6 cfu/ml) or *E. coli* F18 (1 x 10^6 cfu/ml) ± DNP (0.1 mM) for 16 hrs at 37^0C. After treatment, samples of the media (from each set up) were taken and log-fold serial dilutions were performed. Two aliquots of 10 µl from the lowest dilution of each sample were taken and plated onto LB agar plates and incubated overnight at 37^0C/5% CO_2. T84 monolayers were then washed thrice, with sterile room temperature phosphate buffered saline (PBS) and treated with gentamicin (200 µg/ml), diluted in T84 media for 1 hr. To confirm that extracellular bacteria were killed after gentamycin treatment, 10 µl of gentamycin containing medium was taken from 3 randomly selected samples and then plated on agar plates and incubated at 37^0C/5% CO_2 for ~24 hrs. Appearance of any bacterial colonies means extracellular

bacteria were not killed with gentamycin and the experiment would have been deemed as unsuccessful. This never occurred.

To quantify intracellular bacteria, epithelia were twice rinsed again with sterile PBS and lysed with 1.0 ml of 0.1% Triton-X-100/PBS (2 hrs at 4^0C). A log-fold dilution was made from lysed cell samples, from which 10 µl of each were pipetted onto LB agar plates and incubated overnight (37^0C and 5% CO_2) and the number of bacterial colonies counted. Number of intracellular bacteria (colony forming units, cfu) was then determined using the formula:

$$\text{Intracellular cfu/ml} = (\text{number of colonies} \times \text{dilution factor}) \times \frac{\text{volume of Triton X-100 used to lyse the cells}}{\text{volume of cell lysate plated}}$$

The percent internalization was calculated by dividing the absolute number of intracellular bacteria by the absolute number of extracellular bacteria from the same culture well and multiplying the result by 100.(118, 158)

2.5 Fluorescence activated cell sorting (FACS)

FITC-conjugated latex beads (1 µm) and FITC-labeled heat killed *E. coli* (K 12) particles were obtained from Molecular Probes (Eugene, OR). T84 cells were seeded in a 6 well plate. After cells reached ~70% confluency, they were treated with *E. coli* (K-12) particles or FITC-conjugated beads (3 x10^6 beads or particles/ml) ± DNP (0.1 mM) for 16 hrs. Afterwards, cells were rinsed three times with sterile PBS. One ml of 0.4% trypan blue (Sigma) was added into each well for 3 min, to quench extracellular fluorescence, and then the cells were rinsed again thrice with PBS. Next, cells were trypsinized and 10^6 cells were taken per sample and put into flow tubes with 1 ml of flow buffer. Cells were centrifuged at 372 x g for 5 min, and the supernatant was discarded. Fixed perm buffer (Biolegend, London, UK), diluted to 1:3 ratio with

PBS was added to the pellets and incubated for 20 min in the dark at room temperature. Cells were then centrifuged (372 x g, 5 min) and the supernatant was discarded. Cells were further washed with flow buffer, as described previously, three more times. Finally, cells were suspended in 0.5 flow buffer and run through the FACS machine (BD FACS Canto 2, San Jose, CA) and gated for the single cell population that were FITC positive. Data are presented as % positive cells.

2.6 Real time PCR:

Extraction of RNA:

T84 cells (0.5 x 10^6 cells/ well) were seeded into a 12-well plate. Once the cells were ~70% confluent RNA was extracted from untreated T84 cell monolayers or those treated for 6 hrs with *E. coli* (1 x 10^6 cfu/ml) ± DNP (0.1 mM) using the guanidinium thiocynate-phenol-chloroform extraction method with TRIzol® reagent as described by Chomczynski *et al*.(238) After treatment the cells were washed twice with 4^0 C PBS and TRIzol® reagent (500 µl/well) was added into the 12-well plate. Cells were pipetted up and down several times to promote cell lysis and then allowed to sit at room temperature for 5 min for nucleoprotein complexes to be dissociated. Subsequently the samples were transferred to a RNAse / DNAse free 1.5 ml tube and 200 µl of chloroform (EMD Millipore) was added to each tube. Tubes were hand-shaken vigorously for 15 sec or until the solution turned pink. Following incubation of 3 min at room temperature samples were centrifuged at 12,000 x g for 15 min at 4^0 C. After centrifugation, the solution was separated into 3 distinct phases. The top clear phase contains RNA while the middle interphase contains DNA and the lower red phase holds lipids and proteins. The top RNA containing phase was carefully transferred by avoiding contamination with the middle DNA containing interphase into a new RNAse / DNAse free 1.5

ml tube. To precipitate the RNA, 500 µl of isopropanol (EMD Millipore) was added and tubes were allowed to sit at room temperature for 10 min and subsequently centrifuged at 12,000 x g for 10 min at 4^0 C. After pouring off the supernatant, 1 ml of 75% ethanol (EtOH) was added to the pellet, vortexed and centrifuged at 7,600 x g for 5 min at 4^0 C. After removing the supernatant, the pellets were allowed to dry by inverting tubes for 15 min at room temperature, 20 µl of nuclease free water was then added and the samples were heated to 60^0 C for 15 min to solubilize the samples. Quantification of RNA in 1 µl of sample was done by using the NanoDrop 1000 Spectrometer (Thermo Fisher, Wilmington, DE). The measurement of RNA by NanoDrop is done by measuring the absorbance of all the molecules in the sample at the particular wavelength. The quality of samples was assessed by measuring the ratio of absorbance (abs) at 260 and at 280 nm (A260/A280). The ratio of abs A260/A280 > 1.8 is considered as acceptable for RNA.(238)

Generation of complementary deoxyribonucleic acid (cDNA):

Complementary deoxyribonucleic acid (cDNA) from the isolated RNA samples was generated by using the iScript™ cDNA synthesis kit (Bio-Rad, Hercules, CA, USA). One microgram of cDNA per sample was calculated and the volume make up to a maximum volume of 15 µl with PCR-grade H_2O and 4 µl of iScript (containing dNTPs (deoxyribonucleotides), RNAse inhibitor, oligo(dT) primers having a stretch of thymine residues which anneal to the poly(A) tail of mRNA, random primers of six bases long (hexanucleotides), DTT (dithiothreitol, reduces disulfide bridges between two cysteine residues) and $MgCl_2$), and 1 µl of reverse transcriptase with RNAse H (degrades RNA in RNA-DNA hybrid structure formation). The synthesis of cDNA was done by using the MyCycler thermocycler (Bio-Rad) at 42^0 C for 30 min and 5 min at 85^0C to degrade the reverse transcriptase.

Real Time PCR (RT-PCR):

RT-PCR was used to quantify the specific gene (*NOD2*). Required primers were designed using the Primer-Blast program of National Centre for Biotechnology Information (NCBI) and manufactured by Invitrogen (Table 2). While designing the primers, I ensured that they spanned exon-exon junction in order to reduce false positive amplification of any genomic DNA. The primers were validated by making a serial log dilution of a positive control starting with 1 µl of cDNA to create 4 points, a good R^2 value (1.0 - 0.2) and a single (major) peak in the melting curve was considered acceptable. To perform the real time polymerase chain reaction (PCR) a reaction mixture containing 1 µl of cDNA, 0.1 µM of forward and reverse primers, 1x iQ™ SYBER® Green Supermix (BioRad) which contains Taq Polymerase and dNTPs were prepared for each sample and the samples were loaded in duplicate in a 96–well twin-tec PCR plate and loaded on a Mastercycler® Realplex (Eppendrof) real-time PCR machine with the following program settings: 5 min at 95^0C; followed by 40 cycles of 3 sec denaturation at 95^0C, 5 sec annealing at 59^0C and 10 sec extension at 72^0C; and 5 min at 72^0C. Resulting RNA expression was normalized to 18S rRNA (housekeeping gene) expression by the $2^{-\Delta ct}$ method.(239) The following formula was used to calculate the relative gene expression:

$$\text{Relative Gene Expression} = 2^{-(\text{Ct (gene of interest)} - \text{Ct (housekeeping gene)})}$$

Where CT represents the number of cycles required by the fluorescent SYBER green signal to cross the threshold level.(239)

Table 5: List of primers used in the experiment

Gene (Human)	**Forward**	**Reverse**
NOD2	GGGAGCGGGGTTTCGTCAGC	GCTCTGCTGATGGCTCGCACA
18S	ATAGGGCAGACGTTCGAATG	AGATCAAAACCAACCCGGTC

2.7 Transient Transfection of T84 cells with small Interfering (si) RNA

To knock-down the expression of NOD2, siRNAs targeting NOD2 and scramble siRNA were obtained from Santa Cruz Biotechnology Inc (sc-43937-V, sc-4420). Transfection was performed by either using the transfection reagent Lipofectamine (Invitrogen) or through electroporation using the Nucleofactor (Lonza, Cologne, Germany) according to the manufacturer's protocol. Briefly, 6 µl of Lipofectamine was added to 300 µl of Opti-MEM medium (Life Technologies) in a 1.5 ml eppendorf tube. In a second tube, siRNA (120 or 240 pmol) was added to the transfection medium Opti-MEM. The diluted siRNA was then added to the Lipofectamine and incubated for 20 min at room temperature. Following the same procedure the diluted scramble siRNA was also added to the Lipofectamine and incubated for 20 min at room temperature. After 20 min the solution was added to a T84 ($1x10^6$ cells/ml) culture suspension in antibiotic free, 10% FBS containing T84 medium. The cells were seeded into 6 or 12 well plates and after overnight incubation at 37^0 C the medium was changed to antibiotic containing T84 medium. Forty-eight hrs later the desired treatment was done on the polarized monolayer. For electroporation, 100 µl of cell suspension (containing $1x10^6$ T84 cells) in Opti-MEM was placed in a Nucleofactor cuvette and siRNA (120 or 240 pmol) added. The cuvette

was then inserted in the Nucleofactor cuvette holder and Program-T-005 was selected. Once the program was finished the cuvette was removed and 500 µl of 37^0C antibiotic free T84 medium was added. Carefully the content of cuvette was transferred to a 6 well plate already having 1 ml of 37^0C antibiotic free T84 medium. The plates were incubated at 37^0C overnight and the next day medium was changed to antibiotic containing T84 medium and after 48 hours the desired treatment was done on the polarized monolayer. Transfection efficiency was confirmed by BLOCK-iT fluorescent oligo (catalog number: 2013, Thermo Fisher Scientific) according to manufacturer's protocol. Approximately ~75% of cells emitted a strong fluorescence signal up to 48 hrs after transfection as observed under the microscope. Knock-down of NOD2 was confirmed through immunoblot. (see below)

2.8 Development of a Stable NOD2 knock-down (NOD2 KD) T84 Cell line

Stable knock-down of NOD2 was performed using NOD2 shRNA (h) (NOD2 shRNA (h) Lentiviral Particles, sc-43937-V) and GFP control lentiviral particles (copGFP Control Lentiviral Particles sc-108084), transfection reagent Polybrene (sc-134220) and puromycin dihydrochloride (sc-108071) from Santa Cruz Biotechnology, Santa Cruz, CA, USA. Approximately 1 x 10^5 NOD2 or Control GFP shRNA(h) lentiviral particles in polybrene/opti-MEM (5 µg/ml) (Invitrogen) were added to a cell culture suspension of T84 cells (1 x 10^4 cells/ml) in 10% FBS containing antibiotic-free culture medium. Cells were then seeded into a 12 well culture plate. After incubation overnight at 37^0C, the medium was changed to antibiotic-containing T84 cell culture medium with added puromycin (2.5 µg/ml). The puromycin containing T84 medium was changed every third day (1 ml/well). Finally, puromycin resistant colonies were seeded in a 75 ml tissue culture flask. Knock-down of NOD2 was confirmed by immunoblot.

2.9 Western Blotting

Protein Extraction:

T84 cells (1x $1x10^6$) were grown in 6 well-plates and once the cells reached ~70% confluency they were treated with DNP (0.1 mM) ± *E. coli* HB101 (1 x 10^6 cfu/ml), and or mitoTEMPO (10 μM: Santa Cruz Biotechnology), U0126 (25 μM: Sigma-Aldrich) or muramyl di-peptide (MDP: 1-2 μg/ml Invitrogen) for the specified period of time. THP-1 cell-derived macrophages (2.5 x 10^5 cells/well) were treated with *E. coli* HB101 (1 x 10^6 cfu/ml) for 5 hrs to prepare a positive control sample. After treatment, cells were washed three times with 4^0 C PBS and 200 μl of Triton X-100 protein lysis buffer (50 mM Tris-HCl (pH 8.5),150 mM NaCl, 1% Triton-X 100 (Sigma), 25x protease inhibitor cocktail (Roche Molecular Diagnostics, Pleasanton, CA, USA)) was added into each well, and 10 min later the cells were scraped off and samples collected in a 1.5 ml tube and frozen at -80^0 C for 1 hr. Samples were removed from the freezer and thawed on ice and sonicated for 10 sec (Microson™ Ultrasonic Cell Disrupter, SPI supplies, West Chester, PA). After sonication samples were centrifuged at 12,000 x g for 5 min and the supernatant was transferred to new 1.5 ml eppendorf tubes and stored at -80^0 C.

Protein Quantification:

Measurement of protein concentration in samples was done using the Bradford method.(240) Briefly, samples were diluted 1:10 in double distilled water (ddH_2O) and 10 μl from each diluted sample was loaded in duplicate to a 96 well plate. A standard curve was prepared using the known concentration of the protein bovine serum albumin (BSA: New England BioLabs), via making the serial dilution (0-500 mg/ml), and loading 10 μl from each dilution in duplicate to the 96 well. Then 200 μl of 1:4 (Coomassie brilliant blue-G250 (BioRad):ddH_2O) solution was added to each well and incubated for 5 min at room temperature.

During incubation the coomassie blue dye interacts with basic and aromatic groups of amino acids present in the protein leading to the formation of a blue protein-dye complex. The intensity of the color depends on the protein concentration present in the sample. Finally, the absorbance was read at 595 nm on a Wallac 1420 Victor2 spectrophotometer and protein concentration determined.

Gel Electrophoresis for Proteins and Transfer:

Twenty-five micrograms of protein from each sample were added to the 4x Lamelli buffer (8% sodium dodecyl sulfate (SDS), 20% β-mercaptoethanol, 40% glycerol and 0.008% bromophenol blue and 250mM Tris-HCl all obtained from Sigma-Aldrich). The volume of each sample was made equal by adding ddH_2O. Samples were then placed into a boiling water bath for 10 min to denature the proteins. The denatured protein samples were then loaded in SDS-polyacrylamide gel (8%, 10% or 12%) and run at 100-115 V in SDS running buffer (25 mM Tris, 0.1% SDS, 192 mM glycine), until the bromophenol blue dye reached the bottom of the gel (approximately 2-2.5 hrs). The separated proteins on the gel were then transferred to a polyvinylidene difluoride membrane (PVDF) or nitrocellulose membrane (both from VWR, Mississauga, Ontario, Canada) in transfer buffer (20% methanol, 2.5 mM Tris, 19.2 mM glycine) at 4^0 C overnight at 30 V. After that, the membranes were washed with Tris buffered saline-0.1% Tween 20 (TBST).(223)

Blocking, Antibody Staining and Detection:

The membranes were then blocked with 5% non-fat Carnation™ powdered milk prepared in TBST or 5% BSA-TBST (for detection of phospho-proteins) for 1 hr at room temperature to reduce the non-specific binding of detection antibodies in the following steps. After the blocking step, the membranes were incubated with the primary antibodies overnight in 5% BSA-TBST at

4^0 C. A list of primary and secondary antibodies used in the experiments is given in Table 6. Following incubation the membranes were washed 3 times for 5 min in TBST on an orbital shaker. Based on primary antibody specificity, the appropriate secondary antibody (goat anti-rabbit or goat anti-mouse antibodies (1:5000; Santa Cruz-Biotech.)) was applied to membranes for 1 hr at room temperature. After that blots were washed (3x for 5 min) in TBST and once in PBS on an orbital shaker. Blots were processed by chemiluminescence (Western lighting PLUS, PerkinElmer, Waltham, MA) and then exposed to either Kodak XB-1film (Eastman Kodak, Rochester, NY) or MicroChemi (DNR Bio-Imaging System Ltd., Israel). Finally, the membranes were stripped using stripping buffer (0.76 g Tris, 2 g SDS, 700 µl 2-mercaptoethanol, 100 ml dH_2O, pH 7.4) and the membrane blocked again and blotted for Beta actin (1:1000, Santa, Cruz Biotechnology) as a loading control.

Table 6: List of primary and secondary antibodies used for immunoblotting experiments

Antibody	Protein	Specificity	Dilution	Catalogue No, Source
Primary	NOD2	Mouse, human, rat	1:500	sc-30199, Santa Cruz Biotech
Primary	Phospho ERK 1/2	Mouse, human, rat	1:1000	9106S, Cell Signaling
Primary	LC3	Mouse, human, rat	1:500	NB 100-2220, Novus Biologicals
Primary	Caspase -3	Mouse, human, rat	1:1000	9662, Cell signaling
Primary	Cleaved Caspase-3	Mouse, human, rat	1:1000	9661S, Cell signaling
Primary	Beta actin	Mouse, human, rat	1:1000	Sc-1616, Santa Cruz Biotech
Secondary	Goat anti-rabbit IgG-HRP		1:5000	sc-2030, Santa Cruz Biotech
Secondary	Goat anti-mouse IgG-HRP		1:5000	sc-2031Santa Cruz Biotech

2.10 Organoid Culture:

NOD2$^{-/-}$ and wild type (WT) mice were purchased from Jackson Laboratories (Sacramento, CA, USA). Mice were kept in an approved housing facility at University of Calgary Health Science Animal Research Centre (HSARC) under specific-pathogen free conditions and were given unrestricted access to food and water. The experiment was performed following Canadian and Institutional guidelines for animal welfare, administered by the University of Calgary Animal Research and Education Executive Committee (Animal Protocol AC 13-0015).

Colonic crypt isolation from NOD2$^{-/-}$ and WT mice was performed according to the protocol described by Yui *et al*.(241) Briefly, colon was removed from NOD2$^{-/-}$ and WT mice after euthanizing the mice with CO_2 asphyxiation followed by cervical dislocation. The removed colon was then transferred into 50 ml tube with 30 ml PBS and placed on ice. Later the colon was transferred into a Petri dish with 4^0 C cold PBS. After removing the fat, the colon was cut longitudinally and washed in PBS twice. Using scissors the colon was cut into small pieces (~2 mm) and transferred into a 50 ml tube with 20 ml PBS. All the pipettes used in the experiment were coated with PBS (with 2% FBS) to avoid tissues getting stuck inside the pipette. After shaking the tubes by hand for 30 sec the tubes were centrifuged for 30 sec at 290 x g, and the PBS pipetted off. This process was repeated 3-6 times until the solution became clear. After the last washing, 30 ml of ice cold crypt isolation buffer (2 mM EDTA in PBS + 43.4 mM sucrose + 0.5 mM DTT) was added into the tube and was incubated at 4^0 C for 30 min. After incubation the tube was centrifuged at 290 x g, for 30 sec and supernatant was discarded. After that 10 ml of 4^0 C PBS was added into the tube and the solution was pipetted six times keeping the pipette tip at the bottom to dislodge the cells. Once the pieces were settled at the bottom the supernatant was removed and put in a tube marked A on ice, this is the first fraction. The same process was

repeated one more time and the supernatant was collected again into tube A. Tube A is a backup tube, which is used in case we couldn't find a pellet in the subsequent fraction. Again 10 ml of cold PBS was added and pipetted 6 times and supernatant was collected in the second tube marked B and placed on the ice. The process was repeated 5 more times by collecting the fractions (3-7) into tube B. After that tube B was centrifuged at 200 x g at 4^0 C for 5 min and supernatant was removed. The pellet was re-suspended in 10 ml PBS by shaking and the solution was passed through a 100 µm strainer pre-coated with PBS, and the liquid was collected into a new tube. The liquid was again centrifuged at 290 x g at 4^0 C for 5 min and the supernatant was removed through aspiration. The pellet was re-suspended in 1ml pre-warmed TrypLE and incubated at 37^0 C for 10 min in a 50 ml falcon tube. Then tubes were placed on ice and re-suspended in 10 ml 4^0 C ADF (advanced DMEM/F12) and were centrifuged at 290 x g for 5 min at 4^0 C to separate out crypts from the single cells, later supernatant was removed carefully through pipetting.

Matrigel (a reconstituted basement membrane preparation obtained from the Engelbreth-Holm-Swarm mouse sarcoma) was thawed at 4^0 C for 2 hrs before use. The isolated crypts were re-suspended in the matrigel (30 µl/well at ~200-500 crypts/well) using the pipette tip pre-chilled by pipetting 4^0 C PBS up and down. After that 30 µl of matrigel was carefully transferred to the centre of each well in a pre-warmed (37^0 C) 24 well plate. Following transfer of matrigel, the plate was incubated at 37^0 C for 30 min by keeping the plate upside down to facilitate the solidification of the matrigel. Next the plates were removed from the incubator and 500 µl of IntestiCult^{TM} organoid growth medium (15-25^0 C) was added to the side of each well. After putting the lid on the culture plate, the plates were incubated at 37^0 C and 5% CO_2. The culture medium was changed every 2-3 days by removing the existing medium and changing to fresh

500 µl (37^0 C IntestiCult™ organoid growth medium).

After 7 days 3D organoid cultures were ready to be seeded on the transwell filters (3 µm). Preparation for the transwells was done as follows: transwells were coated with 200 µl of 1:30 ratio of matrigel:ADF and incubated at 37^0 C for 2 hrs prior to use. The 1:30 mixture of matrigel:ADF was carefully aspirated and 200 µl of 37^0 C warm ADF was added into each well and kept at 37^0 C in the incubator and left there until the cell suspension was ready to be added onto the transwell. To break the matrigel, culture medium was carefully aspirated from each well and 1 ml of 4^0 C cold ADF was added to each dome. Using the pre-wet 1000 µl tip with PBS, the dome was pipetted vigorously to mechanically break the matrigel. Two 50 ml falcon tubes were taken and 4.5 ml of trypsin-EDTA (0.25% trypsin and 0.5mM EDTA in PBS) was added in each tube. After breaking the matrigel the content of 6 matrigels was transferred to each tube. After that both the tubes were incubated at 37^0 C for 10 min. Later 10 ml of cold ADF was added to inactivate the trypsin and both the tubes were centrifuged at 290 x g, for 5 min. After that, supernatant was removed through careful aspiration leaving ~500 µl of solution on the pellet which was re-suspended by adding 1.2 ml of 37^0 C IntestiCult™ organoid growth medium. The suspensions from both the tubes were pooled together in one tube and re-suspended by adding extra 1 ml of 37^0 C IntestiCult™ organoid growth medium. Then ADF was removed from the transwells and 2.5 ml of 37^0 C IntestiCult™ organoid growth medium was added to the basolateral side of each well followed by the addition of 250 µl of organoid suspension to the apical side of each transwells. The plate was incubated at 37^0 C and the culture medium was changed every second day with 37^0 C IntestiCult™ organoid growth medium. After 10 days *E. coli* HB101 was grown in LB broth and *E. coli* HB101 (1×10^7 cfu/ml) ± DNP (0.1 mM) was added to the apical side of the transwells for 16 hrs. After 16 hrs bacterial translocation and

intracellular bacteria (through gentamycin assay) was measured according to the protocol described in section 2.4 and 2.5.

2.11 Measurement of ROS

T84 or NOD2 KD cells ($3x10^4$ cells/well) were plated into a sterile, tissue culture-treated, clear bottom, dark sided, 96-well microplate and allowed to adhere overnight. The next day, media was removed from the wells and the cells washed by loading 100 µl of 1X buffer from the DCFDA kit (ab11385, Abcam Inc, Toronto, ON). After removing the 1X buffer, 100 µl of 25 µM DCFDA (2^1 7^1-dichlorofluorescin diacetate) was loaded and the plate was kept at 37^0 C for 45 min. Afterwards, the DCFDA solution was removed and cells were washed with 100 µl of 1X buffer. Following washing, cells were treated with DNP (0.1 mM) ± *E. coli* (1 x 10^6 cfu/ml) ± mitoTEMPO (10 µM) or 50 µM tert-butyl hydrogen peroxide (TBHP, supplied with the DCFDA kit as a positive control) in DMEM/F-12 phenol free media with 10% FBS for 4 hrs. Then the absorbance was read on a fluorescence plate reader at excitation and emission wavelength of 485 and 535 nm respectively. All the reagents supplied by the manufacturer were diluted to the used concentration according to manufacturer instructions.

2.12 Enzyme Linked Immunosorbent Assay (ELISA)

T84 cells (0.5 or 1 x 10^6 cells) were grown on a 6-well/12-well plate. After the cells reached ~70% confluency they were incubated with U0126 (25 µM), chloroquine (10 µM), cytochlasin D (0.2 µM), and MyD88 inhibitor (100 µM) for 30 min. Then, the T84 monolayers were treated with beads (3 x 10^6 fluorescent beads/ml), fluorescent heat killed *E. coli* (K12) particles (3 x 10^6 particles/ml), DNP (0.1 µM), *E. coli* HB101 (1 x 10^6 cfu/ml), mitoTEMPO (10 µM), TNFα (40 ng/ml) or LPS (10, 20 or 40 ng/ml) for 16 hrs. Supernatant was collected and centrifuged at

12,000 x g for 5 min at 4^0C. Pellets were discarded and the supernatant was stored in the -80^0 C freezer prior to measurement of IL-8 using the Duo ELISA kit (R & D Systems, Minneapolis, MN, USA) according to the manufacturer's protocol. Briefly, 100 µl (diluted to 1:120 in PBS) of primary antibody was loaded on an ELISA plate (Nunc Immuno-96 plates, Thermo Scientific). After that the plate was incubated overnight at room temperature. The next day, the plate was washed 3 times with the wash buffer (PBS + 0.05% Tween-20) and 300 µl of reagent diluent (prepared following the manufacturer's instruction) was added and the plate incubated at room temperature for 1 hr. After washing (3x with wash buffer), standard (31.2-2,000 pg/ml) and samples were loaded in duplicate to the plate. The plate was incubated for 2 hrs at room temperature. After 2 hrs the plate was washed (3x with wash buffer) and incubated with 100 µl of biotin conjugated secondary antibody diluted in reagent diluent (as per manufacturer's instructions) for 2 hrs at room temperature. The plate was washed again (3x with wash buffer) and incubated with 100 µl of streptavidin-HRP in reagent diluent (1:200 dilution) for 20 min at room temperature in the dark. After 20 min, the plate was washed (3x with wash buffer) and 100 µl of TMB (3,3',5,5'tetramethylbenzidine, Sigma) was added to the each well. Once the blue colour was developed (~20 min) the reaction was stopped by the addition of 50 µl of 2N H_2SO_4. The absorbance was read at 450 nm using the Wallac 1420 Victor2 spectrophotometer, and IL-8 in samples calculated from the standard curve.

2.13 Visualization of intracellular *E. coli* or FITC-conjugated latex beads

NOD2KD or WT T84 cells ($3x10^5$) were grown on 12 mm sterile coverslips in a 24-well plate, and treated with DNP (0.1 mM) ± *E. coli* (1 x 10^6 cfu/ml), or DNP (0.1 mM) ± FITC conjugated latex beads (3 x 10^6, Invitrogen) for 16 hrs. After treatment, the coverslips were washed thrice for 5 min on a rocker by adding 250 µl of 4^0 C PBS, fixed with 4%

paraformaldehyde in PBS (15 min at room temperature) and blocked for 1 hr at room temperature in blocking solution (1% BSA + 10% goat serum in PBS). After that cells were permeablized by adding 200 µl of 0.1% Triton X-100 in blocking solution for 15 min at room temperature. Cells were washed gently on a shaker with 4^0 PBS (3x for 5 min). Monolayers treated with beads were treated with trypan blue (0.4%) for 3 min, rinsed and fixed with 4% paraformaldehyde in PBS by incubating for 15 min at room temperature. Monolayers treated with DNP ± *E. coli* were then treated with FITC conjugated anti-*E. coli* antibody (1:200, in PBS, 10% goat serum, 0.1% Tween) (ab30522; Abcam, Toronto, ON, Canada) for 1 h. Afterwards monolayers were washed (3x with PBS, 5 min each on a rocker), and then DAPI (1:500 in PBS; Molecular Probes) was added and the cells were incubated for 5 min at room temperature. Cells were washed (3x with PBS, 5 min each on a rocker), mounted with Fluorosave (EMD Millipore) and allowed to dry and saved at 4^0 C in dark. Slides were then coded and images were captured by epifluorescence microscopy (Olympus BX41microscope, x40 objective) using QCapture software (Olympus Canada, Mississauga, ON, Canada).

2.14 Statistical analysis and data Presentation

Data are presented as the mean ± standard error of the mean (SEM), where n values represent the number of epithelial observations from a specified number of experiments. In the design of these experiments where typically the variable is internalized bacteria, single group comparisons were performed using Student's t-test. For the multiple group comparison the appropriate statistical test was gauged as one-way analysis of variance (one-way ANOVA) followed by pair-wise post-hoc analysis using Tukey's statistics. A statistically significant difference was accepted at $p < 0.05$.

CHAPTER 3 - Results

3.1 **Disclosure**

Figures 9, 11-26 were published in American Journal of Physiology-Gastrointestinal and Liver Physiology and are reproduced under Rights of Authors of APS Articles (Thesis and dissertations): Saxena A, Lopes F, Poon KKH, and McKay DM. Absence of the NOD2 protein renders epithelia more susceptible to barrier dysfunction due to mitochondrial dysfunction. *American journal of physiology Gastrointestinal and liver physiology.* 2017;313(1):G26-g38.(242)

Reproducibility is the cornerstone of science. So, while the data depicted in figures 8 and 9 replicate similar published data from the McKay laboratory (118, 158), it was important to determine that I could replicate these findings that would pave the way to novel mechanistic studies and allow assessment of NOD2 in the established model.

3.2 DNP does not affect bacterial growth but reduces mitochondrial function

To model the mitochondrial dysfunction observed in some patients with IBD, the chemical 2,4-dinitrophenol (DNP; 0.1 mM) was used. DNP, H^+ ionophore, uncouples oxidative phosphorylation and reduces ATP synthesis.(155) At 0.1 mM concentration, DNP does not inhibit bacterial growth; however, 1 mM of DNP kills bacteria as determined by the standard growth curve. (Figure 8a) However, when the colon-cancer derived, crypt-like, T84 cell monolayer was exposed to DNP (0.1 mM) for 16 hrs, mitochondrial function was reduced as gauged by the MTT (3-(4,5-Dimethylthiazol-2-yl)-2,5,-diphenyltetrazolium bromide) assay (n=18 from 3 experiments, *** $p < 0.001$). (Figure 8b) This confirms previous findings of reduced ATP in DNP treated T84 epithelium (158) and swollen mitochondria, as depicted in transmission electron microscopy micrographs.(157)

Pharmacological agents used at the specified concentration for the experiments were neither bacteriotoxic or bacteriostatic over the 16 hrs experimental period. (Figure 8c)

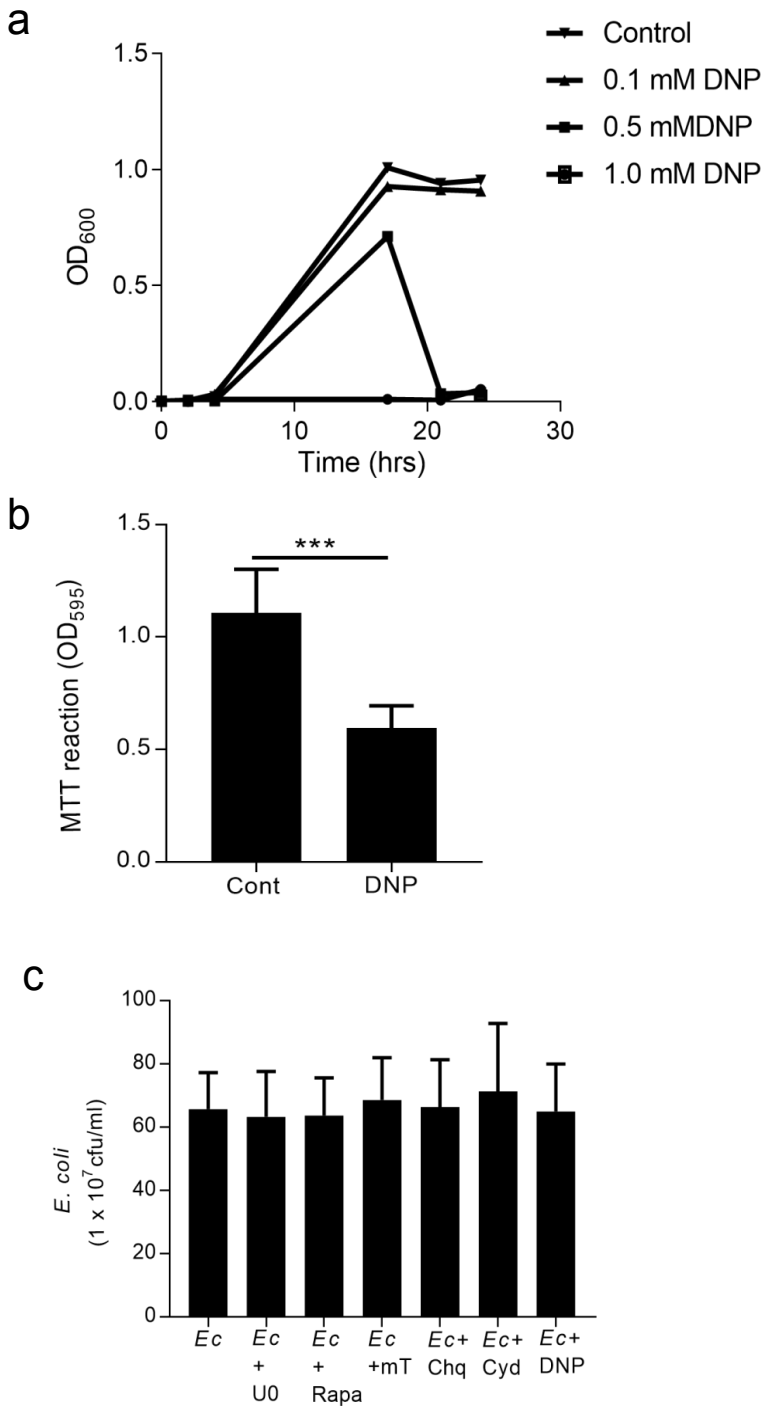
a
Control
0.1 mM DNP
0.5 mMDNP
1.0 mM DNP
OD600
1.5
1.0
0.5
0.0
0
10
20
30
Time (hrs)
b
***
MTT reaction (OD595)
1.5
1.0
0.5
0.0
Cont
DNP
c
E. coli
(1 x 10^7 cfu/ml)
100
80
60
40
20
0
Ec
Ec + U0
Ec + Rapa
Ec +mT
Ec+ Chq
Ec+ Cyd
Ec+ DNP

Figure 8: (a) Representative growth curve of *E. coli* HB101 showing that 0.1 mM concentration of 2,4-dinitrophenol (DNP) does not affect bacterial growth over a 16 hr period, (b) but did significantly reduce mitochondrial function as measured by the MTT assay. (data are mean ± SEM; n=18 from 3 experiments; *** p <0.001). (c) The concentration of pharmacological agents used were neither bacteriotoxic or bacteriostatic over the 16 hr experimental period. T84 monolayers were treated with *E. coli* HB101(1 x 10^6 cfu) ± (DNP; 0.1 mM, U0126; U0 25 μM, rapamycin; Rapa 100 nM, mitoTEMPO; mT 10 μM, chloroquine; Chq 10 μg/ml, cytochalsin D; Cyd 0.25 μM) for 16 hrs. Afterwards 10 μl of outside medium was retrieved and plated on the LB agar and incubated for 24 hrs at 37^0 C and cfu calculated. No significant difference between cfu of *E. coli* treated only and *E. coli* + pharmacological agent were observed (n=9 from 3 experiments).

3.3 Metabolically Stressed Epithelia Display Decreased TER and Greater Translocation and Internalization of *E. coli* HB101

To study the effect of metabolic stress on epithelial barrier function, polarized T84 cells monolayers were exposed to DNP (0.1 mM), *E. coli* HB101 ($1x10^6$ cfu) or both for 16 hrs. Trans-epithelial resistance (TER), was utilized as a measure of tight junction integrity, and hence paracellular permeability. TER values were taken before and after treatment and the percent change from the original values was calculated. Cells treated with DNP alone revealed a small but statistically significant decrease in TER whereas *E. coli* had a more variable impact on TER. However, simultaneous addition of DNP and *E. coli* HB101 consistently reduced TER to 20-40% of pre-treatment values. (Figure 9a)

T84 cell monolayers exposed to DNP + *E. coli* showed ~ 6–fold greater translocation compared to *E. coli* only treated epithelial cells 16 hrs post-treatment. (Figure 9b) Additionally, there were a significantly higher number of internalized viable bacteria in the DNP + *E. coli* co-treated epithelium compared with the epithelium treated with *E. coli* alone. (Figure 9c) The percentage *E. coli* internalization (ratio of number of intracellular bacteria to extracellular bacteria) was also significantly higher in DNP + *E. coli* treated epithelium compared to *E. coli* treated epithelium. (Figure 9d)

These findings were reproduced with the commensal *E. coli* F18 strain (Figure 10) and also replicated with another human epithelial cell line, HT29 (human colorectal adenocarcinoma cell line) as well as the rat small intestine epithelial cell line IEC-6. (Figure 11a-b) None of the treatment groups exhibited increased caspase-3 cleavage, an indicator of apoptosis, 16 hrs post-treatment. (Figure 12) Immunostaining further reveals an increased number of *E. coli* associated with DNP + *E. coli* treated epithelia compared to *E. coli* treated epithelia. (Figure 13)

a

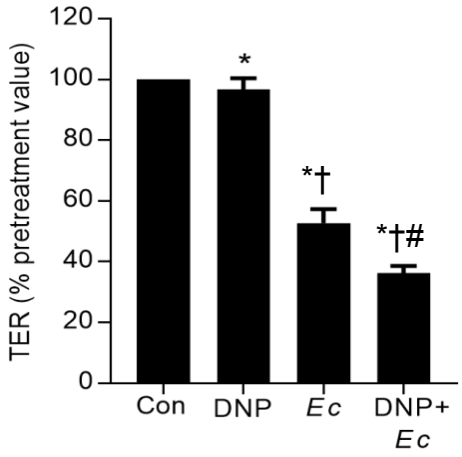
TER (% pretreatment value)
120
100
80
60
40
20
0
*
*†
*†#
Con
DNP
Ec
DNP+ Ec

b

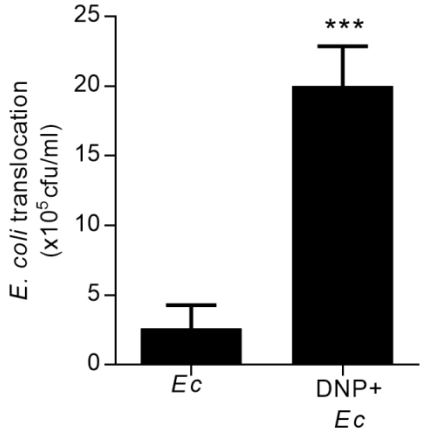
E. coli translocation (x10^5cfu/ml)
25
20
15
10
5
0
***
Ec
DNP+ Ec

c

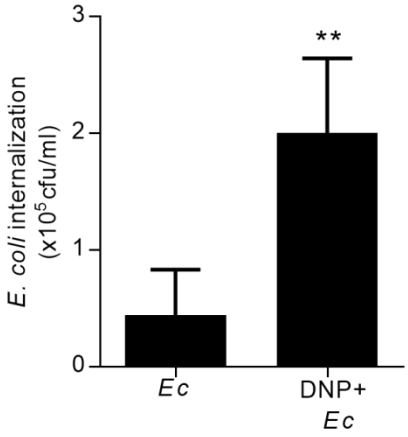
E. coli internalization (x10^5cfu/ml)
3
2
1
0
**
Ec
DNP+ Ec

d

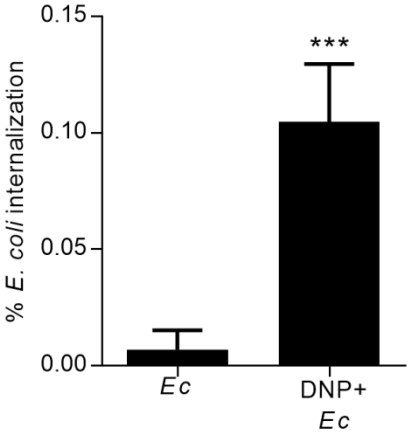
% E. coli internalization
0.15
0.10
0.05
0.00
***
Ec
DNP+ Ec

Figure 9: Mitochondrial dysfunction evoked by DNP (2, 4, dinitrophenol) increases epithelial permeability. Filter grown T84 cells (a-b) were treated with *E. coli* HB101 (*Ec*, 1 x 10^6 cfu/ml) ± DNP (0.1 mM) for 16 hrs and then (a) transepithelial resistance (TER, as pretreatment value) and (b) bacterial translocation was measured (n=9 epithelial monolayers from 3 experiments, data are mean ± SEM; * $p < 0.05$ from control, † $p < 0.005$ from DNP only, # $p < 0.05$ from *E. coli* treated group). Plastic grown T84 cell monolayers were treated with *E. coli* HB101 ± DNP for 16 hrs and then bacteria internalization (c) and % bacterial internalization (d) was measured by the gentamycin assay (n=9 epithelial monolayers from 3 separate experiments, data are mean ± SEM; ** $p < 0.01$ and *** $p < 0.001$).

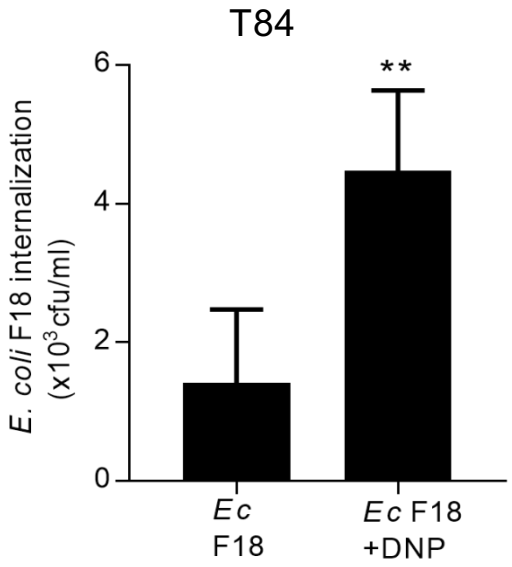

Figure 10: Given that *E. coli* HB101 is a laboratory strain, to add validity findings were reproduced using the commensal strain *E. coli* F18. Plastic grown T84 monolayers were treated with *E. coli* F18 (*Ec* F18, 1 x 10^6 cfu/ml) ± dinitrophenol (DNP, 0.1 mM) for 16 hrs. Bacteria internalization was measured by gentamycin assay (data are mean ± SEM; n=9 monolayers from 3 separate experiments, $^{**}p < 0.005$).

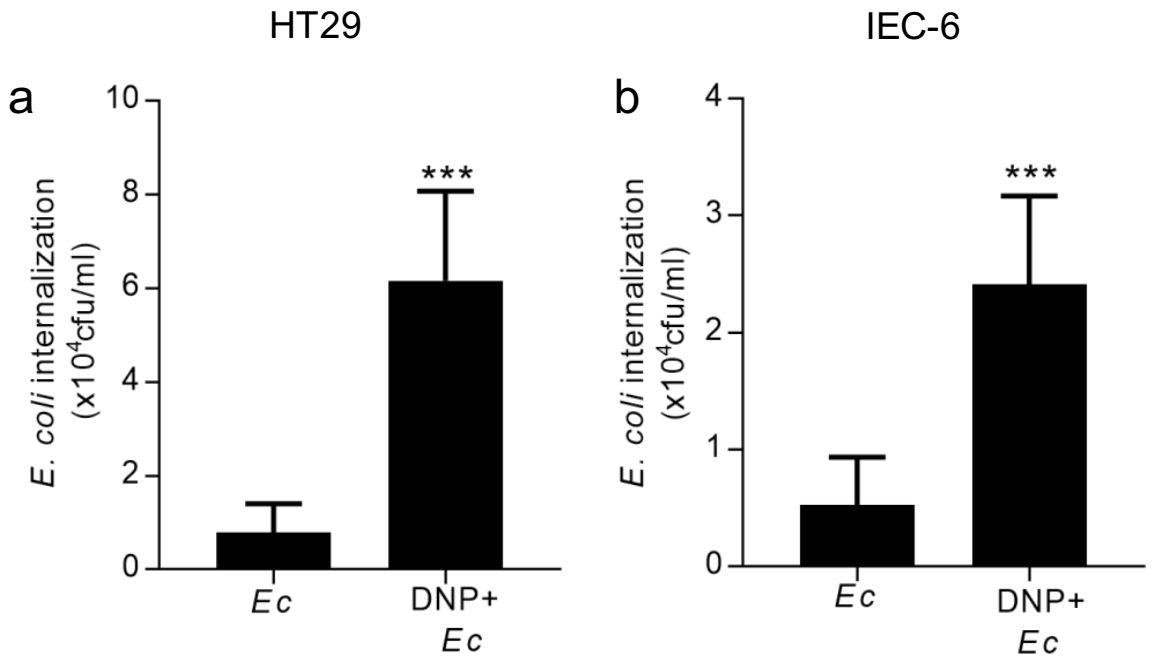

Figure 11: Enhanced bacterial internalization via the metabolic stressor DNP (2, 4, dinitrophenol) is not a cell specific phenomenon. Plastic-grown (a) HT29 (colon cancer cell line) and (b) IEC-6 (non-transformed rat small intestine cell line) were treated with *E. coli* HB101 (*Ec*, 1 x 10^6 cfu/ml) ± dinitrophenol (DNP, 0.1 mM) for 16 hrs and internalized bacteria determined using the gentamycin assay (n=9 monolayers from 3 separate experiments, data are mean ± SEM; ***$p < 0.001$).

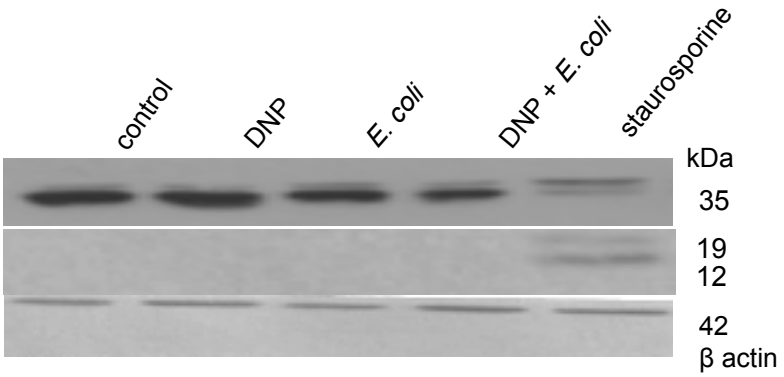

Figure 12: Treatment with *E. coli* (1 x 10^6 cfu/ml) ± dinitrophenol (DNP, 0.1 mM) did not result in increased cleavage of caspase-3 in epithelia. Western blotting of caspase-3 cleavage (12 and 19 kDa) 16 hrs after various treatment of T84 epithelial cells shows no evidence of caspase-3 cleavage. Extract of staurosporine (5 mM for 16 hrs)-treated T84 cell monolayers was used as a positive control. Image representative of 3 experiments.

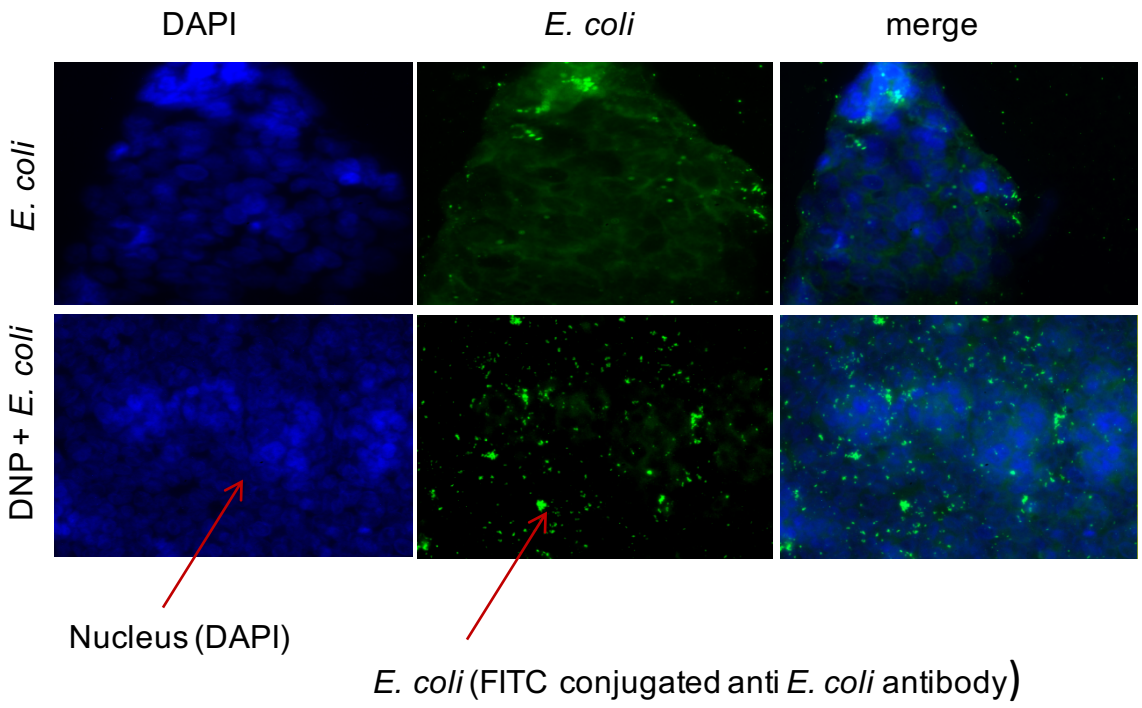

Figure 13: Immunolocalization epifluoresence imaging shows increased numbers of *E. coli* associated with DNP-treated epithelium. T84 cell monolayers were treated with *E. coli* HB101 (1×10^6 cfu) ± DNP (0.1 mM) for 16 hrs. *E. coli* were identified with a FITC-conjugated anti-*E. coli* antibody. Epithelial nuclei were identified with DAPI staining (image is representative of 6 epithelium monolayers from two experiments; original magnification =x20).

3.4 Internalization of commensal *E. coli* in epithelial monolayer increases NOD2 expression

The NOD2 protein coded by the NOD2/Card15 gene is a crucial cytosolic sensor protein responsible for detecting MDP, a product of peptidoglycan present in both gram-positive and gram-negative bacteria. Previous studies have shown that NOD2 is capable of detecting internalized bacteria.(195, 198) However, in transporting enterocytes baseline expression of NOD2 is very low or undetectable.(184) Data from quantitative PCR (qPCR) 6 hrs post-treatment revealed up-regulation of NOD2 mRNA in *E. coli* treated T84 cells, which was significantly increased by DNP co-treatment. (Figure 14a)

To confirm or refute the above findings, T84 epithelia were treated with *E. coli* ± DNP for 6 or 16 hrs. At 6 hrs, NOD2 protein expression was virtually undetectable in T84 cells treated with *E. coli* ± DNP. (Figure 14b) In contrast, at 16 hrs, DNP + *E. coli* treated T84 cells demonstrated significantly higher expression of NOD2 protein compared to *E. coli* treated T84 cells as measured by immunoblot and confirmed by densitometry. (Figure 14c-d)

Additionally, HT29 cells treated with DNP + *E. coli* for 16 hrs also display increased expression of NOD2 compared to HT29 epithelia treated with solely *E. coli* for 16 hrs. (Figure 15a-b).

Immunoblot of T84 epithelia treated with MDP ± DNP (as a positive control) for 24 hrs also display upregulation of NOD2 protein expression. (Figure 16)

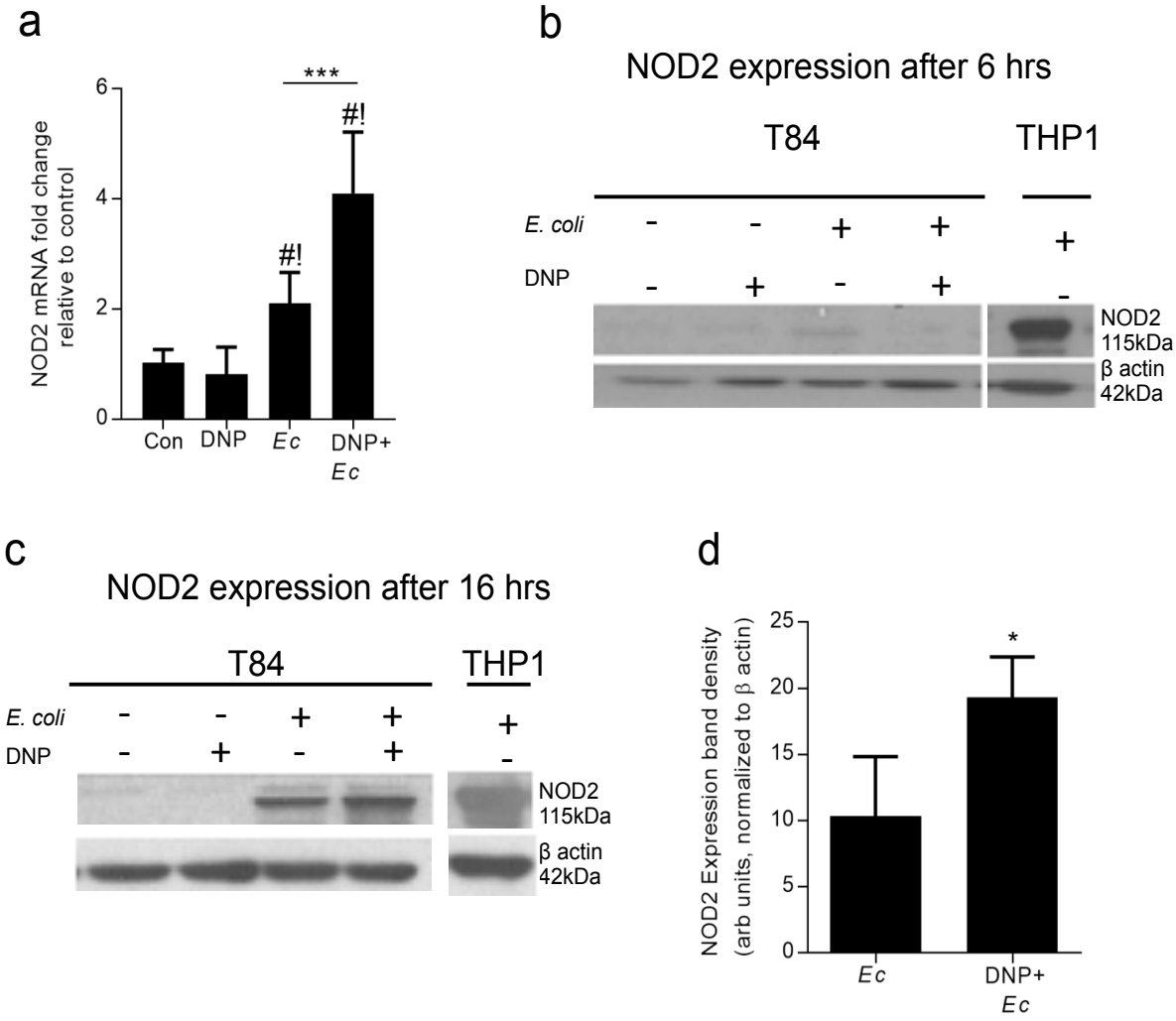

Figure 14: Increased expression of NOD2 in enterocytes exposed to DNP ± *E. coli*. T84 cells treated with *E. coli* HB101(*Ec,* 1 x 10^6 cfu) ± dinitrophenol (DNP: 0.1 mM) shows (a) increase NOD2 mRNA after 6 hrs (data are mean ± SEM; n=9, # p <0.001 from control group, ! p <0.001 from DNP group, ***p <0.0001); NOD2 protein expression was not detectable by western blot after 6 hrs (b). (c) NOD2 protein is significantly increased after 16h of treatment and (d) densitometry analysis of western blots (representative blot of 3 separate experiments n=3, * p <0.05 from *E. coli* group: THP-1 macrophages treated with *E. coli* for 6 hrs used as a positive control, intermediate lanes were cut out in the blots).

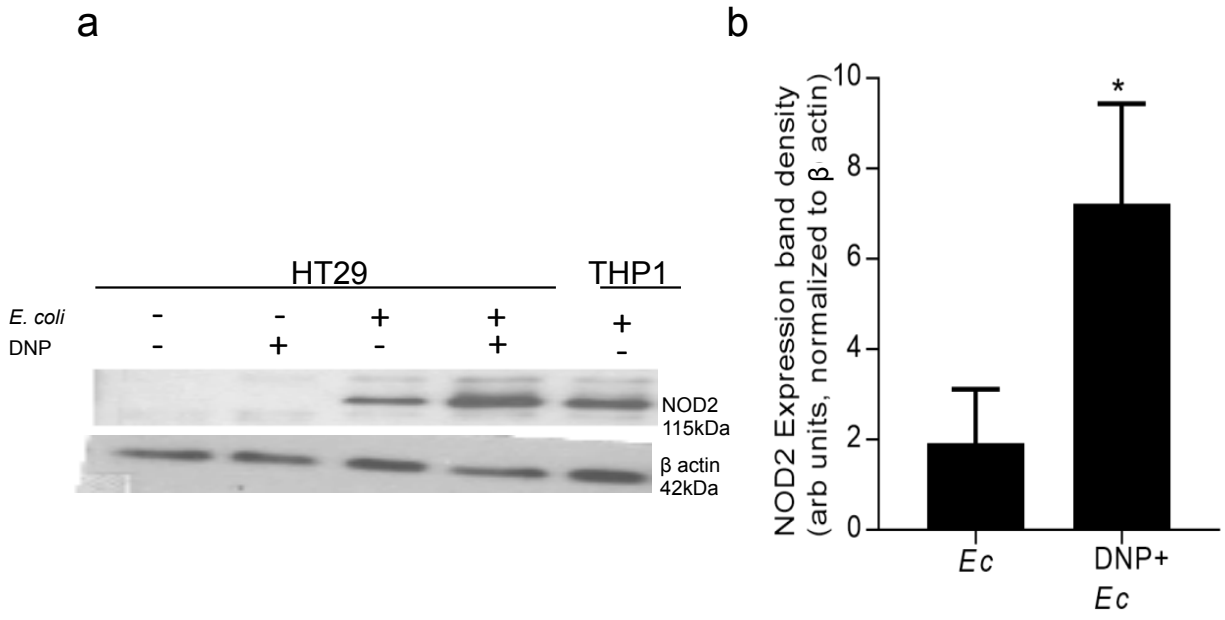

Figure 15: Internalization of *E. coli* in epithelial monolayer increases NOD2 expression in the colon-cancer cell line HT29. Findings from T84 cells were also reproduced in HT29 cells. (a) Increased NOD2 protein expression in HT29 epithelia exposed to *E. coli* HB101(*Ec,* $1x10^6$ cfu) ± dinitrophenol (DNP: 0.1 mM) for 16 hrs, representative blot of 3 separate experiments. (b) Densitometry analysis of NOD2 protein in HT29 cells (data are mean ± SEM; n=3, **p* <0.05 from the *E. coli* treated group).

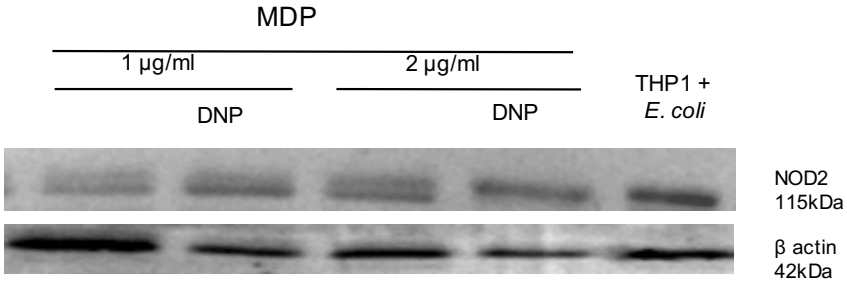

Figure 16: NOD2 protein expression increases after treatment with muramyl di-peptide (MDP). NOD2 senses MDP from both gram +ve and gram –ve bacteria. Hence, to reconfirm the above findings, plastic grown T84 cells were treated with MPD ± DNP (0.1mM) for 24 hrs and NOD2 protein expression was determined through immunoblot. THP-1 macrophages treated with *E. coli* ($1x10^6$ cfu) for 6 hrs used as a positive control.

3.5 Absence of NOD2 in metabolically stressed T84 epithelium results in increased numbers of viable intracellular bacteria

Polymorphism in NOD2 is found to be associated with Crohn's disease.(179) A portion of Crohn's disease patients have defective NOD2 signaling; hence, to imitate this, NOD2 expression was knocked down.(179) In T84 cells, NOD2 expression was knocked-down transiently using siRNA or stably via lentiviral shRNA (NOD2 KD). (Figure 17a-c)

There was no significance difference in paracellular permeability between T84 and NOD2 KD T84 cell monolayers when treated with DNP ± *E. coli* as assessed by changes in TER and flux of FITC dextran (4 KDa). (Figure 18a-b) However, after exposure of T84 and NOD2 KD monolayers to DNP + *E. coli* for 16 hrs, both the number of viable intracellular *E. coli* as well as translocated *E. coli* was significantly greater in the NOD2 KD T84 monolayers compared to wild-type T84 monolayers. (Figure 19)

Non-steroidal anti-inflammatory drugs (NSAID) can cause mitochondrial damage in the epithelial cells lining the intestine, leading to lower ATP levels.(134, 243) Additionally, they can also trigger relapse in IBD.(244) Hence, to validate the use of DNP, indomethacin, an NSAID was used as a metabolic stressor. Both the T84 and NOD2 KD epithelium were treated with indomethacin ± *E. coli* for 16 hrs. Similar to findings with DNP, indomethacin-treated NOD2 KD epithelium showed a greater number of viable intracellular *E. coli* compared to indomethacin-treated WT T84 epithelium.(138) (Figure 20)

To validate findings from cell lines, colonic organoids from $NOD2^{-/-}$ mice and strain matched wild-type mice were grown as monolayers on porous filter supports (Figure 14a-b) and treated with DNP (0.1 mM) ± *E. coli* ($1x10^7$ cfu) for 16 hrs. The $NOD2^{-/-}$ monolayer treated with DNP + *E. coli* also displayed a significantly greater number of translocated and intracellular

viable *E. coli* compared to organoid monolayers from strain-matched wild-type mice treated with DNP + *E. coli*. (Figure 21c-d)

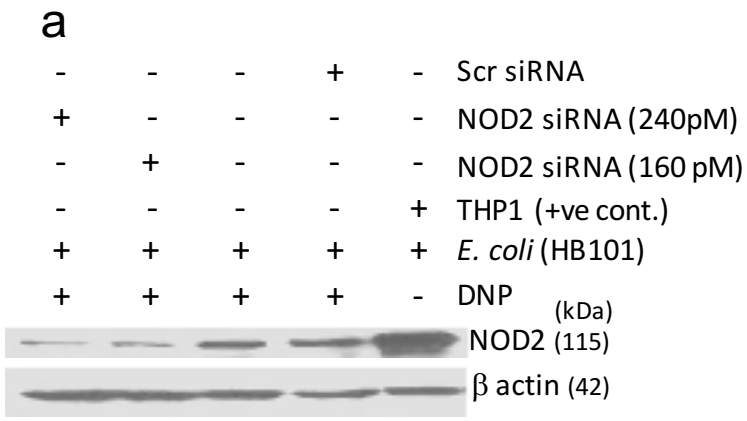
a
- - - + - Scr siRNA
+ - - - - NOD2 siRNA (240pM)
- + - - - NOD2 siRNA (160 pM)
- - - - + THP1 (+ve cont.)
+ + + + + E. coli (HB101)
+ + + + - DNP
(kDa)
NOD2 (115)
β actin (42)

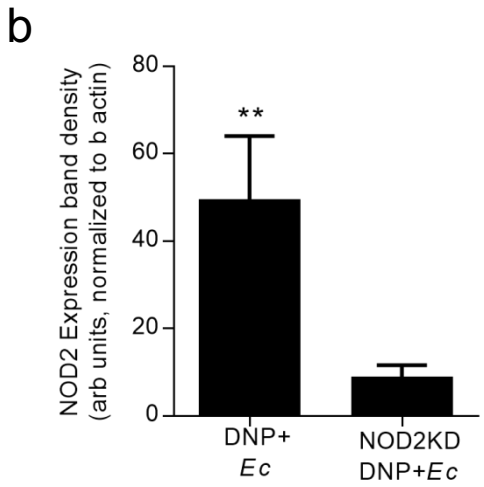
b
NOD2 Expression band density
(arb units, normalized to b actin)
80
60
40
20
0
**
DNP+
Ec
NOD2KD
DNP+Ec

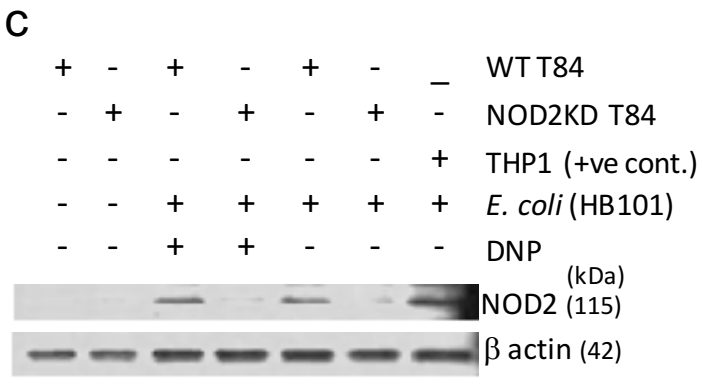
c
+ - + - + - _ WT T84
- + - + - + - NOD2KD T84
- - - - - - + THP1 (+ve cont.)
- - + + + + + E. coli (HB101)
- - + + - - - DNP
(kDa)
NOD2 (115)
β actin (42)

Figure 17: Knock-down of NOD2 expression using siRNA or shRNA. In T84 cells NOD2 expression was knocked down by using (a-b) siRNA (representative image and densitometry; n=3; ** p <0.01 compared to NOD2 knock-down or (c) stably-knocked down using lentivirus shRNA (DNP, dinitrophenol at 0.1 mM; *Ec*, *E. coli* HB101 at $1x10^6$ cfu; WT, wild-type cells; KD, knock down; 16 hrs treatments).

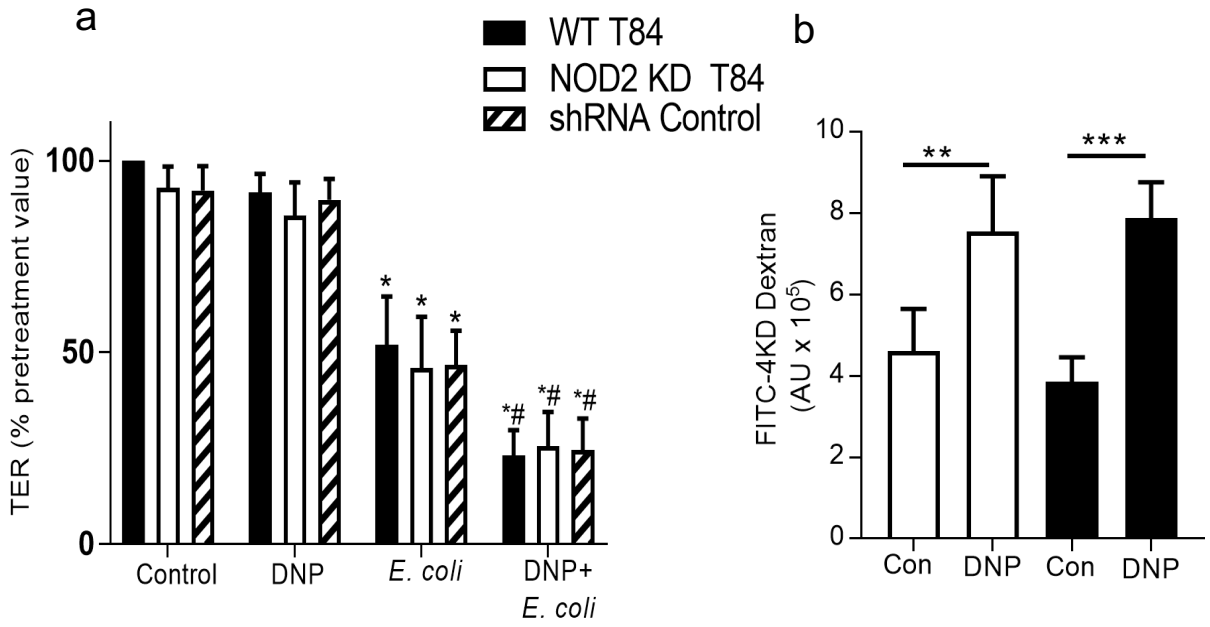

Figure 18: No difference in paracellular permeability between wild-type and NOD2 knock-down epithelium in response to *E. coli* HB101 ± DNP treatment after 16 hrs. Wild-type and NOD2 shRNA knock-down T84 cells were treated for 16 hrs with *E. coli* HB101 (*Ec*, $1x10^6$ cfu) ± dinitrophenol (DNP: 0.1 mM) and paracellular permeability was measured by (a) transepithelial resistance (TER) and (b) transepithelial flux of 4 kDa FITC-dextran (AU, arbitrary fluorescent units; (data are mean ± SEM; n= 9 monolayers from 3 experiments; * $p <$ 0.05 versus control, # $p < 0.05$ versus *E. coli* group, ** $p <0.001$ compare to untreated group, *** $p <0.0001$ compare to untreated group).

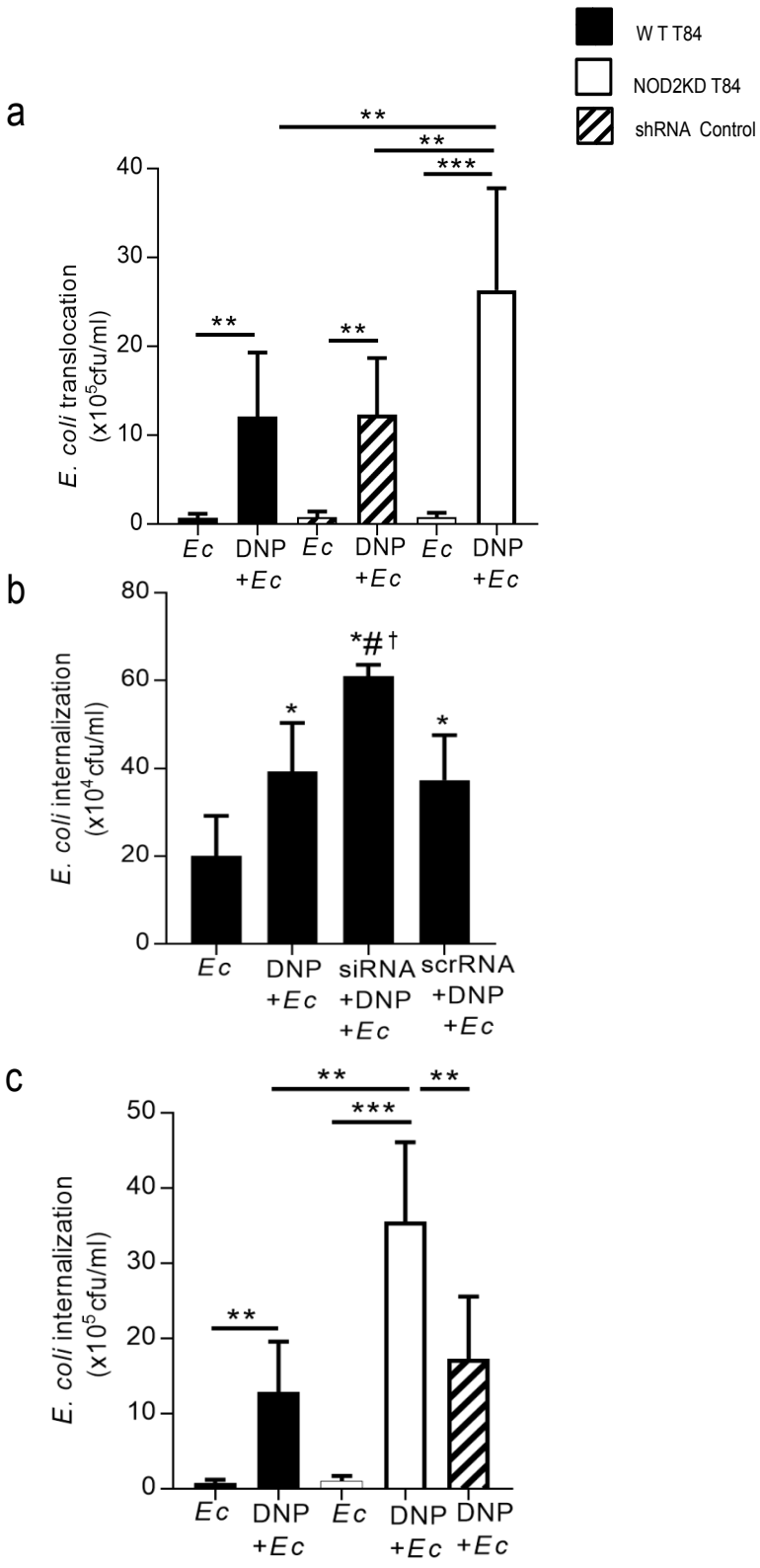
W T T84
NOD2KD T84
shRNA Control
a
E. coli translocation (x10^5cfu/ml)
40
30
20
10
0
**
**
**
***
Ec
DNP +Ec
Ec
DNP +Ec
Ec
DNP +Ec
b
E. coli internalization (x10^4 cfu/ml)
80
60
40
20
0
*
*#†
*
Ec
DNP +Ec
siRNA +DNP +Ec
scrRNA +DNP +Ec
c
E. coli internalization (x10^5cfu/ml)
50
40
30
20
10
0
**
**
***
**
Ec
DNP +Ec
Ec
DNP +Ec
DNP +Ec

Figure 19: T84 epithelium lacking NOD2 exhibit increased numbers of *E. coli* in response to metabolic stress. Wild-type and NOD2 knock-down T84 cells were treated for 16 hrs with *E. coli* HB101 (*Ec*, $1x10^6$ cfu) ± dinitrophenol (DNP: 0.1 mM) (a) bacterial translocation was increased across NOD2 KD cells (data are mean ± SEM; n=9 from 3 experiments, ** $p < 0.001$, *** $p < 0.0001$) and DNP-induced internalization of *E. coli* was increased in T84 cells in which NOD2 was KD with (b) siRNA (data are mean ± SEM; n=3 from 1 experiments; * $p < 0.05$ from *Ec*, # $p < 0.05$ from the DNP + *Ec*, † $p < 0.05$ from DNP + *Ec* + Scr (scrambled) RNA (control), see appendix (Figure 35) for additional experimental data) or (c) shRNA (data are mean ± SEM; n=9 monolayers from 3 experiments; across NOD2 KD cells (data are mean ± SEM; n=9 from 3 experiments, ** $p < 0.001$, *** $p < 0.0001$).

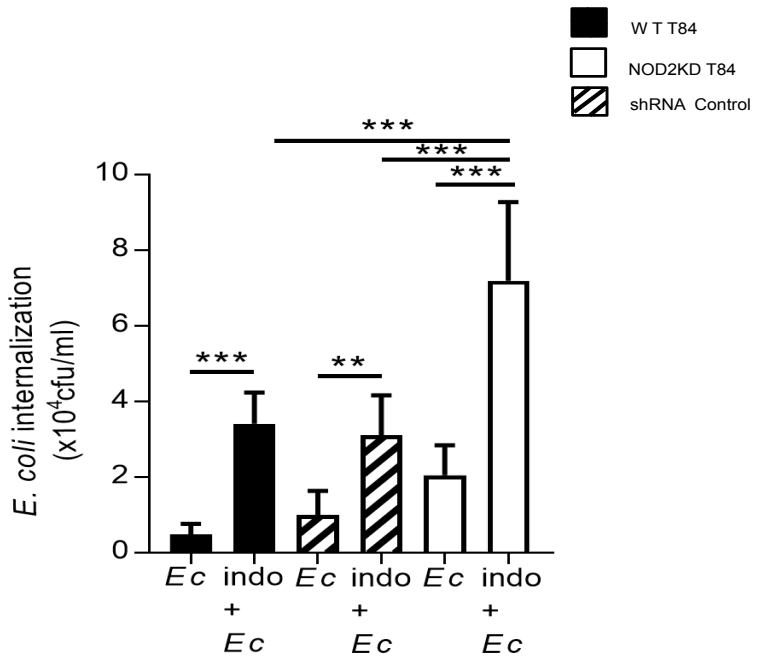

Figure 20: The non-steroidal anti-inflammatory drug (NSAID) indomethacin induced mitochondrial dysfunction increases number of viable intracellular *E. coli* in metabolically stressed wild-type and NOD2 KD epithelium. Increased number of internalized bacteria in *E. coli* HB101 (*Ec*, 1x10^6 cfu) ± indomethacin (indo,1 μM) treated NOD2 KD cells compared to wild-type T84 cells after 16 hrs (data are mean ± SEM; n=9 from 3 experiments, ** $p < 0.001$, *** $p < 0.0001$).

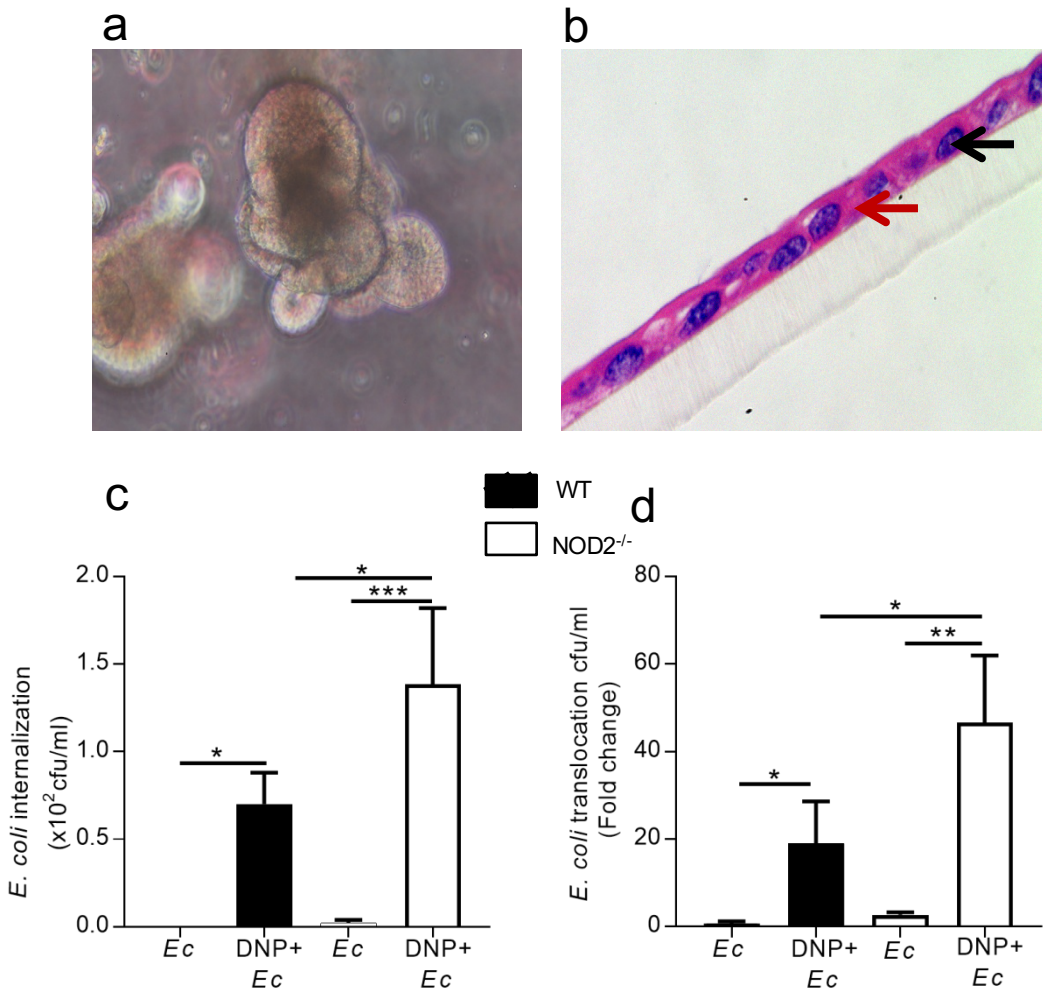

Figure 21: Metabolically stressed colonic organoid monolayer from NOD2$^{-/-}$ mouse displays increased number of viable intracellular bacteria. Findings observed in the cell line model system were recapitulated in stem cell derived colonic organoids from NOD2$^{-/-}$ and age matched wild-type mice. (a) Representative image of colon organoid from NOD2$^{-/-}$ mouse (n=3 images, original magnification = x40) and (b) grown as a monolayer. The monolayer was stained with hematoxylin and eosin. Black arrow points to nucleus stained purple with hemotoxylin. Cytoplasm was stained pink with eosin (red arrow). Filter grown organoid monolayers from NOD2$^{-/-}$ and WT mouse were treated with *E. coli* HB101 (*Ec*, 1x10^7 cfu) ± dinitrophenol (DNP: 0.1 mM) for 16 hrs. After that (c) internalized bacteria and (d) translocated bacteria were quantified through gentamycin assay (data are mean ± SEM; n=3 preprations from 1 mouse, * $p < 0.05$, ** $p < 0.001$, *** $p < 0.0001$).

3.6 Reactive oxygen species (ROS) mediated phosphorylation of ERK1/2 promotes *E. coli* internalization

T84 cells exposed to *E. coli* ± DNP experience increased ROS production.(105) NOD2 KD cells treated with DNP + *E. coli* display increased ROS production by 4 hrs, a time before any bacterial internalization is observed. However, co-treatment with the mitochondria-targeted antioxidant mitoTEMPO, reduces ROS. (Figure 22a) Reduction in ROS also resulted in decreased intracellular bacteria in NOD2 KD and T84 cells elicited by DNP treatment. (Figure 22b)

ROS can activate the MAP kinase ERK1/2.(220) An increase in p-ERK1/2 was observed 4 hrs post-treatment of NOD2 KD and WT T84 epithelia with DNP + *E. coli*. (Figure 23a-b) This increase was significantly ablated when the epithelium was co-treated with mitoTEMPO, suggesting that ROS functions as an upstream signal in ERK1/2 activation. The pharmacological inhibitor U0126 can selectively block ERK activation. Co-treatment of DNP + *E. coli* treated NOD2 KD and WT T84 epithelium with U0126 for 16 hrs significantly reduced the number of viable intracellular *E. coli* compared to the DNP + *E. coli* treated epithelium. (Figure 24a) A similarly significant reduction in number of intracellular beads or dead *E. coli* was observed when the DNP + beads/dead *E. coli* treated NOD2 KD or WT T84 epithelium was co-treated with U0126 compared to epithelia treated with just DNP + beads/dead *E. coli*. (Figure 24b-c) The concentration of pharmacological agents used here (U0126 (25 μM), mitoTEMPO (10 μM)) were neither bacteriotoxic or bacteriostatic over the 16-18 hrs experimental period.(105, 223) (Figure 8c)

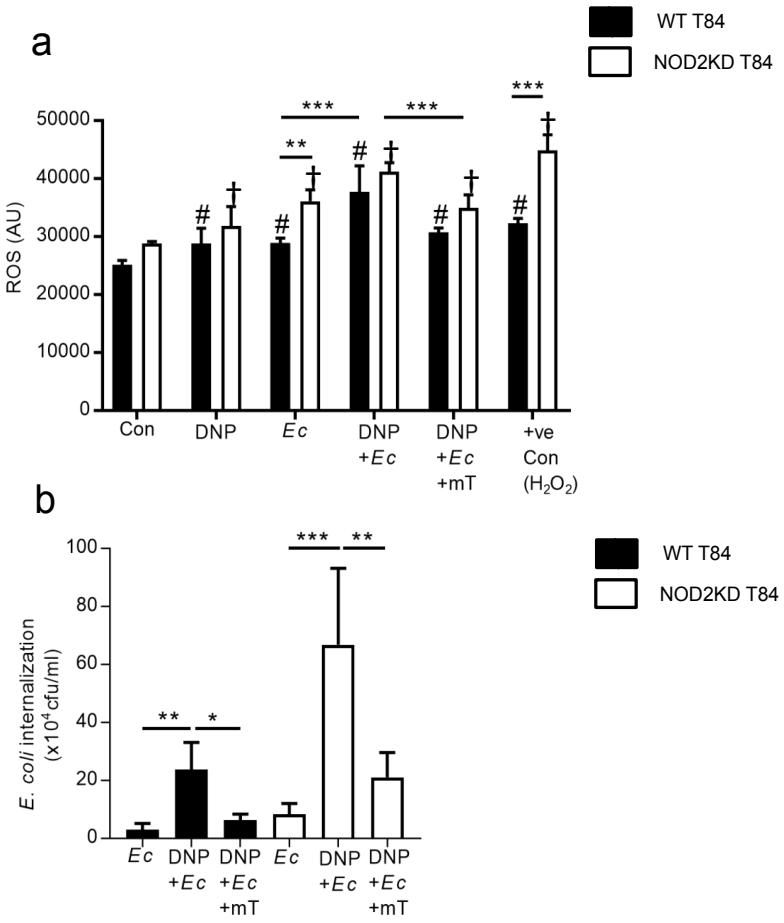

Figure 22: Increased ROS production in DNP ± *E. coli* treated epithelium. (a) Wild-type (WT) and shRNA NOD2 knock-down T84 epithelia exposed to *E. coli* (*Ec*: 1x10^6 cfu) ± dinitrophenol (DNP: 0.1 mM) for 4 hrs results in increased ROS production (AU, arbitrary fluorescent units) that is blocked by co-treatment with the mitochondria-targeted antioxidant, mitoTEMPO (mT: 10 μM) (data are mean ± SEM; n=4, ** p <0.01,*** p <0.001; # and † p <0.05 compared to WT and NOD2KD control (Con), respectively; +ve control, H_2O_2 treated cells (0.5 mM)). (b) Co–treatment with mitoTempo reduced the DNP-evoked internalization of *E. coli* into WT T84 and NOD2KD T84 cells (data are mean ± SEM; n=9 from 3 separate experiments, * p <0.05, ** p <0.001).

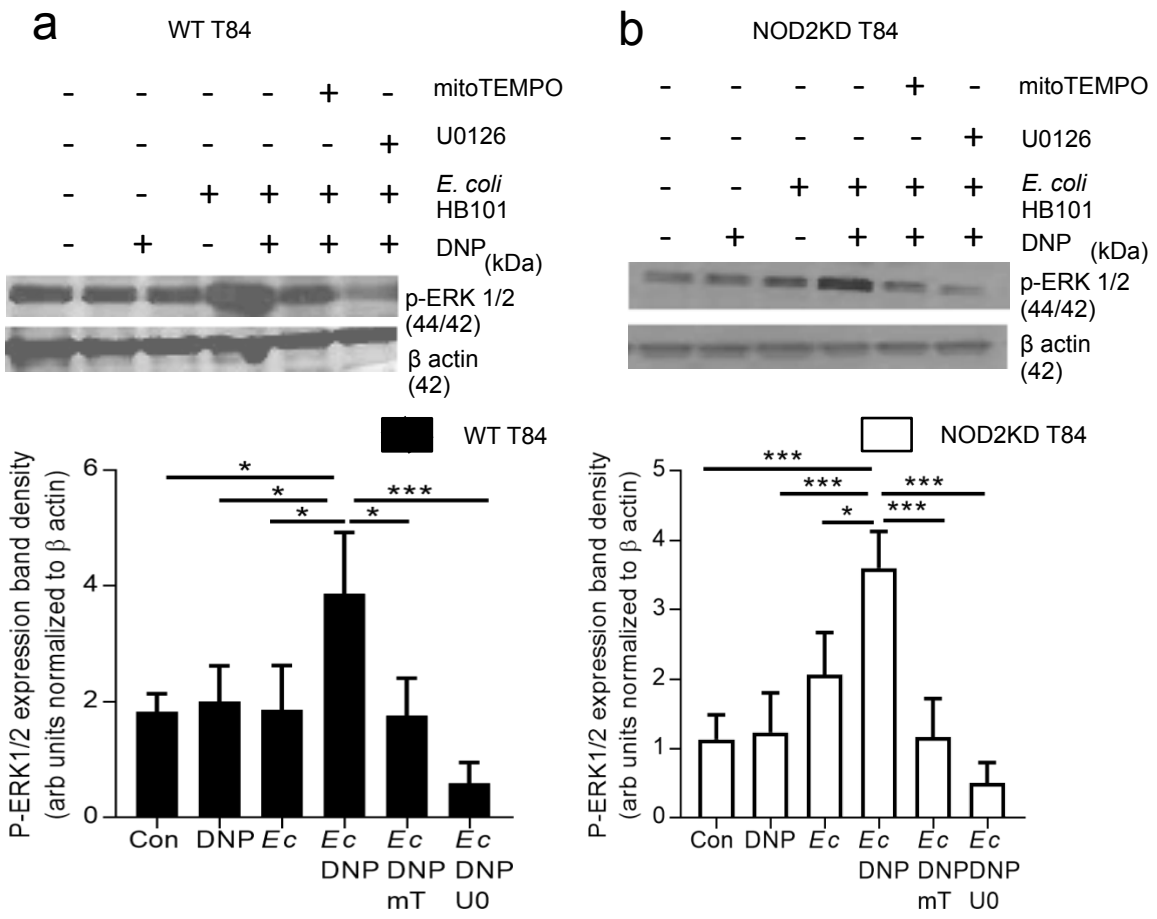

Figure 23: Reactive oxygen species (ROS) mediated phosphorylation of ERK 1/2.
Immunoblots and densitometry (representative blot of three separate experiments) showing that (a) WT and (b) NOD2KD T84 cells have increased ERK1/2 activation (i.e. p-ERK) after 4 hrs of DNP (0.1 mM) + *E. coli* ($1x10^6$ cfu) treatment that is suppressed in the presence of the pharmacological inhibitor, U0126 (25 μM) or mitoTEMPO (mT, 10 μM) (n=3). WT and NOD2KD epithelium was pretreated with U0126 (25 μM) or mitoTEMPO (10 μM) for 30 min before treating the epithelia with DNP.

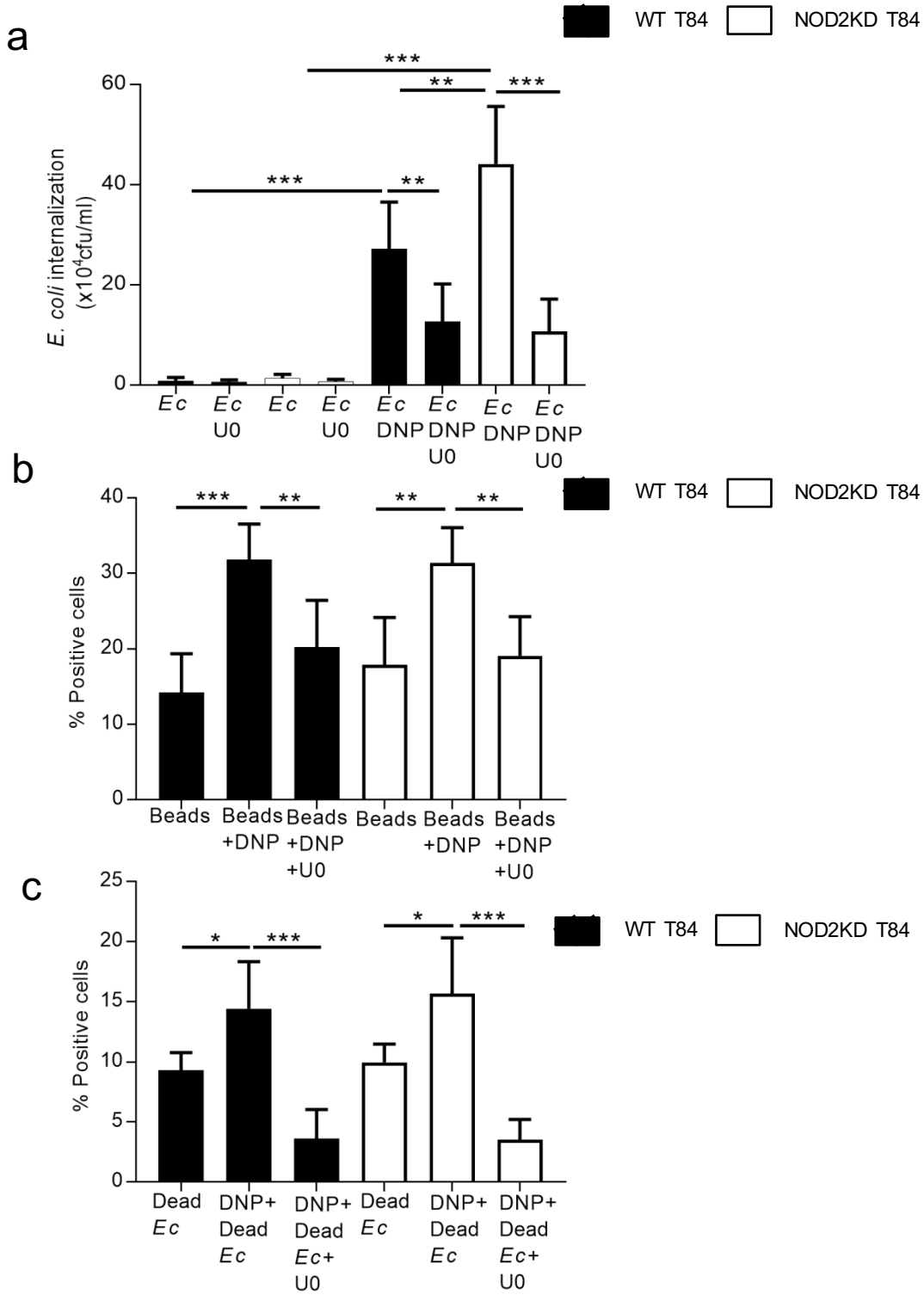
a
WT T84
NOD2KD T84
E. coli internalization (x10^4cfu/ml)
60
40
20
0
***
**
***
***
**
Ec
Ec U0
Ec
Ec U0
Ec DNP
Ec DNP U0
Ec DNP
Ec DNP U0
b
WT T84
NOD2KD T84
% Positive cells
40
30
20
10
0
***
**
**
**
Beads
Beads +DNP
Beads +DNP +U0
Beads
Beads +DNP
Beads +DNP +U0
c
WT T84
NOD2KD T84
% Positive cells
25
20
15
10
5
0
*
***
*
***
Dead Ec
DNP+ Dead Ec
DNP+ Dead Ec+ U0
Dead Ec
DNP+ Dead Ec
DNP+ Dead Ec+ U0

Figure 24: Reactive oxygen species (ROS) mediated phosphorylation of ERK1/2 promotes *E. coli* internalization. (a) Dinitrophenol (DNP, 0.1 mM)-invoked internalization of *E. coli* HB101($1x10^6$ cfu) in WT and NOD2KD T84 cells was significantly reduced by 30 min pretreatment and after that co-treatment with the ERK 1/2 inhibitor U0126 (25 μM) (data are mean ± SEM; n=9 epithelial monolayers from 3 experiments; * p <0.5, ** p <0.001, *** p <0.0001). (b-c) T84 cells and NOD2KD T84 were exposed to inert fluorescent 1 μm diameter beads ($1x10^6$ beads) or dead fluorescent *E. coli* (Dead *Ec*; $1x10^6$ cfu) ± DNP ± U0126 and 16 hrs later internalized bead and bacteria were assessed by flow cytometry and are presented as the number of positive cells. (data are mean ± SEM; n=9 from 3 experiments; * p <0.05, * p <0.5, ** p <0.001, *** p <0.0001).

3.7 Absence of NOD2 augments epithelial barrier defect via defective killing of intracellular bacteria

NOD2 recruits ATG16L1 at the bacterial entry site within dendritic cells, epithelial cells as well as in macrophages and induces xenophagy.(212, 213) Hence, we asked if the increase in the number of intracellular bacteria in NOD2 KD cells was due to an increase in uptake or defective killing of intracellular bacteria. To test this, NOD2 KD and WT T84 epithelia were treated with inert fluorescent beads or FITC-conjugated dead *E. coli* in conjunction with DNP for 16 hrs. No significant difference between the number of intracellular beads or dead *E. coli* was observed between the NOD2 KD and WT T84 epithelia. (Figure 25a-b)

To further assess this issue, WT T84 and NOD2 KD epithelia were treated with *E. coli* ± DNP for 4, 7 and 16 hrs. After 4 and 7 hrs the extracellular *E. coli* were killed using gentamycin and fresh medium was added, allowing the epithelium to continue to grow for another 9 or 12 hrs, respectively, to match the 16 hrs experimental time point. In both cases, increased numbers of bacteria were observed in NOD2 KD epithelium after 16 hrs compared to the WT T84 epithelium, in accordance with the previous finding of reduced killing of bacteria in NOD2 KD cells. (Figure 26)

One method of measuring autophagy is conversion of cytosolic LC3-1 protein to LC3-II (autophagosome associated form of LC3-1). Immunoblot of LC3-I/LC3-II revealed reduced conversion of LC3-I to LC3-II in NOD2 KD cells after treatment of the epithelia with *E. coli* ± DNP compared to WT T84 epithelia treated with DNP ± *E. coli.* (Figure 27) Moreover, induction of autophagy via rapamycin reduced the number of viable intracellular *E. coli* in both WT T84 and NOD2 KD epithelium treated with DNP ± *E. coli* by inducing xenophagy. (Figure 27c)

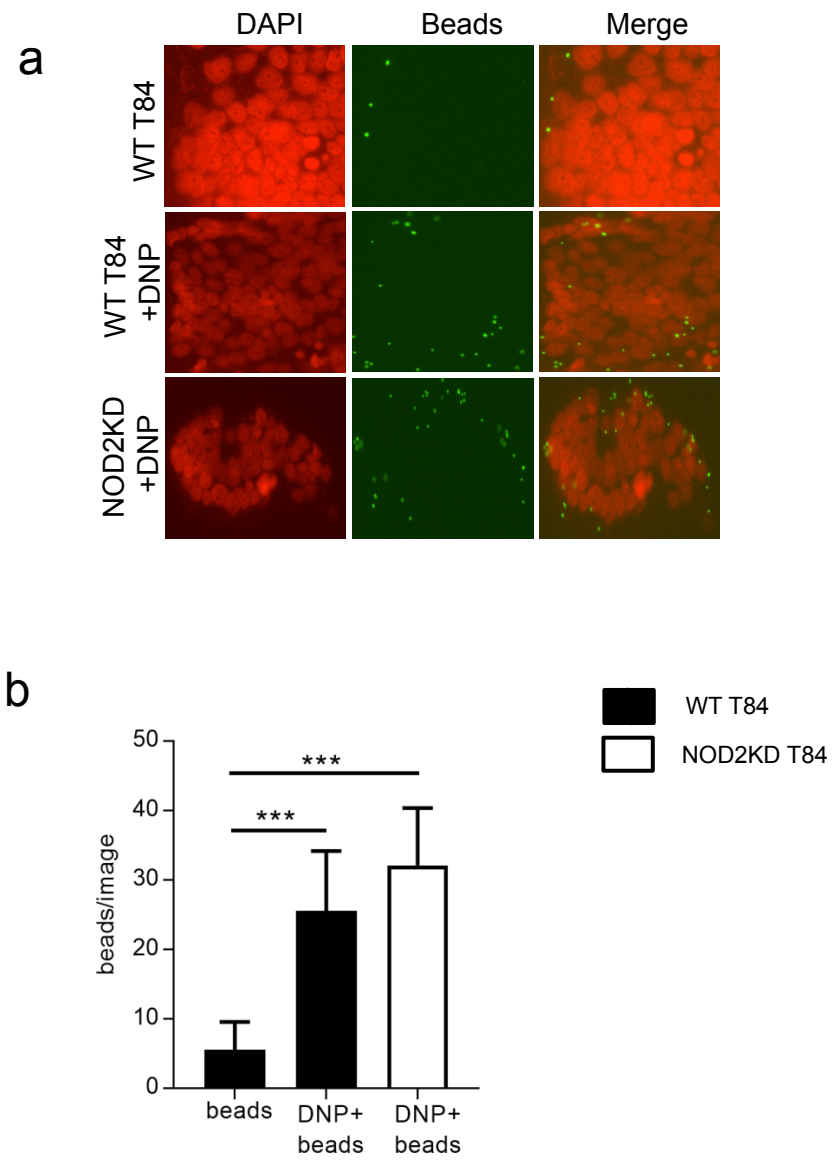

Figure 25: No significant difference in number of internalized beads in metabolically stressed WT and NOD2KD epithelium. (a) Immunolocalization of the fluorescent beads (1x10^6 beads) shows a similar increased uptake in dinitrophenol (DNP: 0.1 mM) treated WT and NOD2 KD T84 epithelial after 16 hrs (representative image of 6 epithelium preparations from 3 experiments; original magnification = x40). After treatment, the fluorescence of outside beads were quenched by trypan blue. The nuclei stained with DAPI and after images were taken, it was recolored in red while FITC conjugated beads are in green. (b) quantification of intracellular beads by counting on coded slides (data are mean ± SEM; n=9 from 3 separate experiment, *** p <0.0001).

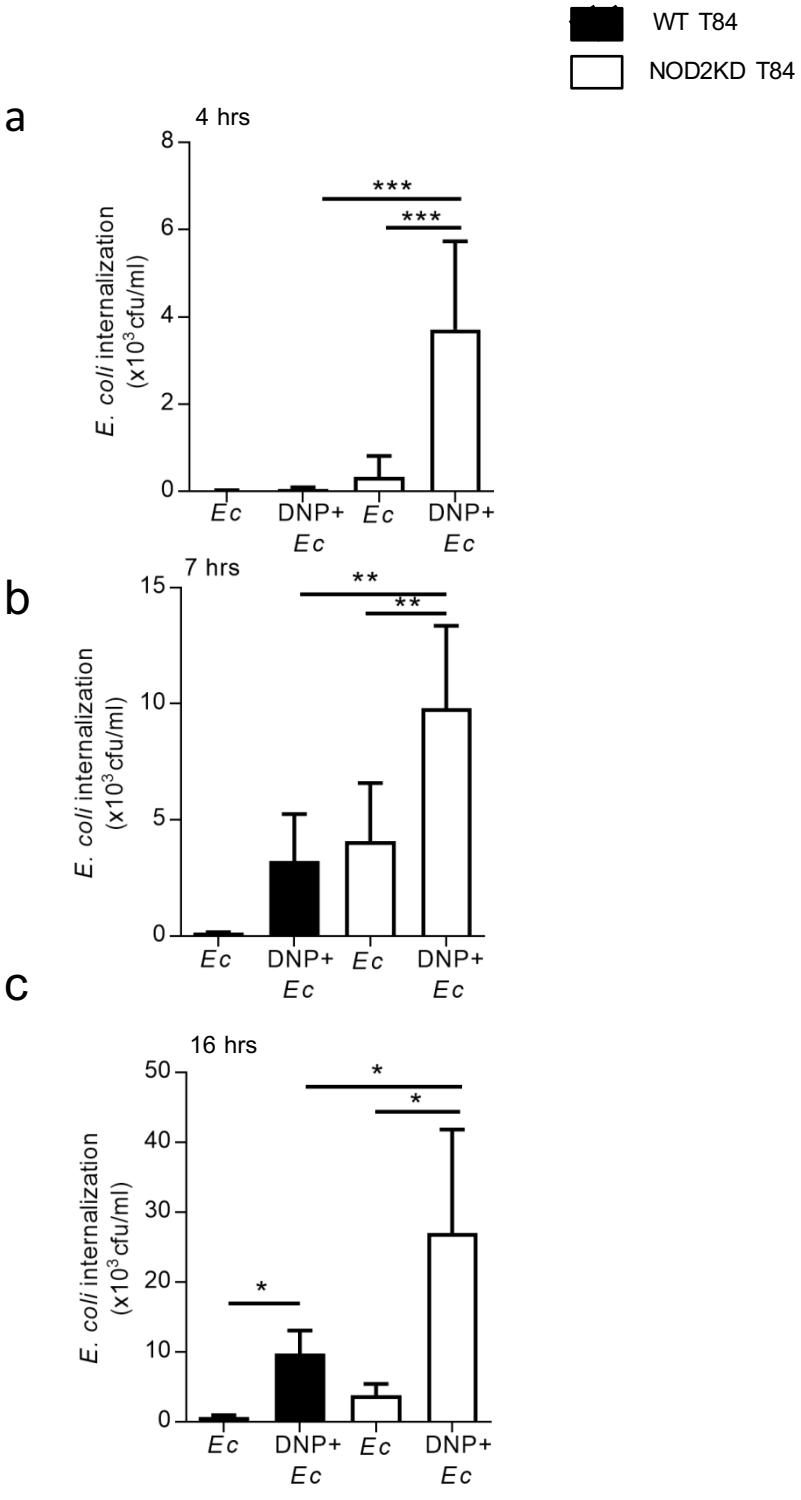
WT T84
NOD2KD T84
a
4 hrs
E. coli internalization
(x10^3 cfu/ml)
***
***
Ec
DNP+ Ec
Ec
DNP+ Ec
b
7 hrs
**
**
c
16 hrs
*
*
*

Figure 26: Reduced killing of internalized *E. coli* in NOD2 KD cells. The increased number of intracellular bacteria in metabolically-stressed epithelia is due to reduced killing. Wild-type (WT) and NOD2 KD T84 epithelial monolayers were treated with dinitrophenol (DNP: 0.1 mM) and *E. coli* HB101 (*Ec*, $1x10^6$ cfu/ml) for (a) 4 hrs, (b) 7 hrs or (c) 16 hrs. Following the defined period of exposure to *E. coli*, extracellular bacteria were killed by gentamycin and the in the case of the 4 hrs and 7 hrs treatments the cells were returned to 37^oC for 12 hrs or 9 hrs, respectively, to align with a total 16 hrs experiment as in (c). At this point, cells were rinse, lysed and intracellular viable bacteria counted after growth on LB agar plates (data are mean ± SEM; n=6 epithelial preparations from 2 experiments, see appendix (Figure 36) for additional experimental data; * p <0.05, ** p <0.001, *** p <0.0001).

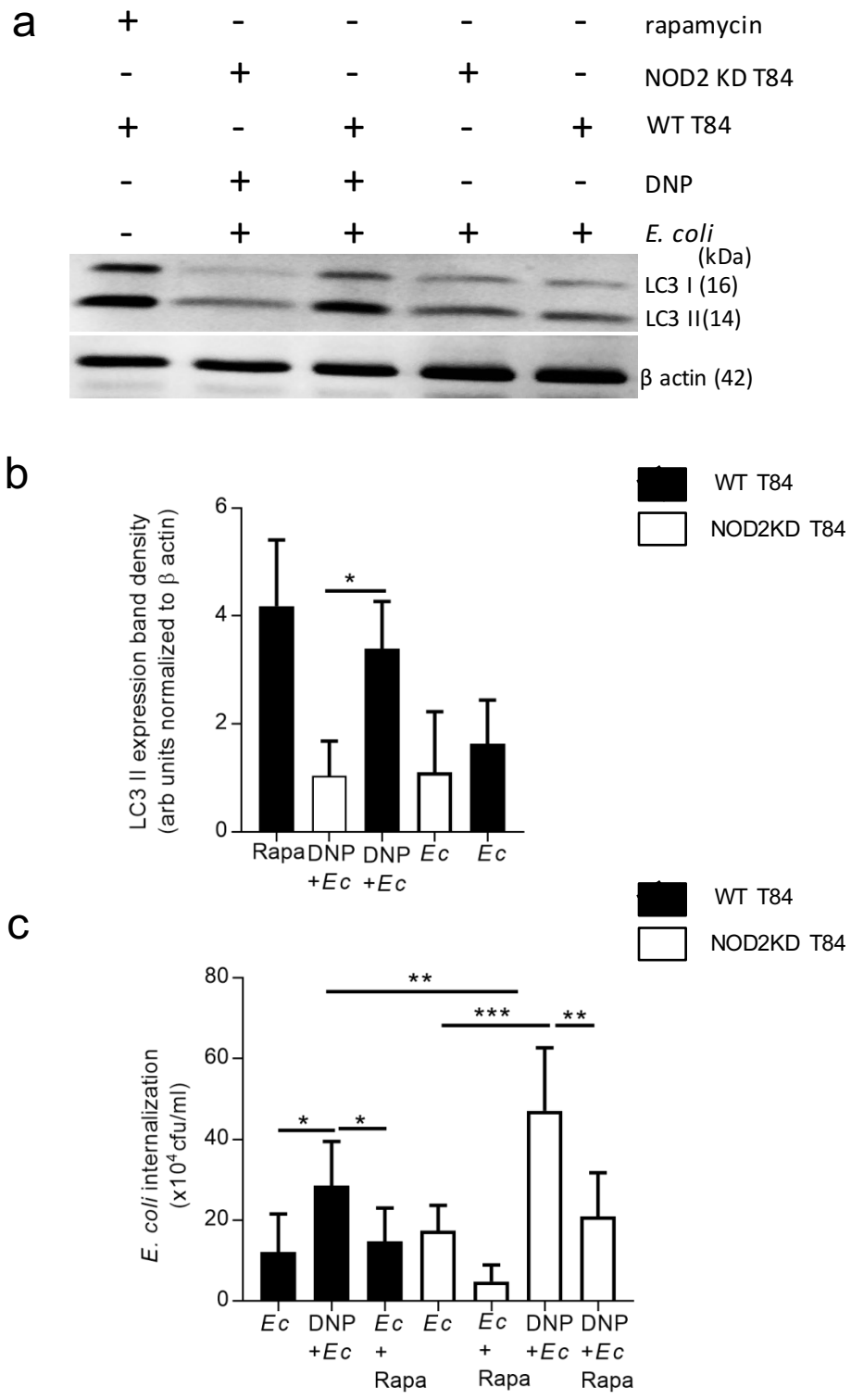
a
+ - - - - rapamycin
- + - + - NOD2 KD T84
+ - + - + WT T84
- + + - - DNP
- + + + + E. coli
(kDa)
LC3 I (16)
LC3 II(14)
β actin (42)
b
WT T84
NOD2KD T84
LC3 II expression band density
(arb units normalized to β actin)
0
2
4
6
*
Rapa
DNP +Ec
DNP +Ec
Ec
Ec
c
WT T84
NOD2KD T84
E. coli internalization
(x10^4 cfu/ml)
0
20
40
60
80
*
*
**
***
**
Ec
DNP +Ec
Ec + Rapa
Ec
Ec + Rapa
DNP +Ec
DNP +Ec Rapa

Figure 27: Reduced autophagy was observed in NOD2 KD cells. (a) Representative immunoblot shown activation of autophagy, that is increased expression of LC3II in WT or NOD2KD T84 epithelia after 16 hrs of the various treatments, and quantified in panel (b) (n=3 epithelia; * p <0.05; dinitrophenol (DNP: 0.1 mM; *E. coli* (*Ec*, $1x10^6$ cfu/ml); the inducer of autophagy, rapamycin (Rapa,100 nM). (c) The number of viable intracellular *E. coli* in NOD2 KD T84 and WT T84 under basal or DNP stimulated (16 hrs) conditions is significantly reduced by co-treatment with rapamycin (data are mean ± SEM; n=9 epithelial preparations from 3 experiments; *p < 0.05, **p < 0.001).

3.8 IL-8 production increases in T84 monolayers 16 hrs post-treatment with *E. coli* ± DNP in a time dependent manner

IL-8 is a major proinflammatory cytokine secreted by intestinal epithelial cells and a potent neutrophil chemoattractant. Colonic mucosa from patients with ulcerative colitis can show ~10-fold increase of IL-8 production over the control.(229) IL-8 is well known to play an important role in the anti-bacterial response (230); understanding whether metabolic stress is sufficient to trigger IL-8 production will enable us to understand the former role in potentially triggering inflammation in IBD. T84 cell monolayers were treated with either: TNFα (positive control 10 ng/ml), medium only (negative control), DNP (0.1 mM), *E. coli* HB101 ($1x10^6$ cfu/ml) or DNP + *E. coli* to test how bacterial exposure in a stressed epithelium affects IL-8 production. Cells were incubated for different time intervals (6, 16, and 24 hrs) and IL-8 was measured through ELISA. T84 cells exposed to DNP + *E. coli* for 16 hrs produced a significantly greater amount of IL-8 compared to the control or *E. coli* only treated epithelium alone. (Figure 28a) Additionally, a time dependent (6-42 hrs) increase in IL-8 production in DNP + *E. coli* HB101 treated T84 monolayers was seen compared to *E. coli* HB101 treated epithelium alone. (Figure 28b)

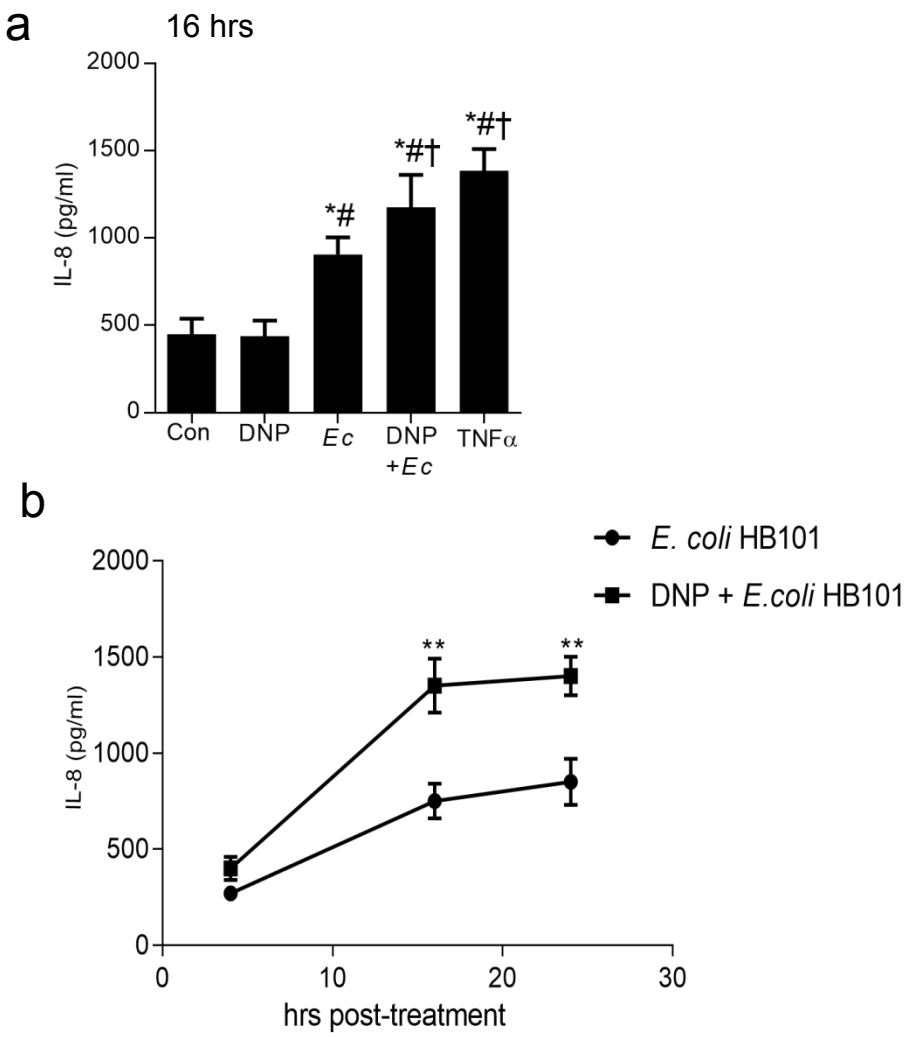

Figure 28: Increase in IL-8 production in T84 cell monolayer 16 hrs post-treatment with DNP ± *E. coli* in a time dependent manner. T84 cell monolayers were treated with, *E. coli* HB101(*Ec,* $1x10^6$ cfu) ± DNP (0.1mM), or the control for 4, 16, or 24 hrs, then medium collected and IL-8 levels quantified using ELISA. Results were then presented as a bar graph for 16 hrs (a) and time course (b). (data are mean ± SEM; * $P < 0.05$ versus control, # $P < 0.05$ versus DNP, † $P < 0.05$ from *E. coli* treated group, n=9 from 3 experiments, * $p < 0.05$, ** $p < 0.005$, *** $p < 0.005$, TNFα 10ng/ml).

3.9 Bacteria or bacteria derived products are required for IL-8 production from a metabolically stressed epithelium

The T84 cell monolayer was treated with either: (a) dead *E. coli* ($3x10^6$ cfu/ml), or (b) inert latex beads ($3x10^6$ cfu/ml; 1 μm) for 16 hrs with or without DNP. Controls mimicked the earlier experiment with the addition of a T84 monolayer treated with DNP + *E. coli* as another positive control; T84 cells treated with dead *E. coli* particles ± DNP and T84 cells incubated with latex beads ± DNP served as the experimental groups. The T84 cell monolayer treated with DNP + dead *E. coli* particles showed a significant increase in IL-8 production compared with untreated or dead *E. coli* particles only. No significant difference in IL-8 production between the control, beads or DNP + beads treated epithelia was observed. (Figure 29a-b)

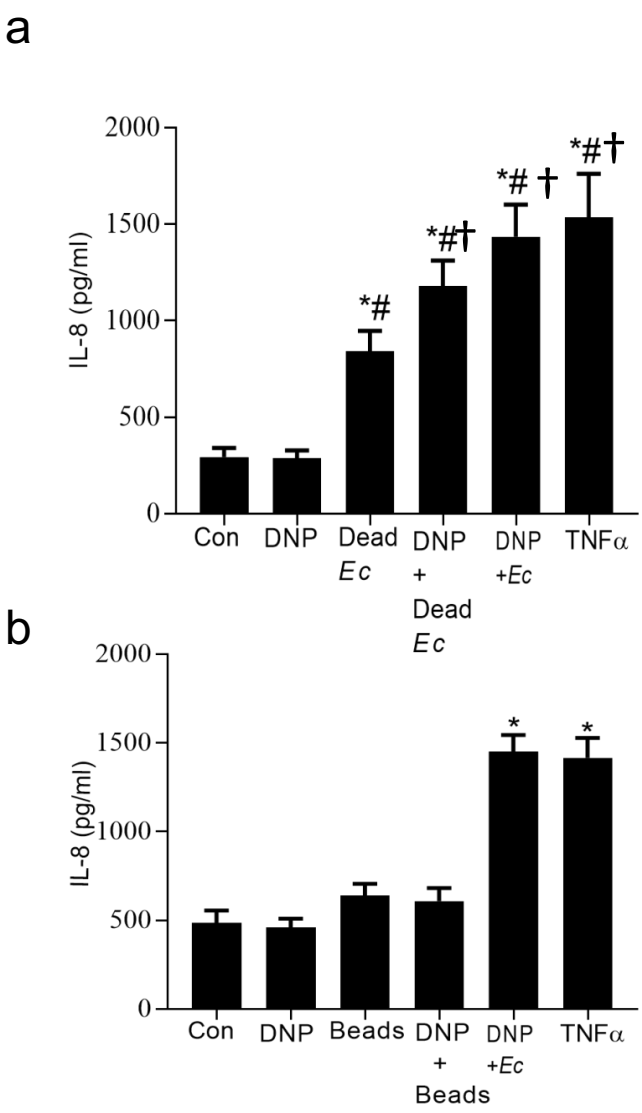

Figure 29: Production of IL-8 from metabolically stressed epithelium is dependent on bacteria or bacteria derived products. (a) T84 cell monolayers treated with DNP (0.1 mM) or dead *E. coli* particles (3 x 10^6 particles/ml) ± DNP for 16 hrs. IL-8 was measured by ELISA in the culture medium (data are mean ± SEM; n = 9 from 3 separate experiments, * p <0.5 from control group, # p < 0.5 versus DNP, † p <0.5 from dead *E. coli* treated group). (b) T84 monolayers treated with DNP or Beads (3 x 10^6 Beads/ml) ± DNP for 16 hrs (data are mean ± SEM; n=9 from 3 experiments, * p <0.05 from the control group). IL-8 measured from DNP (0.1 mM) + *E. coli* HB101 (*Ec,* 1 x 10^6 cfu/ml) and TNFα (10 ng/ml) treated epithelium serve as a positive control for both the experiments).

3.10 IL-8 production in DNP + *E. coli* treated epithelia is dependent on TLR signaling

To investigate the role of TLRs in IL-8 secretion, TLR signal inhibitors such as the MyD88 inhibitory peptide were used. MyD88 is an important adaptor molecule in the upstream signaling cascades of TLRs. MyD88 inhibitory peptide inhibits MyD88-dependent signaling activity by interfering with MyD88 homodimer formation.(245, 246) Chloroquine inhibits endosome maturation, which is required for the activation of intracellular TLRs, such as TLR7 and TLR9 which are present in endosome compartments. TLR9 recognizes bacterial DNA which contains repeated unmethylated CpG motifs.(247) This is in contrast to TLR7 which recognizes single stranded viral RNA.(248, 249) T84 cells express TLR9 mRNA which is upregulated in HT29 cells when exposed to DNA from the pathogenic bacteria *Salmonella enterica* serovar Dublin. (231, 250) Expression of TLR4 in colonic epithelial cells is low.(251, 252) Co-treatment of DNP + *E. coli* treated T84 monolayers with the MyD88 inhibitory peptide significantly reduced IL-8 production compared to DNP + *E. coli* treated epithelium 16 hrs post-treatment. (Figure 30a) Additionally, co-treatment with chloroquine to a DNP + *E. coli* treated epithelium significantly attenuated IL-8 production compared with DNP + *E. coli* treated epithelium but didn't alter TNFα induced IL-8 synthesis from T84 cells 16 hrs post-treatment. (Figure 30b) Cytochalasin D inhibits actin polymerization. Co-treatment of DNP + *E. coli* treated T84 cell monolayers with cytochalasin D significantly reduces DNP mediated *E. coli* internalization 16 hrs post-treatment. (Figure 31a) Treatment of the T84 cell monolayers with cytochalasin D significantly reduced DNP + *E. coli* induced IL-8 synthesis but not TNFα induced IL-8 synthesis. (Figure 31b) TLR4 is an extracellular TLR which recognizes LPS from gram negative bacteria.(231) To assess the possibility of LPS being the major contributor of IL-8 synthesis, we treated T84 cells with LPS for 16 hrs. LPS induced IL-8 production was significantly lower than

IL-8 produced by DNP + *E. coli* treated epithelium. (Figure 32) The concentration of pharmacological agents used here (chloroquine (10 μM/ml), cytochalsin D (0.25 μM),were neither bacteriotoxic or bacteriostatic over the 16-18 hrs experimental period.(158, 231) (Figure 8c)

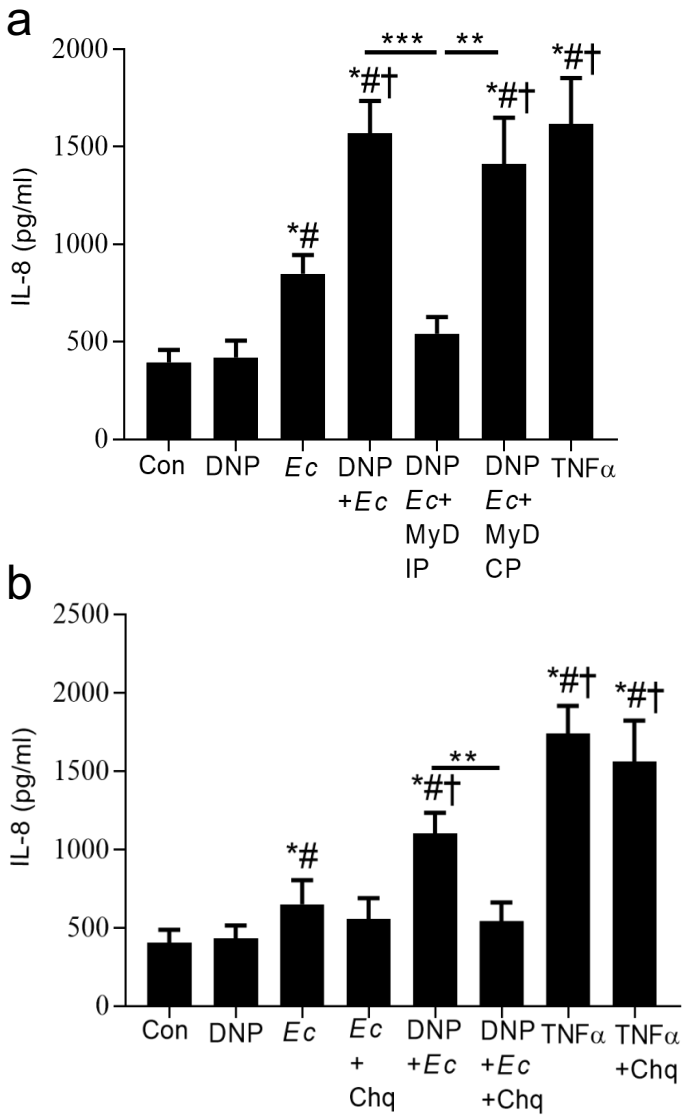

Figure 30: IL-8 production in DNP + *E. coli* treated epithelia is dependent on TLR signaling. (a) TLR signaling is involved in IL-8 production from the metabolic stressed epithelium. T84 cell monolayers were treated with dinitrophenol (DNP, 0.1 mM), *E. coli* HB101 (1 x 10^6 cfu/ml) ± DNP. Additionally, T84 cell monolayers were pretreated with MyD88 inhibitory peptide (MyD IP, 100 μM) and MyD88 control peptide (MyD CP, 100 μM) for 30

min before treating the epithelia for 16 hrs. IL-8 was measured through ELISA. Untreated and TNFα (10 ng/ml) treated epithelium served as negative and positive controls (data are mean ± SEM; n=6 from 2 separate experiments, * p <0.5 from control group, # p <0.5 from DNP group, † p <0.5 from *E. coli* treated group). (b) Decrease in IL-8 production in T84 monolayer after treatment with choloroquine an inhibitor of endosome maturation. T84 cell monolayers were pretreated with choloroquine (Chq, 10 μM) for 30 min. Afterwards co-treatment of choloroquine to DNP + *E. coli* treated epithelium significantly reduced the IL-8 production 16 hrs post-treatment (data are mean ± SEM; n=9 from 3 experiments, *p <0.05 from the control group, # p <0.05 versus DNP, † p <0.05 from the *E. coli* treated group, * p <0.05).

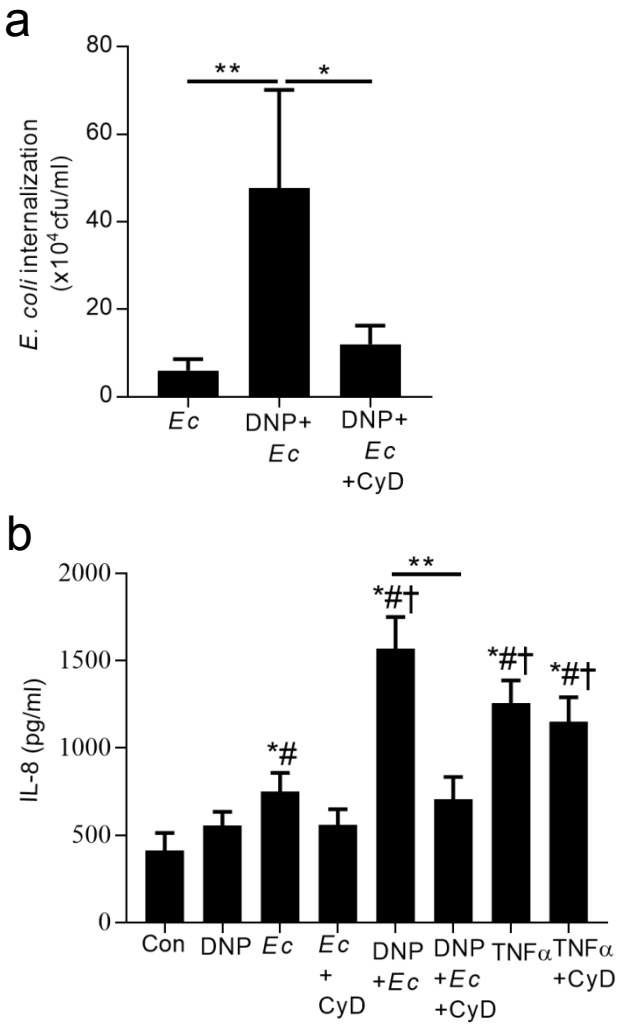

Figure 31: Disruption of actin cytoskeleton reduces both *E. coli* internalization as well as IL-8 production in DNP co-treated epithelium. (a) T84 cell monolayers were treated with *E. coli* (1 x 10^6 cfu/ml) ± dinitrophenol (DNP, 0.1 mM). T84 cell monolayer were pretreated with cytochalasin D (CyD, 0.2 μM) for 30 min and then treated with DNP + *E. coli* + cytochalasin D for 16 hrs and *E. coli* internalization was measured through gentamycin assay. (b) T84 cell monolayers were treated with DNP, DNP ± *E. coli* ± cytochalasin D or TNFα (10 ng/ml) ± cytochalasin D for 16 hrs and IL-8 was measured (data are mean ± SEM; n=9 from 3 separate experiments * p <0.05 from the control group, # p <0.05 versus DNP, † p <0.05 from the *E. coli* treated group, ** p <0.005).

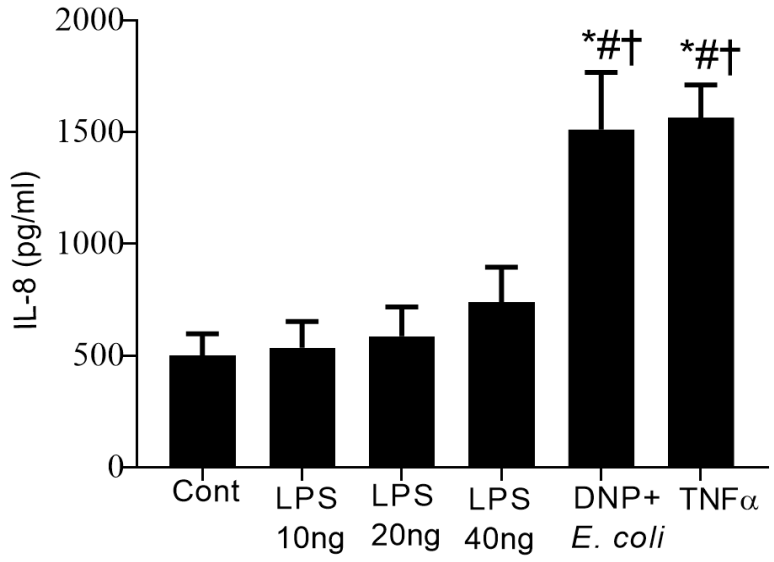

Figure 32: Treatment of T84 cell monolayers with different concentrations of LPS for 16 hrs do not exhibit increase in IL-8 production. T84 cell monolayers treated with *E. coli* HB101 (1 x 10^6 cfu/ml) ± dinitrophenol (DNP, 0.1 mM) or TNFα (10 ng/ml) for 16 hrs served as positive control (data are mean ± SEM; n=9 from 3 experiments, * p <0.05 from LPS (10 ng/ml), # p <0.05 from LPS (20 ng/ml), † p <0.05 from LPS (40 ng/ml).

3.11 IL-8 synthesis in DNP + *E. coli* treated T84 epithelium is mediated by MAPK, ERK and ROS

Increased P-ERK1/2 expression was observed in the DNP + *E. coli* treated T84 monolayer 4-hrs post-treatment. This was reduced by co-treatment with the ERK inhibitor U0126 as well as mitoTEMPO. (Figure 23) Additionally, co-treatment with U0126 or mitoTEMPO reduces the DNP evoked increase in intracellular bacteria (Figure 22 & 24) as well as IL-8 production. (Figure 33)

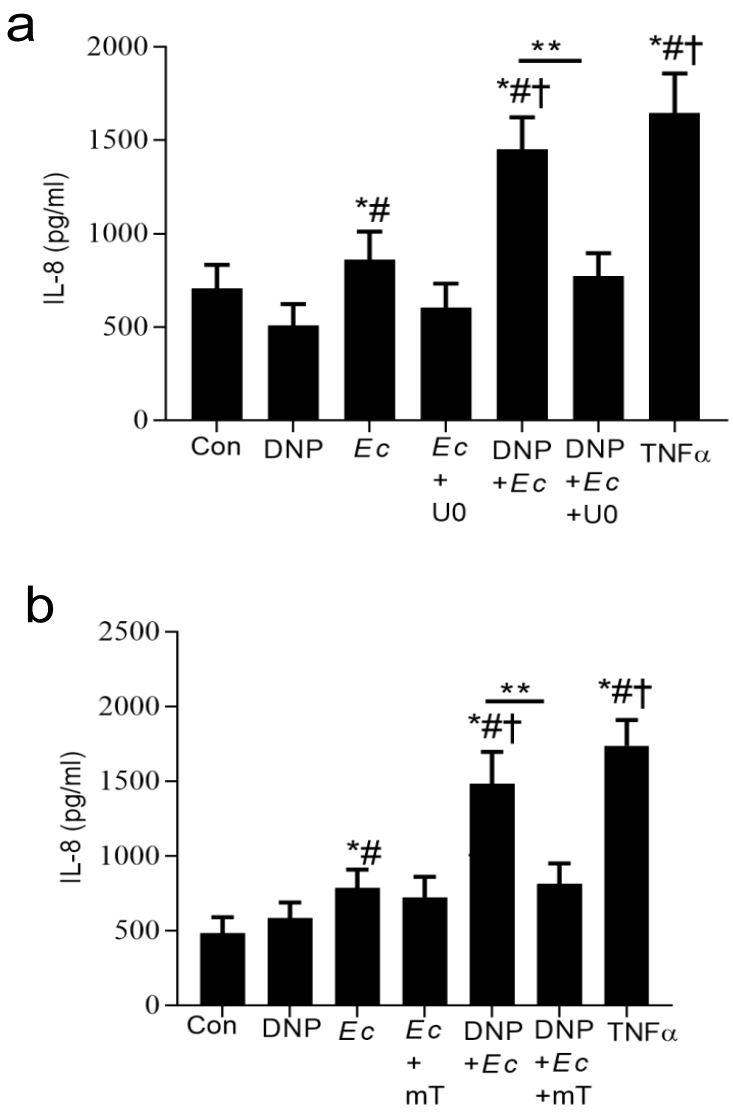

Figure 33: IL-8 synthesis in DNP + *E. coli* treated epithelium is mediated by MAPK, ERK and ROS. ERK signaling and ROS is involved in IL-8 production from the dinitrophenol (DNP) + *E. coli* HB101 treated epithelium. (a) Co-treatment of DNP (0.1 mM) + *E. coli* (1 x 10^6 cfu/ml) treated T84 monolayer with ERK inhibitor U0126 (U0, 25 μM) exhibit significant reduction in IL-8 production compared to DNP + *E. coli* treated epithelium 16 hrs post-treatment (data are mean ± SEM; n=9 from 3 separate experiments; * p <0.05 from control group, # p <0.05 versus DNP, † p <0.05 from the *E. coli* treated group, ** p <0.005). (b) Additionally, co-treatment of mitochondria targeted antioxidant mitoTEMPO (mT, 10 μM) to DNP + *E. coli* treated epithelium significantly reduced the IL-8 production compared to DNP + *E. coli* treated epithelium (data are mean ± SEM; n=9 from 3 separate experiments; * p <0.05 from control group, # p <0.05 versus DNP, † p <0.05 from *E. coli* treated group, * p <0.05, ** p <0.005). T84 cell monolayers were

pretreated with ERK inhibitor U0126 (25 μM) or mitoTEMPO (10 μM) for 30 min before they were co-treated with DNP + *E. coli* + U0126 (25 μM)/ mitoTEMPO (10 μM).

3.12 Absence of NOD2 in DNP + *E. coli* treated T84 epithelium resulted in increased IL-8 production

The absence of NOD2 in a metabolically stressed epithelium resulted in an increased number of viable intracellular bacteria compared to the metabolically stressed wild type epithelium as shown earlier. (Figure 18d-e) Stable knock-down of NOD2 in T84 cells was performed through shRNA. Exposing NOD2 knock-down T84 monolayers to DNP and nonpathogenic *E. coli* HB101 evokes increased IL-8 production compared with DNP ± *E. coli* HB101 treated WT T84 monolayers. (Figure 34)

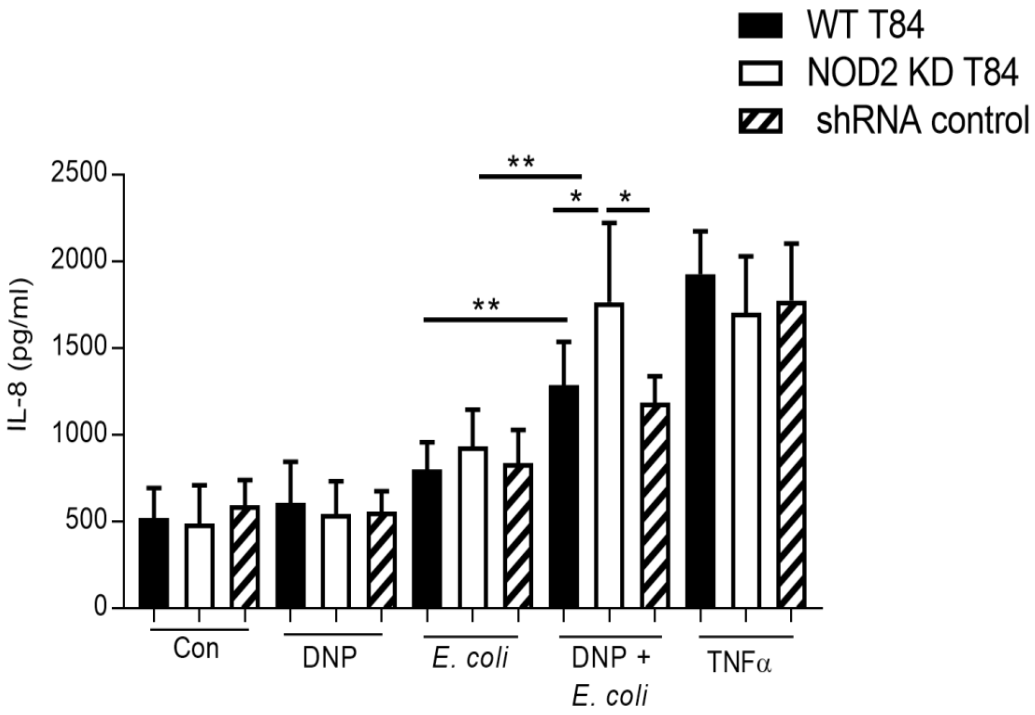

Figure 34: Knock-down of NOD2 (NOD2 KD) from T84 epithelium resulted in increased IL-8 production when treated with DNP + *E. coli*. Absence of NOD2 from the T84 epithelium (NOD2 KD) resulted in increased IL-8 production when treated with dinitrophenol (DNP) + *E. coli* HB101 compared to wild type (WT) epithelium treated with DNP (0.1 mM) + *E. coli* (1 x 10^6 cfu/ml) 16 hrs post-treatment (data are mean ± SEM; n=9 from 3 separate experiments, * p <0.05, ** p <0.005, *** p <0.0005). TNFα (10 ng/ml) treated epithelium serve as a positive control.

CHAPTER 4- DISCUSSION

4.1 Experimental design - pros and cons of the experimental system

T84 cells, a human colonic carcinoma derived cell line, were utilized as our main tissue culture model of the colonic epithelium.(236) These cells form electrically tight monolayers if grown on collagen-coated transwell supports in conjunction with serum.(253) These cells were selected for the following reasons: 1) to maintain consistency in the model system utilized in several studies conducted by the McKay lab (118, 156-158); 2) T84 cells maintain polarity akin to differentiated epithelial cells, having distinct apical and basal sides; 3) T84 monolayers can grow as a confluent monolayer with tight junctions, which restricts paracellular flux, enabling closer examination of transcellular migration of bacteria; 4) T84 cells show minimal mucus production, which benefits our study as defective mucus production has been linked to IBD and mice lacking mucin genes develop colitis spontaneously (254, 255); and, 5) this cell line has been important in defining mechanisms of chloride secretion and regulation of tight junction form and function, i.e. paracellular permeability.(256, 257)

In defining and assessing the principles underlying the control of epithelial permeability, human-colon derived epithelial cell lines have repeatedly proven to be useful tools (257, 258); however, a caveat of this model is that the cells are immortalized. Immortalization necessarily coincides with genetic instability and other non-representative physiological characteristics such as native functions as well as responsiveness to various stimuli, which may limit the generalizability of the results.(257) However, our results don't rely on a single cell line as we reconfirm our results in another human colon-cancer cell line, HT29.

Subsequently, we sought to recapitulate the observed phenomena *in vitro* by utilizing intestinal organoids from NOD2$^{-/-}$ and WT mice. Primary stem cell-derived colonic organoids have a cellular composition similar to the colonic epithelium, and retain the crypt structures, but

are devoid of any mesenchymal or immune cells. Within the context of our investigation of epithelial-microbial interactions, growing colonic organoids on a monolayer was relevant and useful.(259)

At the same time, the mechanistic studies conducted could have been complemented by assessment of colonic biopsies from Crohn's disease patients carrying the specific NOD2 mutations (R702W, G9008R and L1007fsC), as well as control patients. These mutations result in a loss of function of NOD2 and are major risk factors associated with Crohn's disease.(260) Biopsies could be placed into Ussing chambers and treated with DNP ± *E. coli* HB101 or DNP + FITC conjugated dead *E. coli.* Colonic permeability could be gauged by TER and *E. coli* flux across the epithelial barrier.(105) Pharmacological studies could also be performed such as testing the effect of mitoTEMPO or the ERK inhibitor, U0126, on *E. coli* flux across the epithelial barrier.

Our model for metabolic stress was 2,4-dintrophenol (DNP), an oxidative phosphorylation uncoupler. It functions by disrupting the mitochondrial proton gradient.(155) DNP was chosen for its specific ability to reduce cellular ATP levels, as they are often lower in tissues from IBD patients.(119) At 0.1 mM, DNP significantly lowered ATP levels inside T84 cells by 4 hours of incubation.(158) DNP has been used in other cell lines besides IECs to evoke metabolic stress; 1 mM of DNP was found to half ATP production in the human Jurkat T-cell lymphoma cell line after 6 hours of incubation.(261) Importantly apoptosis is mechanistically energy-dependent and ATP depletion was shown to disfavor apoptosis in Jurkat cells.(261) It is feasible that increased bacterial transcytosis stemmed from cell-death; however, DNP (0.1mM, 16 hrs) is incapable of evoking caspase-3-mediated apoptosis (Figure 12) or DNA laddering, indicators of apoptosis, in T84 epithelia.(156) At 0.1 mM DNP does not cause bacterial death

(Figure 8a). At the same time, 24 hrs incubation with DNP did induce necrosis as shown by trypan-blue staining or lactate dehydrogenase release (an indicator of necrosis).(157)

Following previous work in the McKay lab, indomethacin, a common NSAID, was also utilized as a metabolic stressor.(138) Indomethacin inhibits both cyclooxygenase-1 (COX-1) and cyclooxygenase-2 (COX2), and blocks prostaglandin production.(136, 137) Indomethacin can also solubilize lipids from phospholipids allowing the NSAID to enter the epithelium.(262) Importantly, it has been previously shown in *in vitro* and *in vivo* studies that NSAID uncouples oxidative phosphorylation.(136, 263) In turn, this results in lowered ATP levels and increased ROS and Ca^{2+} efflux from the cell. We hypothesized that this decrease in energy levels (ATP) could be a driving factor in increasing epithelial permeability, both paracellular and transcellular, resulting in increased translocation of mucosal antigens including bacteria and a trigger for inflammation.(137, 138, 156, 262)

A decline in energy (ATP) levels as a result of mitochondrial dysfunction also affects intercellular (paracelluar) permeability. Importantly, apical junctional complexes are controlled by ATP dependent actin-myosin complexes and therefore decreases in energy levels can increase paracelluar permeability.(131) In one study, Caco-2 epithelial cells treated with rotavirus, which targets mitochondria in its mechanism of action, displayed a significant drop in mitochondrial activity after 10 hrs followed by a drop in TER at 24 hrs post-infection.(131) Another study in which HeLa cells (cervical epithelium) were treated with *Citrobacter rodentium* showed similar findings; cells displayed decreased mitochondrial membrane potentials followed by a decrease in TER.(130) These findings were recapitulated in our lab in multiple contexts; metabolically stressed T84 epithelia – those treated with DNP + *E. coli* alone - showed a significant decline in TER compared to epithelia treated solely with *E. coli* HB101, while indomethacin (NSAID)

treatment also enhanced paracellular permeability after co-treatment with *E. coli*.(138) Taken together, it is evident that mitochondrial dysfunction greatly enhances paracellular permeability; however, the primary focus of our study was bacterial entry into the mucosa via the transcellular pathway. We chose to prioritize transcellular translocation because our work demonstrated that it precedes the increase in paracellular flux; initiating ~4 hrs post-treatment of T84 monolayers with DNP + *E. coli*, long before any significant changes in paracellular permeability occur.(157)

The commensal microbiota plays an important role in intestinal function and many studies have implicated this community in IBD.(170, 264) Remarkably, reduced diversity of the colonic microbiota has been found in cohorts of patients with IBD based on 16s rRNA profiling.(265) Indeed, in a healthy gut 64% of bacteria are *Firmicutes*, while IBD patients show reduced diversity in this phylum, with specific decreases in the *Clostridium leptum* group.(265) There are also higher levels of colonic *Proteobacteria*, gram negative bacteria that include the IBD-implicated *Escherichia coli*, in some IBD patients.(127, 266-268) Indeed, luminal concentrations of *E. coli* are markedly different in Crohn's disease patients, and titers to *E. coli* specific antibodies are typically higher in Crohn's disease patient serum.(269) One study found 37-55% of IBD patients have antibodies to *E. coli*, while the same was true for fewer than 5% of control subjects.(270) Critically, differences in microbiota composition have also been associated with IBD-susceptibility genes NOD2 and ATG16L1.(127)

Because of the important association of *E. coli* with IBD, the *E. coli* strain HB101 was the predominant bacterial strain utilized in our study. *E. coli* HB101 is a non-pathogenic, non-invasive, laboratory strain of bacteria, akin to a commensal organism. We chose HB101 for our model so we could confidently attribute changes in bacterial internalization to mitochondrial dysfunction as opposed to invasion by the *E. coli* or effect of pathogenic *E. coli*. One example of

such a strain is *E. coli* LF82, an adherent/invasive *E. coli* (AIEC) that has been detected in Crohn's disease patients.(271) These bacteria are capable of adhering to and invading IECs, while also surviving in macrophages without host cell death for a sustained period of time.(272) Consequently, they would not be a suitable choice for our model system as they are likely to show high levels of internalization without any metabolic stress. Importantly, however, we were able to confirm our *E. coli* HB101 findings with another commensal bacterium, *E. coli* F18. It would, however be of interest to determine if the invasion of epithelia (or macrophages) by *E. coli* LF82 is increased by metabolic stress.

4.2 Discussion (Results)

NOD2, a member of the NOD-like Receptor Family (NLR) is the intracellular sensor of muramyl dipeptide (MPD), the smallest constituent of peptidoglycan of gram positive and gram-negative bacteria.(202) NOD2 variants associated with Crohn's disease result in loss of protein function.(212) NOD2 deficiency is insufficient for spontaneous intestinal inflammation, but exacerbates murine susceptibility to dextran sodium sulfate-induced colitis.(205, 273) A study by Jing *et al.* shows that *Pglyrp*$^{-/-}$ (peptidoglycan recognition protein expressed in intestinal epithelium) and *NOD2*$^{-/-}$ double knock-out mice have increased susceptibility to DSS-colitis compared to single gene deficiency.(274) Increased sensitivity to DSS in these mice is dependent upon enhanced apoptosis of the intestinal epithelium as well as changes in the gut microflora.(274) Another study determined that *NOD2*$^{-/-}$ mice display an increased risk of DSS-induced colitis instigated by microbial dysbiosis; this effect was alleviated by fecal implants from the control mice (*NOD2* sufficient mice).(204) The role of NOD2, has been extensively studied in macrophages and dendritic cells.(275) In these APCs (antigen presenting cells), NOD2

deficiency has been implicated in defective killing of internalized bacteria.(275) NOD2 is expressed at low levels in transporting enterocytes, which comprise the body's largest interface with the microbiota.(184) This convergence of findings provided strong motivation for assessing the role of NOD2, and any subsequent implications for its deficiency, within IECs in conjunction with mitochondrial deficiency and a commensal-rich environment.

Basal expression of NOD2 in non-stimulated IEC (T84 cells) is minute (below detection on immunoblots), and metabolic stress induced by DNP, was insufficient to heighten NOD2 expression in T84 epithelia (Figure 14b). However, T84 cells incubated with *E. coli* alone for 16 hrs showed enhanced NOD2 mRNA and protein expression, which was further exaggerated in cells co-treated with *E. coli* and DNP. This aligns with literature on NOD2 in infected cells showing that NOD2 is a cytosolic sensor of intracellular bacteria (195, 276); that is, metabolic stress decreases barrier function and enables increased uptake of extracellular bacteria. Given that NOD2 levels increase significantly in response to intracellular bacteria, understanding the implications of NOD2 depletion on the enterocyte was an essential follow-up question, especially given loss of function mutation-NOD2 as the major genetic susceptibility trait of Crohn's disease.

To investigate how NOD2 deficiency affects enterocyte function, we chose to consider levels of bacterial internalization as a proxy of barrier function. Wild-type T84 cells treated with DNP + *E. coli* for 16 hrs showed obvious and consistent increases in levels of bacterial internalization (Figure 9c-d & Figure, 10-11); knock out of NOD2 (Figure 17a-c) along with uncoupling of oxidative phosphorylation resulted in significantly increased levels of intracellular bacteria when compared to metabolically stressed wild-type (WT) T84 epithelium

(Figure 19a-c). Taken together, this signifies that NOD2 loss-of-function renders the enterocyte more vulnerable to the effects of transcellular permeability instigated by metabolic stress. This assertion is reinforced by the dual findings: 1) NOD2 KD cells treated with indomethacin, showed a substantially greater number of intracellular *E. coli*, relative to T84 WT (Figure 20); and, 2) epithelia isolated from a $NOD2^{-/-}$ mice and treated with DNP also exhibited a significant increase in intracellular bacteria compared to primary cultures derived from WT mice (Figure 21c-d).

Mitochondrial generation of ROS is the result of ATP production by the electron transport chain because of leakage of electrons onto molecular oxygen. However, during metabolic stress lower ATP generation leads to heightened respiration rates, which ultimately cause a rise in ROS levels. ROS are potent intracellular signaling molecules that modulate many cell functions such as disulfide bond formation and protein folding, and cross talk with transcription factors such as NF-kB of the cell.(277) To counteract ROS generated during oxidative phosphorylations, antioxidants are produced by the cell such as superoxidases. However, in times of metabolic stress, ROS generation can overtake antioxidant generation; excess ROS has been shown to be both a by-product and an instigator of inflammation and has been linked to IBD.(2, 121, 278, 279) Most of the studies done on ROS generation in IBD are related to the phagocytic activities of inflammatory cells (e.g. neutrophils and macrophages); however, few studies have examined the enterocytes as a source of ROS in IBD and the relationship with microbiota.(116, 280)

In the presence of excess ROS, the cell experiences oxidative stress that can culminate in apoptosis.(281) In addition to the potency of intra-cellular ROS, application of H_2O_2 (extracellular ROS) to epithelial monolayers has been shown to increase enterocyte

permeability.(282, 283) Topical application of mitoTEMPO (a mitochondrial-targeted antioxidant), to human colonic biopsies mounted in Ussing chambers, and co-treated with DNP attenuated *E. coli* translocation, while systemic mitoTEMPO treatment of mice suffering DSS-induced colitis reduced disease severity and reinforced barrier function.(105) Thus, I investigated whether ROS levels were changed in NOD KD cells; analyses showed that NOD2 KD T84 epithelium treated with DNP + *E. coli* generated more ROS than similarly treated normal WT-cells (Figure 22a). Following this result, mitoTEMPO treatment was found to rescue bacterial internalization in NOD2 KD enterocytes, reducing both ROS levels as well as the number of intact, intracellular bacteria present in the cells (Figure 22a-b). This difference in ROS generation between NOD2 KD cells and WT cells could have many differing roots; possibilities range from heightened sensitivity to the oxidative un-coupler, or it being a consequence of the enhanced number of intracellular bacteria. Thus, additional evidence is presented in support of manipulating ROS as a means to control epithelial barrier function in various IBD phenotypes.

Wild-type T84 epithelia treated with DNP + *E. coli* show lower levels of IκB, which is degraded as NF-κB is activated.(157) NOD2, as a cytosolic sensor of MDP, can trigger downstream NF-κB and MAPK signaling.(202) MAPKs, including ERK1/2 regulate endocytosis.(221, 222) It has been observed that both WT-T84 and NOD2 KD T84 cells exhibit increased phosphorylation of ERK1/2 in response to treatment with DNP + *E. coli* and a significant reduction was subsequently observed after co-treatment with both mitoTEMPO and U0126, an inhibitor of the MAPK-ERK pathway (Figure 23a-b). I also found that U0126 treatment significantly reduced the DNP-directed increase in intracellular *E. coli* HB101, latex beads, and dead *E. coli* in WT and NOD2KD T84 cells (Figure 24a-c). ERK1/2 activates ADP ribosylation factor (ARF)-6 a protein implicated in endocytosis and intracellular trafficking.(284)

A study by Smyth *et al.* showed that IFNγ-induced *E. coli* HB101 internalization into the T84 epithelial cell line is ERK1/2 dependent.(223) Additionally, they showed ERK1/2 dependent activation of ARF-6 in IFNγ treated T84 cells. Pharmacological inhibition of ERK1/2 by U0126 or siRNA mediated knock-down of ARF-6 reduced the IFNγ induced increased *E. coli* HB101 internalization in T84 cells.(223) My results are consistent with the findings of Smyth *et al*.(223) Subsequently studies should be directed towards the role of ARF-6 in DNP + *E. coli* treated wild-type and NOD2 KD, as a potential target to manipulate epithelial-microbial interaction in the context of metabolic stress.

It would be valuable to investigate the effect of metabolic stress on murine models bearing inducible intestinal epithelium specific knock-out of ERK1/2. Primary intestinal epithelial cells could be isolated from $NOD2^{-/-}$ and WT mice and then treated with DNP ± *E. coli;* intracellular bacteria levels can be determined through the gentamycin assay. Additionally, colonic organoids (as a monolayer) can be grown from colonic tissues isolated from these mice and the effect of metabolic stress in the context of epithelial–microbial interaction investigated. Previous studies have reported the role of ERK1/2 activation on IEC proliferation and migration (285, 286), and deletion of ERK1/2 from IECs may have deleterious developmental effects, rendering the mice unable to survive. However, further investigation on how ERK 1/2 modulation affects barrier permeability may prove to be useful in deciphering intestinal inflammation.

MitoTEMPO's reduction of both viable bacteria in the enterocyte and P-ERK levels reinforces the role of disrupted-mitochondria-derived ROS in instigating the internalization of extracellular material, in an ERK 1/2 dependent manner. Intriguingly, the pattern holds for both WT and NOD2KD cells, with an exacerbated impact in the latter (Figure 22b, 23a-b). This

follows previous research done by Wang *et al.* demonstrating that mitochondrial ROS inhibition by mitoTEMPO reduces DNP-instigated *E. coli* internalization into T84 monolayers.(105)

While it had been established that DNP + *E. coli* treatment in NOD2 KD cells results in increased bacterial internalization, the cause had yet to be determined: were the elevated numbers caused by increased enterocytic permeability, or were they a consequence of reduced bacterial killing? To answer this question, I differentially treated WT and NOD2 KD monolayers with DNP + dead fluorescent bacteria or inert fluorescent beads, and saw no disparity in uptake, indicating that increased uptake was unlikely to be the sole cause of the increased intracellular bacterial levels. However, because of ROS's involvement with ERK signaling, a modulator of epithelial permeability, I cannot wholly discard the possibility of increased bacterial uptake rates. At the same time, NOD2 depleted T84 cells treated with DNP + *E. coli* for 4 hrs yielded significantly higher numbers of viable intracellular bacteria 12 hrs later than the corresponding WT control, suggesting that bacteria initially taken up into NOD2 KD cells survived for longer and potentially multiplied. Taken together, I speculate that the attenuated sensing, an essential effector function of NOD2, and subsequent killing of internalized bacteria is the major cause of heightened bacterial levels. Future studies should specifically address bacterial replication in the model.

NOD2 sensing of internalized bacteria is strongly tied to autophagy. Upon entry of bacteria, NOD2 recruits ATG16L1 and helps initiate xenophagy.(213) Autophagy is a process of self-degradation that is used for organelle recycling during periods of starvation, but can also be redirected as a line of defense against invading microorganisms, vis-a-vis xenophagy.(208, 210, 275) Indeed, previous studies showed defective killing of *Salmonella* in epithelial cells harboring Crohn's disease associated NOD2 variants.(212) This is followed by studies in macrophages and

dendritic cells showing NOD2 depletion increases the number of viable, intracellular bacteria through attenuated killing.(200, 287) Thus, taken together, I assert that increased bacterial internalization, enabled by metabolic stress, is potentiated by reduced IEC sensing stemming from NOD2 depletion, which ultimately results in reduced bacterial killing, possibly via reduced autophagy as indicated by reduced LC3-lI levels (Figure 27a-b). The role of autophagy can be further supplemented by growing the colonic organoids from the *ATG16L1*$^{-/-}$ and WT mice as a monolayer and treating them with DNP ± *E. coli* for 16 hrs. After 16 hrs, the number of intracellular bacteria can be measured by gentamycin assay.

Microtubule-associated protein 1 light chain (LC3-I) is a cytosolic protein that contains a glycine residue at the amino terminal end.(288) Following initiation of autophagy, the C-terminal glycine is conjugated to the lipophilic phosphatidylethanolamine (PE) moiety to form LC3-II.(288, 289) The presence of phosphatidylethanolamine facilitates the integration of LC3-II into the autophagosome through Atg (autophagy related) protein activity; LC3-II is reported to be involved in cargo selection for degradation.(288-290) Additionally, *in vitro* studies have suggested that LC3-II promotes membrane tethering and fusion.(290) LC3-II is a protein that specifically localizes to the autophagosome (289), therefore western blot for LC3-I and LC3-II (reliable antibodies are available from different commercial sources) following normalization for overall levels of LC3-II via a loading control such as ß actin is a widely used method of measuring autophagy.(291)

Rapamycin is a lipophilic macrolide antibiotic that induces autophagy by inhibiting mTOR (mammalian target of rapamycin; a negative regulator of autophagy).(292) Induction of autophagy with rapamycin resulted in decreased numbers of viable intracellular bacteria in WT and NOD2$^{-/-}$ T84 epithelium treated with DNP (Figure 27c), eliminating the differences between

the two cell types through promotion of xenophagy. This is consistent with previous research demonstrating that MDP stimulated autophagy can be reactivated in epithelial cells harboring NOD2 mutations after rapamycin treatment.(212) The increased load of bacteria inside the NOD2 KD epithelium can lead to apoptosis, exaggerating the barrier defect. Therefore, reducing the number of intracellular bacteria inside the NOD2 KD epithelium by enhancing the autophagy through rapamycin treatment is a good potential intervention strategy to decrease the barrier defect.

Methods beyond LC3-II assessment exist to evaluate autophagy; other markers exist, such as Beclin-1. Beclin-1 is a Bcl-2-homology (BH)-3 domain only protein, and the mammalian homologue of yeast Atg6/Vsp30. Beclin-1is a constituent of the type III phosphtidylinositol 3-kinase complex involved in the formation of autophagic vesicles.(293) The death associated protein kinase (DAPK) phosphorylates Beclin-1 to promote its dissociation from Bcl-2-like proteins, which then induces autophagy.(294) Consequently, Beclin-1 could be measured to assess autophagy to complement measurement of the LC3-II protein. This can be performed via western blot of cell lysates from DNP + *E. coli* treated wild-type and NOD2 KD T84 epithelia.

Neutrophils play an important role in the gut by removing microbes that traverse the epithelium. However, in addition to their defensive role, excessive recruitment of neutrophils to the intestinal mucosa is part of an inflammatory response. Neutrophils are important actors in IBD; contributing to inflammation and tissue damage by generating excessive ROS in order to kill the phagocytosed bacteria which at the same time damages the surrounding tissue.(295) IECs serve as the first line of defense in the gut, and produce the potent neutrophil chemoattractant, IL-8.(227) Elevated levels of IL-8 have been found in the mucosa of IBD patients compared to control.(229) As discussed previously, metabolic stress has also been shown to be a prominent

contributing factor in IBD; colonic biopsies from IBD patients revealed swollen mitochondria with irregular cristae, as well as reduced levels of intestinal ATP.(118, 296) Subsequently, I chose to examine the effects of metabolic stress on enterocytic IL-8 production in the presence of non-invasive, non-pathogenic *E. coli* HB101.

At four hours, metabolically stressed epithelial cells co-treated with DNP + *E. coli* did not show increased IL-8 production compared to untreated or *E. coli* only treated cells, but did after 16, 24, and 42 hrs (Figure 28a-b). The lack of difference after 4 hours likely reflects the time it takes for bacterial internalization to happen and to trigger IL-8 gene upregulation, transcription and finally translation. Importantly, metabolic stress alone was insufficient to increase IL-8 secretion, as was *E. coli* alone. However, as our earlier work has shown, oxidative phosphorylation uncoupling increases transcellular permeability, which enables the passage of bacteria into the enterocyte (156, 158) and potentially activation of intracellular pattern recognition receptors; indeed, this is compatible with the increased number of intracellular bacteria in NOD2 KD cells.

To confirm whether it was bacterial uptake itself, or the uptake of particular products instigating increase in IL-8 secretion, epithelia were differentially treated with inert bacteria – sized beads, dead *E. coli*, and live *E. coli*, in the presence of DNP. We found that DNP + inert bead treated epithelia evoked significantly less IL-8 production compared to epithelial treated with DNP + *E. coli* (Figure 29b). In contrast, T84 cells treated with dead *E. coli* showed comparable IL-8 production to monolayers exposed to DNP and *E. coli* HB101 (Figure 29a). Taken together, this means that IL-8 production in a metabolically stressed epithelium is dependent on bacterial components, but not necessarily intact, living bacteria. This further

suggests that PAMPs from internalized bacteria are responsible for downstream induction of IL-8 production.

IECs express PRRs (pattern recognition receptors) intracellularly – TLR-7 (recognizes ds RNA from virus), TLR-9 (recognizes CpG DNA from bacteria) and transmembrane membrane TLR-4 (low expression, recognizes LPS from gram negative bacteria).(231, 251) To assess the possibility that increased IL-8 production was due to TLR-4 mediated signaling, I treated T84 monolayers with different concentrations of LPS. LPS treated epithelia showed significantly lower production of IL-8 compared to DNP + *E. coli* treated epithelium (Figure 32), suggesting intracellular TLR activation and signaling occurs in metabolically stressed epithelia. Another feasible experiment to assess the role of LPS in invoking IL-8 secretion in a DNP + *E. coli* HB101 treated epithelium would be to co-treat with the LPS inhibitor, Polymyxin B, and then further evaluate if IL-8 secretion is attenuated. To assess whether extracellular uptake of bacteria is required for IL-8 generation by enterocytes, I targeted two components of the internalization process: endosome formation and the actin cytoskeleton.(158) Chloroquine, an endosome maturation inhibitor, was administered to metabolically stressed epithelia and resulted in a significantly lower IL-8 yield compared to cells treated with DNP + *E. coli* alone (Figure 30b). Addition of cytochlasin D, a disrupter of actin polymerization, also manifested in significantly lower IL-8 secretion compared to matched cells treated with DNP + *E. coli* alone (Figure 31b).

Bacteria are typically taken up via endocytosis, and enterocytes have been shown to undergo membrane ruffling after DNP + *E. coli* exposure.(157) My work shows that disruption of either endocytosis or actin polymerization is sufficient to reduce IL-8 production, indicating that IL-8 generation is caused by the endocytosis of bacterially-derived products. Importantly,

TLR-9, a detector of microbial DNA, is localized to the endosome and has been previously shown to facilitate IL-8 secretion in IECs after CpG DNA exposure.(231) However, there was no significant difference in IL-8 production between the TNFα treated T84 monolayers co-treated with chloroquine or cytochlasin D compared to the epithelium treated with TNFα alone. To confirm the role of TLR-9 beyond pharmacological inhibition, we can knock-down TLR-9 expression via siRNA.

Nearly all TLR signaling heavily relies on MYD88, a TIR domain containing adaptor molecule which enables the activation of the NF-κB and MAPK pathways leading to the expression of pro-inflammatory cytokines.(245) Therefore, to understand if TLR signaling was involved in IL-8 expression in a metabolically stressed epithelia I treated monolayers with the MyD88 inhibitory peptide in addition to the typical metabolic stressor and *E. coli*. Again, I found attenuated IL-8 production from the epithelium (Figure 30a). This reduction reinforces the role of TLR signalling in IL-8 secretion in metabolically stressed epithelia.

Previous work showed that the severity of DSS-induced colitis in mice is reduced by systemic delivery of mitoTEMPO, an antioxidant.(105) To understand whether antioxidant treatment can reduce IL-8, IECs were treated with mitoTEMPO + DNP + *E. coli*. Such treated monolayers showed a significant decrease in IL-8 levels compared to matched monolayers lacking mitoTEMPO (Figure 33b). Co-treatment of DNP + *E. coli* treated epithelium with mitoTEMPO significantly reduced bacterial internalization compared to DNP + *E. coli* treated epithelium alone, further reiterating that intracellular bacteria is one of the major contributors to IL-8 production (Figure 22b). This implicates ROS as a potential therapeutic target for reducing inflammation in IBD, corroborating a variety of other studies.(297-299)

My work showed that mitochondrial perturbation triggers increased MAPK signaling and subsequently increased epithelial permeability (Figure 23a-b). Here, I show that ROS generation due to dysfunctional mitochondria is also capable of eliciting pro-inflammatory, IL-8 signaling. MAPK signaling, particularly ERK1/2 has also been implicated as regulators of AP-1 transcription factors that modulate IL-8 gene expression.(215) I have shown through immunoblotting that the epithelium treated with DNP + *E. coli* + mitoTEMPO displayed reduced expression of P-ERK1/2 compared to epithelium treated with DNP + *E. coli* alone. Epithelia treated with U0126, an ERK 1/2 inhibitor, also showed significantly less IL-8 production than untreated epithelia (Figure 33a). As a result, ROS-driven IL-8 production in enterocytes can be regarded as ERK 1/2 dependent, yielding an additional therapeutic possibility for enteropathies like IBD.

Finally, NOD2 is an important cytosolic sensor protein that facilitates xenophagy and subsequently enables killing of bacteria.(200, 287). I hypothesized that since NOD2 depletion would result in increased numbers of viable, intracellular bacteria, intracellular PRRs would detect microbial components more often, resulting in a stronger inflammatory response. To test this, I differentially treated WT and NOD2 KD T84 monolayers with DNP + *E. coli* for 4 or 7 hrs; upon the conclusion of the incubation period, I killed external bacteria and let the monolayers grow for 12 or 9 more hours and measured intracellular bacteria levels afterwards. In this experiment, NOD2 KD cells showed significantly greater intracellular bacteria counts. In tandem, I measured IL-8 levels in WT and NOD2 KD T84 monolayers that were exposed to DNP + *E. coli* and, as predicted, observed greater IL-8 production in NOD2 KD cells relative to the WT (Figure 34). Taken together, these data strongly suggest that heightened intracellular

bacterial loads correspond to enhanced IL-8 production in NOD2 KD cells; for full confirmation, I can repeat the bacteria experiment but directly measure IL-8 levels in the supernatant instead.

While NOD2 is responsible for RIP2 activation and subsequent NF-κB and MAPK activation, depletion did not reduce epithelial IL-8 expression, but indeed increased it. This may be because NOD2 is also implicated in instigating autophagic and xenophagic activity; loss of NOD2 leads to greater numbers of viable, intracellular bacteria, up taken through endocytosis. Aside from NOD2, other intracellular PRRs exist, such as the NLR and RLR family, that can also detect the increased bacterial load. NOD1, for example, recognizes the γ-D-Glu-mDAP (IE-DAP) peptide, which is another peptidogylan derivative found in gram-negative bacteria.(159) NOD1 also triggers NF-κB activation and can hereby enhance IL-8 production. Taken together, my study demonstrates that loss of bacterial killing in NOD2 deficient patients contributes to enhanced IL-8 production through increased retention of live bacteria in the metabolically stressed epithelia.

4.3 Future work

In the McKay lab, it was reported that treatment of the T84 epithelium with DNP (0.1mM) for 6 hrs results in an increased number of pseudopodial extensions of 0.5-1.0 μm; pseudopodial extension numbers were further increased in epithelia co-treated with DNP + *E. coli*.(157) Previous studies have indicated the involvement of the small GTPase, ADP-ribosylation factor-6 (ARF6), in receptor mediated endocytosis via membrane trafficking, endosome recycling and exocytosis of secretory granules.(284, 300) At the same time, ARF-6 has been reported to be a component of actin-rich membrane protrusions and ruffles.(300, 301) Subsequently, it would be insightful to investigate the role of ARF-6 in DNP-induced

transcytosis of *E. coli* HB101 in WT and NOD2 KD T84 cells. ARF activity can be measured in WT and NOD2 KD T84 cells following their treatment with DNP + *E. coli* through an ARF-6 pull-down assay. At the same time, the effect of the absence of ARF6 (instigated through ARF-6 specific siRNA knock-down) in DNP-induced transcytosis in epithelium could be measured.

Additionally, we have previously reported on the involvement of the Src kinase Fyn in IFN**γ**-induced transcytosis of *E. coli* HB101 in the T84 epithelium. It would be intriguing to further explore whether Fyn is also involved in DNP-mediated transcytosis of *E. coli* HB101.(235) Wild-type or NOD2 KD T84 epithelium could either be treated with the Fyn inhibitor PP1 (60 nM; a dose with specificity to Fyn (235)), or Fyn could be knocked-down using siRNA (235) and DNP-induced changes in epithelial permeability (TER and bacterial transcytosis) or ROS generation could be assessed.

Another interesting future experiment could be to assess whether metabolic stress can instigate internalization of *E. coli* HB101 in a colonic epithelium model in an *in vitro* setting. In my study, I observed that metabolic stress can instigate a greater number of intracellular bacteria in WT epithelium; however, when NOD2 was knocked-down from these cells, there was a significantly greater number of intracellular bacteria compared to the WT T84. To investigate these results in a more complex model system, we can grow colonic organoid from WT or $NOD2^{-/-}$ mice, or from control or Crohn's disease patients having NOD2 mutations and induce metabolic stress with DNP ± GFP tagged *E. coli* HB101 into the lumen of the organoid through microinjection. After a specified period of time, the outside bacteria can be killed by gentamycin, so we can assess the number of internalized bacteria. Alternatively, we can image the organoid by quenching the external bacteria. For a more realistic metabolic stressor, we can also treat the organoids with TNFα ± IFNγ + *E. coli* HB101 and assess intracellular bacteria counts. Another

option, however, could be to grow these colonic organoids as monolayers as described by Fernando *et al.* and then treat them with metabolic stressors and *E. coli* HB101 and assess intracellular bacteria counts by gentamycin assay. (302) Doing this will enable us to visualize bacterial translocation in an organ-mimicking environment. Our current study aimed to assess translocation rather than paracellular flux, and this procedure will let us visualize it directly.

We can also assess where in the cell, *E. coli* HB101 localizes to, and whether co-localization of bacteria and NOD2 occurs. For this, we can perform immunoflourescence and immunolabel the NOD2, cellular compartments and *E. coli*, or alternatively, use fluorescent *E. coli*. After differential treatment of the WT T84 and NOD2 KD epithelium with DNP + *E. coli* at different time intervals, cells can be fixed, and the bacteria co-localized with a variety of markers that include ARF6 (marker of vesicle trafficking) or EEA1, a marker of early endosomes, LAMP1 for late endosomes, cathepsin B for phagosomes, microtubule associated protein 1 light chain 3 (LC3II) for the autophagosome and NOD2. The finding would help us attain further visual confirmation on the endocytic pathway as a mechanism for bacterial uptake in autophagy. We can also use this to further understand NOD2's involvement throughout the process and why NOD2 depletion has such profound effects on intracellular levels of bacteria. We can also trace the journey of internalized bacteria through the cell; do they remain in vesicles, or do they leak into the cytoplasm? By elucidating the path taken by internalized bacteria, we can target them with greater specificity.

We also observed that mitoTEMPO attenuates bacterial internalization and IL-8 production in a metabolically stressed epithelium. Liang *et al.* have shown that mitoTEMPO can also help prevent the opening of the mitochondrial permeability transition pore (PTP).(303) Subsequently, we can look for increased openings of PTP in *E. coli* HB101 ± DNP treated

epithelium using commercially available kits. Additionally, increased internalization as well as mitochondrial dysfunction can increase ROS production. Taken together, ROS induced opening of PTP can disrupt intracellular Ca^{2+} homeostasis and these changes in Ca^{2+} signaling could be one of the factors instigating increased IL-8 production. Importantly, mitochondria form contacts with the endoplasmic reticulum (ER) at certain sites where Ca^{2+} exchange between ER and mitochondria can take place.(304) When the exchange of Ca^{2+} from the ER to mitochondria is at physiological levels, it aides ATP production; however when mitochondria are overloaded with Ca^{2+} from the ER, PTPs form, which can subsequently lead to cell death via apoptosis.(162, 305) Taking this into account, we can further assess whether Ca^{2+} entry in mitochondria is heightened in metabolic stress by using the mitochondria specific long wave calcium indicators such as Rhod-2 and subsequently performing imaging or FACS analysis. We can also consider the ultrastructure of mitochondria and ER during metabolic stress and bacterial entry, by performing transmission electron microscopy. This will enable us to decipher the interplay between ER function and mitochondria during metabolic stress.

4.4 Significance of this Research

Understanding the factors controlling intestinal barrier integrity is of paramount importance in IBD research. A leaky intestinal epithelial barrier has been strongly linked to dysfunctional immune responses. Indeed, the translocation of commensal bacteria from the gut lumen to the blood circulation can lead to sepsis, organ failure, and death. Increases in epithelial permeability are often reported in IBD.(32) Genomic studies have implicated loss-of-function mutations in molecules key to barrier maintenance as major factors in IBD pathogenesis. My studies focused primarily on NOD2, a cytosolic sensor of peptidoglycan derivatives. Many

studies have shown NOD2 mutations to be associated with the development of Crohn's disease.(2, 175, 176) Loss of NOD2 protein function in metabolically stressed enteric epithelial cells can modify their functional capabilities. Indeed, it has been shown by Kurgatasam *et al.* that children with Crohn's disease who carry certain allelic variations of NOD2 develop a significantly increased risk for surgery compared with children with Crohn's disease who lack the NOD2 mutation.(306) My study investigates the implications of NOD2 depletion in metabolically stressed enterocytes on epithelial permeability and inflammatory chemokine production. In a multi-hit hypothesis for the development of IBD, I hypothesized that the loss of NOD2 would exaggerate epithelial abnormalities caused by metabolic stress as defined by loss of barrier function and increased IL8.

Metabolic stress can be caused by a host of factors including inflammatory mediators like IFNγ, microbial dysbiosis, and NSAID treatment.(124, 128, 137) Previous work by Bjarnson *et al*. suggested NSAIDs break down epithelial phospholipids and also damage mitochondria. Work by the McKay group showed that T84 cells treatment with indomethacin, one NSAID, showed mitochondrial defects and enhanced commensal bacterial internalization.(137, 138) My study, performed with a different metabolic stressor indomethacin reinforces the ability of mitochondrial dysfunction to deleteriously impact barrier integrity, shedding light on the appropriateness of NSAID usage in different patient care situations. Understanding the effects of metabolic stress on the epithelium and its underlying mechanism will enable us to formulate specific therapeutic targets to alleviate intestinal inflammation, and make better informed choices about specific medications. The successful use of mitoTEMPO to attenuate internal bacterial levels suggests that ROS in inflamed or otherwise metabolically stressed epithelia are viable targets for treatment.

Understanding how the convergence of NOD2 depletion and metabolic stress manifests in reduced epithelial integrity and pro-inflammatory output will help us better understand the etiology of IBD and advance development of targeted therapeutics. Previous research has shown that NOD2 deletion is highly impactful in both Paneth cells and macrophages by reducing killing of bacteria; here, I show that loss of NOD2 has deleterious implications for IECs under metabolic stress, modifying the enterocyte-microbe interaction and enhancing the transcellular transcytosis of non-invasive bacteria across the epithelial layers.

4.5 Summary Statement

In conclusion, this thesis offers many novel findings that provide insight into the effects of lack of NOD2 (loss of function mutation; a Crohn's disease susceptibility trait) in metabolically stressed transporting enterocytes. We learn that:

- Increased bacterial internalization of noninvasive *E. coli* occurs in metabolically stressed epithelia
- Increased bacterial uptake in metabolically stressed epithelia results in increased expression of NOD2 (mRNA and protein expression)
- There is an increased epithelial barrier defect in metabolically stressed epithelia lacking NOD2 (increased number of intracellular bacteria)
- Mitochondria regulate epithelial transcellular permeability via the ROS to ERK1/2 pathway
- The increased number of viable *E. coli* in metabolically stressed epithelia lacking NOD2 is due to reduced killing (xenophagy)

- Induction of xenophagy by treating the metabolically stressed epithelia lacking NOD2 with Rapamycin ameliorates the barrier defect by reducing the number of intracellular *E. coli*
- Metabolically stressed epithelia lacking NOD2 produce increased levels of IL-8 when treated with noninvasive *E. coli*

These novel findings could translate into better disease management (e.g., mitochondrial-targeted antioxidants) for Crohn's disease patients carrying loss-of-function mutations in the NOD2 gene.

Summary Figure

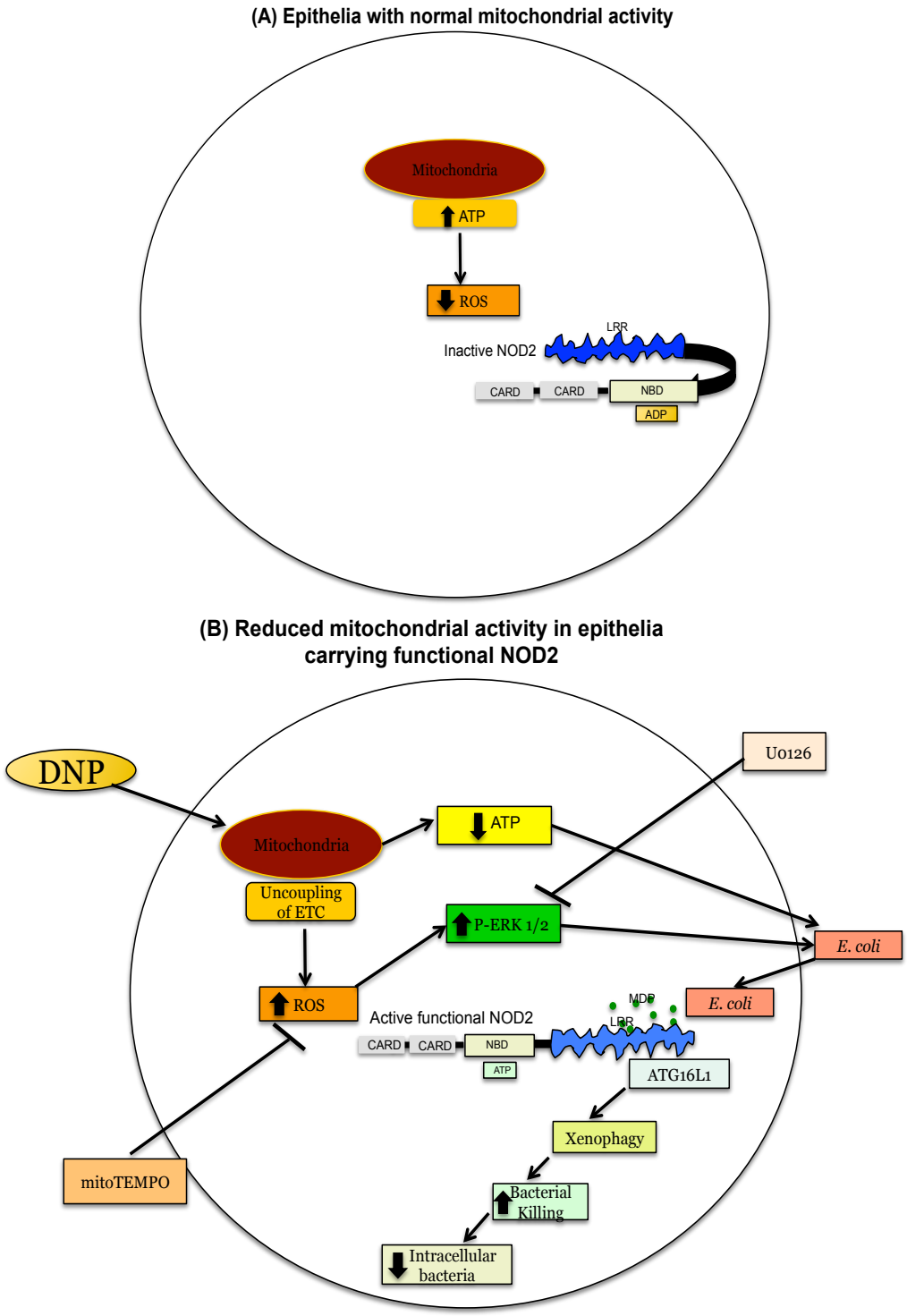

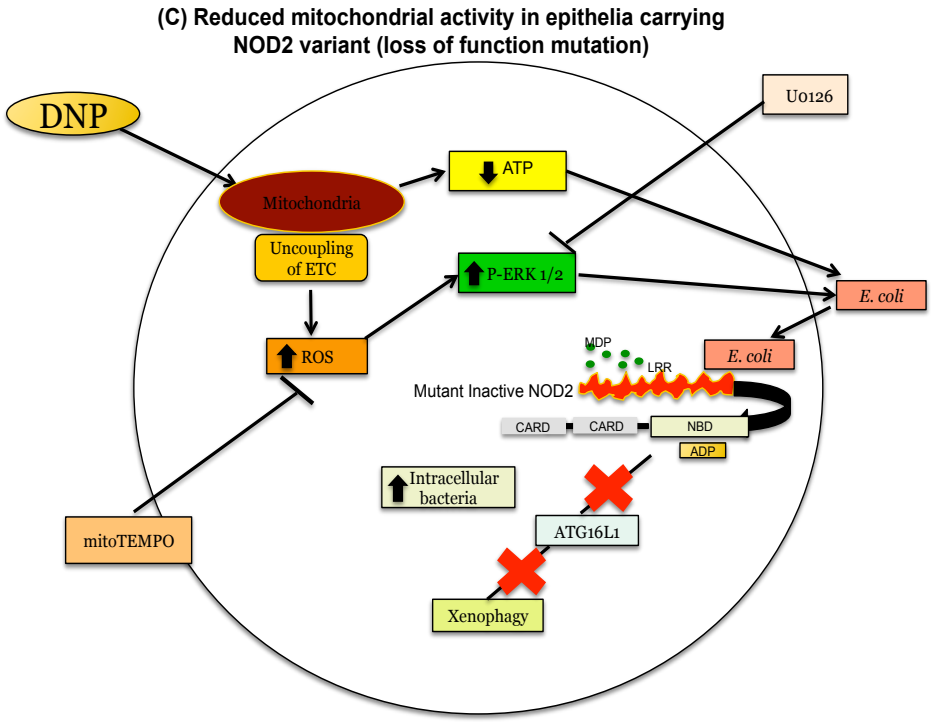

Summary figure: Depiction of the interplay between different associates that results in increased numbers of intracellular bacterial in my model system. (During normal mitochondrial activity, there is normal ATP production and low ROS and bacteria are largely restricted to the lumen, leading to little or no bacterial internalization. (B-C) Normal conditions are perturbed by reduced mitochondrial activity (evoked experimentally with dinitrophenol (DNP; uncoupler of mitochondrial electron transport chain (ETC)) which results in both increased ROS generation, and decreased ATP production (enterocyte starvation). The generated ROS activate MAPK, ERK 1/2 (P-ERK1/2). Activated P-ERK1/2 in conjunction with reduced ATP leads to increased uptake of commensal *E. coli* (noninvasive lab strain *E. coli* HB101 in my model system) into the enterocyte. Inhibition of upstream ROS by mitoTEMPO and downstream ERK 1/2 activation by U0126 treatment, reduces the entry of *E. coli* into the epithelium. (B) Metabolically stressed epithelia carrying functional NOD2 recognize muramyl dipeptide (MPD) from bacterial

peptidoglycan and recruit ATG16L1 (a protein involved in autophagy) and subsequently reduces the number of intracellular *E. coli* through xenophagy. (C) Metabolically stressed epithelia carrying the mutant NOD2 (loss of function mutation) which cannot sense its ligand, MDP, fails to both recruit ATG16L1 and carry out xenophagy of the internalized bacteria - this results in an increased number of viable intracellular *E. coli.*

REFRENCES

1. Abraham C, and Cho JH. Inflammatory bowel disease. *The New England journal of medicine.* 2009;361(21):2066-78.

2. Khor B, Gardet A, and Xavier RJ. Genetics and pathogenesis of inflammatory bowel disease. *Nature.* 2011;474(7351):307-17.

3. Loftus EV, Jr., and Sandborn WJ. Epidemiology of inflammatory bowel disease. *Gastroenterology clinics of North America.* 2002;31(1):1-20.

4. Rocchi A, Benchimol EI, Bernstein CN, Bitton A, Feagan B, Panaccione R, Glasgow KW, Fernandes A, and Ghosh S. Inflammatory bowel disease: a Canadian burden of illness review. *Canadian journal of gastroenterology = Journal canadien de gastroenterologie.* 2012;26(11):811-7.

5. Talley NJ, Abreu MT, Achkar JP, Bernstein CN, Dubinsky MC, Hanauer SB, Kane SV, Sandborn WJ, Ullman TA, and Moayyedi P. An evidence-based systematic review on medical therapies for inflammatory bowel disease. *The American journal of gastroenterology.* 2011;106 Suppl 1(S2-25; quiz S6.

6. Graff LA, Vincent N, Walker JR, Clara I, Carr R, Ediger J, Miller N, Rogala L, Rawsthorne P, Lix L, et al. A population-based study of fatigue and sleep difficulties in inflammatory bowel disease. *Inflammatory bowel diseases.* 2011;17(9):1882-9.

7. Sajobi TT, Lix LM, Clara I, Walker J, Graff LA, Rawsthorne P, Miller N, Rogala L, Carr R, and Bernstein CN. Measures of relative importance for health-related quality of life. *Quality of life research : an international journal of quality of life aspects of treatment, care and rehabilitation.* 2012;21(1):1-11.

8. Bernstein CN, and Nabalamba A. Hospitalization, surgery, and readmission rates of IBD in Canada: a population-based study. *The American journal of gastroenterology.* 2006;101(1):110-8.

9. Pithadia AB, and Jain S. Treatment of inflammatory bowel disease (IBD). *Pharmacological reports : PR.* 2011;63(3):629-42.

10. Zareie M, Singh PK, Irvine EJ, Sherman PM, McKay DM, and Perdue MH. Monocyte/macrophage activation by normal bacteria and bacterial products: implications for altered epithelial function in Crohn's disease. *The American journal of pathology.* 2001;158(3):1101-9.

11. Issenman RM, Jenkins RT, and Radoja C. Intestinal permeability compared in pediatric and adult patients with inflammatory bowel disease. *Clinical and investigative medicine Medecine clinique et experimentale.* 1993;16(3):187-96.

12. Soderholm JD, Peterson KH, Olaison G, Franzen LE, Westrom B, Magnusson KE, and Sjodahl R. Epithelial permeability to proteins in the noninflamed ileum of Crohn's disease? *Gastroenterology.* 1999;117(1):65-72.

13. Mowat AM, and Agace WW. Regional specialization within the intestinal immune system. *Nature reviews Immunology.* 2014;14(10):667-85.

14. van der Flier LG, and Clevers H. Stem cells, self-renewal, and differentiation in the intestinal epithelium. *Annual review of physiology.* 2009;71(241-60.

15. Heel KA, McCauley RD, Papadimitriou JM, and Hall JC. Review: Peyer's patches. *Journal of gastroenterology and hepatology.* 1997;12(2):122-36.

16. Brandtzaeg P. Function of mucosa-associated lymphoid tissue in antibody formation. *Immunological investigations.* 2010;39(4-5):303-55.

17. Johansen FE, and Kaetzel CS. Regulation of the polymeric immunoglobulin receptor and IgA transport: new advances in environmental factors that stimulate pIgR expression and its role in mucosal immunity. *Mucosal immunology.* 2011;4(6):598-602.

18. Stubbe H, Berdoz J, Kraehenbuhl JP, and Corthesy B. Polymeric IgA is superior to monomeric IgA and IgG carrying the same variable domain in preventing Clostridium difficile toxin A damaging of T84 monolayers. *Journal of immunology (Baltimore, Md : 1950).* 2000;164(4):1952-60.

19. Lycke N, Erlandsson L, Ekman L, Schon K, and Leanderson T. Lack of J chain inhibits the transport of gut IgA and abrogates the development of intestinal antitoxic protection. *Journal of immunology (Baltimore, Md : 1950).* 1999;163(2):913-9.

20. Turner JR. Intestinal mucosal barrier function in health and disease. *Nature reviews Immunology.* 2009;9(11):799-809.

21. Johansson ME, Phillipson M, Petersson J, Velcich A, Holm L, and Hansson GC. The inner of the two Muc2 mucin-dependent mucus layers in colon is devoid of bacteria. *Proceedings of the National Academy of Sciences of the United States of America.* 2008;105(39):15064-9.

22. Meyer-Hoffert U, Hornef MW, Henriques-Normark B, Axelsson LG, Midtvedt T, Putsep K, and Andersson M. Secreted enteric antimicrobial activity localises to the mucus surface layer. *Gut.* 2008;57(6):764-71.

23. Vaishnava S, Yamamoto M, Severson KM, Ruhn KA, Yu X, Koren O, Ley R, Wakeland EK, and Hooper LV. The antibacterial lectin RegIIIgamma promotes the spatial segregation of microbiota and host in the intestine. *Science (New York, NY).* 2011;334(6053):255-8.

24. Shen L. Functional morphology of the gastrointestinal tract. *Current topics in microbiology and immunology.* 2009;337(1-35.

25. Keita AV, and Soderholm JD. Barrier dysfunction and bacterial uptake in the follicle-associated epithelium of ileal Crohn's disease. *Annals of the New York Academy of Sciences.* 2012;1258(125-34.

26. Stadnyk AW. Cytokine production by epithelial cells. *FASEB journal : official publication of the Federation of American Societies for Experimental Biology.* 1994;8(13):1041-7.

27. Schoenenberger CA, and Matlin KS. Cell polarity and epithelial oncogenesis. *Trends in cell biology.* 1991;1(4):87-92.

28. John LJ, Fromm M, and Schulzke JD. Epithelial barriers in intestinal inflammation. *Antioxidants & redox signaling.* 2011;15(5):1255-70.

29. Anderson JM, and Van Itallie CM. Physiology and function of the tight junction. *Cold Spring Harbor perspectives in biology.* 2009;1(2):a002584.

30. Rook GA, and Brunet LR. Microbes, immunoregulation, and the gut. *Gut.* 2005;54(3):317-20.

31. Rook GA, and Brunet LR. Give us this day our daily germs. *Biologist (London, England).* 2002;49(4):145-9.

32. Laukoetter MG, Nava P, and Nusrat A. Role of the intestinal barrier in inflammatory bowel disease. *World journal of gastroenterology.* 2008;14(3):401-7.

33. De-Souza DA, and Greene LJ. Intestinal permeability and systemic infections in critically ill patients: effect of glutamine. *Critical care medicine.* 2005;33(5):1125-35.

34. Furuse M, Fujita K, Hiiragi T, Fujimoto K, and Tsukita S. Claudin-1 and -2: novel integral membrane proteins localizing at tight junctions with no sequence similarity to occludin. *The Journal of cell biology.* 1998;141(7):1539-50.

35. Itoh M, Furuse M, Morita K, Kubota K, Saitou M, and Tsukita S. Direct binding of three tight junction-associated MAGUKs, ZO-1, ZO-2, and ZO-3, with the COOH termini of claudins. *The Journal of cell biology.* 1999;147(6):1351-63.

36. Smith T. Picture story. Personalized PDZ domains. *Nature structural biology.* 1999;6(2):107.

37. Van Itallie CM, and Anderson JM. Claudins and epithelial paracellular transport. *Annual review of physiology.* 2006;68(403-29.

38. Furuse M, Furuse K, Sasaki H, and Tsukita S. Conversion of zonulae occludentes from tight to leaky strand type by introducing claudin-2 into Madin-Darby canine kidney I cells. *The Journal of cell biology.* 2001;153(2):263-72.

39. Furuse M, Hata M, Furuse K, Yoshida Y, Haratake A, Sugitani Y, Noda T, Kubo A, and Tsukita S. Claudin-based tight junctions are crucial for the mammalian epidermal barrier: a lesson from claudin-1-deficient mice. *The Journal of cell biology.* 2002;156(6):1099-111.

40. Van Itallie CM, Holmes J, Bridges A, Gookin JL, Coccaro MR, Proctor W, Colegio OR, and Anderson JM. The density of small tight junction pores varies among cell types and is increased by expression of claudin-2. *Journal of cell science.* 2008;121(Pt 3):298-305.

41. Colegio OR, Van Itallie C, Rahner C, and Anderson JM. Claudin extracellular domains determine paracellular charge selectivity and resistance but not tight junction fibril architecture. *American journal of physiology Cell physiology.* 2003;284(6):C1346-54.

42. Furuse M, Hirase T, Itoh M, Nagafuchi A, Yonemura S, Tsukita S, and Tsukita S. Occludin: a novel integral membrane protein localizing at tight junctions. *The Journal of cell biology.* 1993;123(6 Pt 2):1777-88.

43. Furuse M, Itoh M, Hirase T, Nagafuchi A, Yonemura S, Tsukita S, and Tsukita S. Direct association of occludin with ZO-1 and its possible involvement in the localization of occludin at tight junctions. *The Journal of cell biology.* 1994;127(6 Pt 1):1617-26.

44. Saitou M, Fujimoto K, Doi Y, Itoh M, Fujimoto T, Furuse M, Takano H, Noda T, and Tsukita S. Occludin-deficient embryonic stem cells can differentiate into polarized epithelial cells bearing tight junctions. *The Journal of cell biology.* 1998;141(2):397-408.

45. Schulzke JD, Gitter AH, Mankertz J, Spiegel S, Seidler U, Amasheh S, Saitou M, Tsukita S, and Fromm M. Epithelial transport and barrier function in occludin-deficient mice. *Biochimica et biophysica acta.* 2005;1669(1):34-42.

46. Furuse M, Fujimoto K, Sato N, Hirase T, Tsukita S, and Tsukita S. Overexpression of occludin, a tight junction-associated integral membrane protein, induces the formation of intracellular multilamellar bodies bearing tight junction-like structures. *Journal of cell science.* 1996;109 (Pt 2)(429-35.

47. Chen ML, Pothoulakis C, and LaMont JT. Protein kinase C signaling regulates ZO-1 translocation and increased paracellular flux of T84 colonocytes exposed to Clostridium difficile toxin A. *The Journal of biological chemistry.* 2002;277(6):4247-54.

48. Nunbhakdi-Craig V, Machleidt T, Ogris E, Bellotto D, White CL, 3rd, and Sontag E. Protein phosphatase 2A associates with and regulates atypical PKC and the epithelial tight junction complex. *The Journal of cell biology.* 2002;158(5):967-78.

49. Suzuki T, Elias BC, Seth A, Shen L, Turner JR, Giorgianni F, Desiderio D, Guntaka R, and Rao R. PKC eta regulates occludin phosphorylation and epithelial tight junction integrity. *Proceedings of the National Academy of Sciences of the United States of America.* 2009;106(1):61-6.

50. Santhanam S, Rajamanickam S, Motamarry A, Ramakrishna BS, Amirtharaj JG, Ramachandran A, Pulimood A, and Venkatraman A. Mitochondrial electron transport chain complex dysfunction in the colonic mucosa in ulcerative colitis. *Inflammatory bowel diseases.* 2012;18(11):2158-68.

51. Bazzoni G. The JAM family of junctional adhesion molecules. *Current opinion in cell biology.* 2003;15(5):525-30.

52. Laukoetter MG, Nava P, Lee WY, Severson EA, Capaldo CT, Babbin BA, Williams IR, Koval M, Peatman E, Campbell JA, et al. JAM-A regulates permeability and inflammation in the intestine in vivo. *The Journal of experimental medicine.* 2007;204(13):3067-76.

53. Bazzoni G, Martinez-Estrada OM, Mueller F, Nelboeck P, Schmid G, Bartfai T, Dejana E, and Brockhaus M. Homophilic interaction of junctional adhesion molecule. *The Journal of biological chemistry.* 2000;275(40):30970-6.

54. Srinivasan B, Kolli AR, Esch MB, Abaci HE, Shuler ML, and Hickman JJ. TEER measurement techniques for in vitro barrier model systems. *Journal of laboratory automation.* 2015;20(2):107-26.

55. Hermiston ML, and Gordon JI. In vivo analysis of cadherin function in the mouse intestinal epithelium: essential roles in adhesion, maintenance of differentiation, and regulation of programmed cell death. *The Journal of cell biology.* 1995;129(2):489-506.

56. Nollet F, Kools P, and van Roy F. Phylogenetic analysis of the cadherin superfamily allows identification of six major subfamilies besides several solitary members. *Journal of molecular biology.* 2000;299(3):551-72.

57. Gooding JM, Yap KL, and Ikura M. The cadherin-catenin complex as a focal point of cell adhesion and signalling: new insights from three-dimensional structures. *BioEssays : news and reviews in molecular, cellular and developmental biology.* 2004;26(5):497-511.

58. Yap AS, Niessen CM, and Gumbiner BM. The juxtamembrane region of the cadherin cytoplasmic tail supports lateral clustering, adhesive strengthening, and interaction with p120ctn. *The Journal of cell biology.* 1998;141(3):779-89.

59. Aberle H, Butz S, Stappert J, Weissig H, Kemler R, and Hoschuetzky H. Assembly of the cadherin-catenin complex in vitro with recombinant proteins. *Journal of cell science.* 1994;107 (Pt 12)(3655-63.

60. Shifflett DE, Clayburgh DR, Koutsouris A, Turner JR, and Hecht GA. Enteropathogenic E. coli disrupts tight junction barrier function and structure in vivo. *Laboratory investigation; a journal of technical methods and pathology.* 2005;85(10):1308-24.

61. Madara JL, and Stafford J. Interferon-gamma directly affects barrier function of cultured intestinal epithelial monolayers. *The Journal of clinical investigation.* 1989;83(2):724-7.

62. Hiribarren A, Heyman M, L'Helgouac'h A, and Desjeux JF. Effect of cytokines on the epithelial function of the human colon carcinoma cell line HT29 cl 19A. *Gut.* 1993;34(5):616-20.

63. Menard S, Lebreton C, Schumann M, Matysiak-Budnik T, Dugave C, Bouhnik Y, Malamut G, Cellier C, Allez M, Crenn P, et al. Paracellular versus transcellular intestinal permeability to gliadin peptides in active celiac disease. *The American journal of pathology.* 2012;180(2):608-15.

64. Cossart P, and Sansonetti PJ. Bacterial invasion: the paradigms of enteroinvasive pathogens. *Science (New York, NY).* 2004;304(5668):242-8.

65. Kaiser P, Diard M, Stecher B, and Hardt WD. The streptomycin mouse model for Salmonella diarrhea: functional analysis of the microbiota, the pathogen's virulence factors, and the host's mucosal immune response. *Immunological reviews.* 2012;245(1):56-83.

66. Coburn B, Li Y, Owen D, Vallance BA, and Finlay BB. Salmonella enterica serovar Typhimurium pathogenicity island 2 is necessary for complete virulence in a mouse model of infectious enterocolitis. *Infection and immunity.* 2005;73(6):3219-27.

67. Muller AJ, Kaiser P, Dittmar KE, Weber TC, Haueter S, Endt K, Songhet P, Zellweger C, Kremer M, Fehling HJ, et al. Salmonella gut invasion involves TTSS-2-dependent epithelial traversal, basolateral exit, and uptake by epithelium-sampling lamina propria phagocytes. *Cell host & microbe.* 2012;11(1):19-32.

68. Kalischuk LD, Leggett F, and Inglis GD. Campylobacter jejuni induces transcytosis of commensal bacteria across the intestinal epithelium through M-like cells. *Gut pathogens.* 2010;2(14.

69. Kalischuk LD, Inglis GD, and Buret AG. Campylobacter jejuni induces transcellular translocation of commensal bacteria via lipid rafts. *Gut pathogens.* 2009;1(1):2.

70. Clark E, Hoare C, Tanianis-Hughes J, Carlson GL, and Warhurst G. Interferon gamma induces translocation of commensal Escherichia coli across gut epithelial cells via a lipid raft-mediated process. *Gastroenterology.* 2005;128(5):1258-67.

71. McKay DM, Watson JL, Wang A, Caldwell J, Prescott D, Ceponis PM, Di Leo V, and Lu J. Phosphatidylinositol 3'-kinase is a critical mediator of interferon-gamma-induced

increases in enteric epithelial permeability. *The Journal of pharmacology and experimental therapeutics.* 2007;320(3):1013-22.

72. Hopkins CR, Miller K, and Beardmore JM. Receptor-mediated endocytosis of transferrin and epidermal growth factor receptors: a comparison of constitutive and ligand-induced uptake. *Journal of cell science Supplement.* 1985;3(173-86.

73. Anderson RG, Brown MS, and Goldstein JL. Role of the coated endocytic vesicle in the uptake of receptor-bound low density lipoprotein in human fibroblasts. *Cell.* 1977;10(3):351-64.

74. McMahon HT, and Boucrot E. Molecular mechanism and physiological functions of clathrin-mediated endocytosis. *Nature reviews Molecular cell biology.* 2011;12(8):517-33.

75. Stan RV. Structure of caveolae. *Biochimica et biophysica acta.* 2005;1746(3):334-48.

76. Lipardi C, Mora R, Colomer V, Paladino S, Nitsch L, Rodriguez-Boulan E, and Zurzolo C. Caveolin transfection results in caveolae formation but not apical sorting of glycosylphosphatidylinositol (GPI)-anchored proteins in epithelial cells. *The Journal of cell biology.* 1998;140(3):617-26.

77. Pelkmans L, Puntener D, and Helenius A. Local actin polymerization and dynamin recruitment in SV40-induced internalization of caveolae. *Science (New York, NY).* 2002;296(5567):535-9.

78. Shin JS, Gao Z, and Abraham SN. Involvement of cellular caveolae in bacterial entry into mast cells. *Science (New York, NY).* 2000;289(5480):785-8.

79. Lane N, and Martin W. The energetics of genome complexity. *Nature.* 2010;467(7318):929-34.

80. Vafai SB, and Mootha VK. Mitochondrial disorders as windows into an ancient organelle. *Nature.* 2012;491(7424):374-83.

81. Pagliarini DJ, Calvo SE, Chang B, Sheth SA, Vafai SB, Ong SE, Walford GA, Sugiana C, Boneh A, Chen WK, et al. A mitochondrial protein compendium elucidates complex I disease biology. *Cell.* 2008;134(1):112-23.

82. Sickmann A, Reinders J, Wagner Y, Joppich C, Zahedi R, Meyer HE, Schonfisch B, Perschil I, Chacinska A, Guiard B, et al. The proteome of Saccharomyces cerevisiae mitochondria. *Proceedings of the National Academy of Sciences of the United States of America.* 2003;100(23):13207-12.

83. Forner F, Foster LJ, Campanaro S, Valle G, and Mann M. Quantitative proteomic comparison of rat mitochondria from muscle, heart, and liver. *Molecular & cellular proteomics : MCP.* 2006;5(4):608-19.

84. Bogenhagen DF. Mitochondrial DNA nucleoid structure. *Biochimica et biophysica acta.* 2012;1819(9-10):914-20.

85. Meeusen S, and Nunnari J. Evidence for a two membrane-spanning autonomous mitochondrial DNA replisome. *The Journal of cell biology.* 2003;163(3):503-10.

86. Anderson S, Bankier AT, Barrell BG, de Bruijn MH, Coulson AR, Drouin J, Eperon IC, Nierlich DP, Roe BA, Sanger F, et al. Sequence and organization of the human mitochondrial genome. *Nature.* 1981;290(5806):457-65.

87. Taanman JW. The mitochondrial genome: structure, transcription, translation and replication. *Biochimica et biophysica acta.* 1999;1410(2):103-23.

88. Javadov S, and Karmazyn M. Mitochondrial permeability transition pore opening as an endpoint to initiate cell death and as a putative target for cardioprotection. *Cellular physiology and biochemistry : international journal of experimental cellular physiology, biochemistry, and pharmacology.* 2007;20(1-4):1-22.

89. Schoultz I, Soderholm JD, and McKay DM. Is metabolic stress a common denominator in inflammatory bowel disease? *Inflammatory bowel diseases.* 2011;17(9):2008-18.

90. Baughman JM, Perocchi F, Girgis HS, Plovanich M, Belcher-Timme CA, Sancak Y, Bao XR, Strittmatter L, Goldberger O, Bogorad RL, et al. Integrative genomics identifies MCU as an essential component of the mitochondrial calcium uniporter. *Nature.* 2011;476(7360):341-5.

91. De Stefani D, Raffaello A, Teardo E, Szabo I, and Rizzuto R. A forty-kilodalton protein of the inner membrane is the mitochondrial calcium uniporter. *Nature.* 2011;476(7360):336-40.

92. Roediger WE. The colonic epithelium in ulcerative colitis: an energy-deficiency disease? *Lancet.* 1980;2(8197):712-5.

93. Singh S, Graff LA, and Bernstein CN. Do NSAIDs, antibiotics, infections, or stress trigger flares in IBD? *The American journal of gastroenterology.* 2009;104(5):1298-313; quiz 314.

94. Rodenburg W, Keijer J, Kramer E, Vink C, van der Meer R, and Bovee-Oudenhoven IM. Impaired barrier function by dietary fructo-oligosaccharides (FOS) in rats is accompanied by increased colonic mitochondrial gene expression. *BMC genomics.* 2008;9(144.

95. Murphy MP. How mitochondria produce reactive oxygen species. *The Biochemical journal.* 2009;417(1):1-13.

96. Martin HM, Hancock JT, Salisbury V, and Harrison R. Role of xanthine oxidoreductase as an antimicrobial agent. *Infection and immunity.* 2004;72(9):4933-9.

97. Droge W. Free radicals in the physiological control of cell function. *Physiological reviews.* 2002;82(1):47-95.

98. Thannickal VJ, and Fanburg BL. Reactive oxygen species in cell signaling. *American journal of physiology Lung cellular and molecular physiology.* 2000;279(6):L1005-28.

99. Pavlick KP, Laroux FS, Fuseler J, Wolf RE, Gray L, Hoffman J, and Grisham MB. Role of reactive metabolites of oxygen and nitrogen in inflammatory bowel disease. *Free radical biology & medicine.* 2002;33(3):311-22.

100. Restivo NL, Srivastava MD, Schafer IA, and Hoppel CL. Mitochondrial dysfunction in a patient with crohn disease: possible role in pathogenesis. *Journal of pediatric gastroenterology and nutrition.* 2004;38(5):534-8.

101. Buffinton GD, and Doe WF. Depleted mucosal antioxidant defences in inflammatory bowel disease. *Free radical biology & medicine.* 1995;19(6):911-8.

102. Sido B, Hack V, Hochlehnert A, Lipps H, Herfarth C, and Droge W. Impairment of intestinal glutathione synthesis in patients with inflammatory bowel disease. *Gut.* 1998;42(4):485-92.

103. You Y, Fu JJ, Meng J, Huang GD, and Liu YH. Effect of N-acetylcysteine on the murine model of colitis induced by dextran sodium sulfate through up-regulating PON1 activity. *Digestive diseases and sciences.* 2009;54(8):1643-50.

104. Kwon KH, Ohigashi H, and Murakami A. Dextran sulfate sodium enhances interleukin-1 beta release via activation of p38 MAPK and ERK1/2 pathways in murine peritoneal macrophages. *Life sciences.* 2007;81(5):362-71.

105. Wang A, Keita AV, Phan V, McKay CM, Schoultz I, Lee J, Murphy MP, Fernando M, Ronaghan N, Balce D, et al. Targeting mitochondria-derived reactive oxygen species to reduce epithelial barrier dysfunction and colitis. *The American journal of pathology.* 2014;184(9):2516-27.

106. Novak EA, and Mollen KP. Mitochondrial dysfunction in inflammatory bowel disease. *Frontiers in cell and developmental biology.* 2015;3(62.

107. Galluzzi L, Kepp O, and Kroemer G. Mitochondria: master regulators of danger signalling. *Nature reviews Molecular cell biology.* 2012;13(12):780-8.

108. Kroemer G, Galluzzi L, and Brenner C. Mitochondrial membrane permeabilization in cell death. *Physiological reviews.* 2007;87(1):99-163.

109. Galluzzi L, Vitale I, Abrams JM, Alnemri ES, Baehrecke EH, Blagosklonny MV, Dawson TM, Dawson VL, El-Deiry WS, Fulda S, et al. Molecular definitions of cell death subroutines: recommendations of the Nomenclature Committee on Cell Death 2012. *Cell death and differentiation.* 2012;19(1):107-20.

110. Zamzami N, Marchetti P, Castedo M, Zanin C, Vayssiere JL, Petit PX, and Kroemer G. Reduction in mitochondrial potential constitutes an early irreversible step of programmed lymphocyte death in vivo. *The Journal of experimental medicine.* 1995;181(5):1661-72.

111. Galluzzi L, Kepp O, Trojel-Hansen C, and Kroemer G. Non-apoptotic functions of apoptosis-regulatory proteins. *EMBO reports.* 2012;13(4):322-30.

112. Beesoo R, Neergheen-Bhujun V, Bhagooli R, and Bahorun T. Apoptosis inducing lead compounds isolated from marine organisms of potential relevance in cancer treatment. *Mutation research.* 2014;768(84-97.

113. Elmore S. Apoptosis: a review of programmed cell death. *Toxicologic pathology.* 2007;35(4):495-516.

114. Hongmei Z. *Extrinsic and Intrinsic Apoptosis Signal Pathway Review.* 2012.

115. Roediger WE. Colonic epithelial metabolism in ulcerative colitis. *Gut.* 1993;34(11):1646.

116. Santhanam S, Venkatraman A, and Ramakrishna BS. Impairment of mitochondrial acetoacetyl CoA thiolase activity in the colonic mucosa of patients with ulcerative colitis. *Gut.* 2007;56(11):1543-9.

117. Meddings JB, Jarand J, Urbanski SJ, Hardin J, and Gall DG. Increased gastrointestinal permeability is an early lesion in the spontaneously diabetic BB rat. *The American journal of physiology.* 1999;276(4 Pt 1):G951-7.

118. Nazli A, Yang PC, Jury J, Howe K, Watson JL, Soderholm JD, Sherman PM, Perdue MH, and McKay DM. Epithelia under metabolic stress perceive commensal bacteria as a threat. *The American journal of pathology.* 2004;164(3):947-57.

119. Schurmann G, Bruwer M, Klotz A, Schmid KW, Senninger N, and Zimmer KP. Transepithelial transport processes at the intestinal mucosa in inflammatory bowel disease. *International journal of colorectal disease.* 1999;14(1):41-6.

120. Soderholm JD, Olaison G, Peterson KH, Franzen LE, Lindmark T, Wiren M, Tagesson C, and Sjodahl R. Augmented increase in tight junction permeability by luminal stimuli in the non-inflamed ileum of Crohn's disease. *Gut.* 2002;50(3):307-13.

121. Beltran B, Nos P, Dasi F, Iborra M, Bastida G, Martinez M, O'Connor JE, Saez G, Moret I, and Ponce J. Mitochondrial dysfunction, persistent oxidative damage, and catalase inhibition in immune cells of naive and treated Crohn's disease. *Inflammatory bowel diseases.* 2010;16(1):76-86.

122. Hsieh SY, Shih TC, Yeh CY, Lin CJ, Chou YY, and Lee YS. Comparative proteomic studies on the pathogenesis of human ulcerative colitis. *Proteomics.* 2006;6(19):5322-31.

123. de Mattos BR, Garcia MP, Nogueira JB, Paiatto LN, Albuquerque CG, Souza CL, Fernandes LG, Tamashiro WM, and Simioni PU. Inflammatory Bowel Disease: An Overview of Immune Mechanisms and Biological Treatments. *Mediators of inflammation.* 2015;2015(493012.

124. Kuwano Y, Tominaga K, Kawahara T, Sasaki H, Takeo K, Nishida K, Masuda K, Kawai T, Teshima-Kondo S, and Rokutan K. Tumor necrosis factor alpha activates transcription of the NADPH oxidase organizer 1 (NOXO1) gene and upregulates superoxide production in colon epithelial cells. *Free radical biology & medicine.* 2008;45(12):1642-52.

125. Gavillet M, Allaman I, and Magistretti PJ. Modulation of astrocytic metabolic phenotype by proinflammatory cytokines. *Glia.* 2008;56(9):975-89.

126. Sokol H, Seksik P, Furet JP, Firmesse O, Nion-Larmurier I, Beaugerie L, Cosnes J, Corthier G, Marteau P, and Dore J. Low counts of Faecalibacterium prausnitzii in colitis microbiota. *Inflammatory bowel diseases.* 2009;15(8):1183-9.

127. Frank DN, St Amand AL, Feldman RA, Boedeker EC, Harpaz N, and Pace NR. Molecular-phylogenetic characterization of microbial community imbalances in human inflammatory bowel diseases. *Proceedings of the National Academy of Sciences of the United States of America.* 2007;104(34):13780-5.

128. Manichanh C, Rigottier-Gois L, Bonnaud E, Gloux K, Pelletier E, Frangeul L, Nalin R, Jarrin C, Chardon P, Marteau P, et al. Reduced diversity of faecal microbiota in Crohn's disease revealed by a metagenomic approach. *Gut.* 2006;55(2):205-11.

129. He D, Sougioultzis S, Hagen S, Liu J, Keates S, Keates AC, Pothoulakis C, and Lamont JT. Clostridium difficile toxin A triggers human colonocyte IL-8 release via mitochondrial oxygen radical generation. *Gastroenterology.* 2002;122(4):1048-57.

130. Ma C, Wickham ME, Guttman JA, Deng W, Walker J, Madsen KL, Jacobson K, Vogl WA, Finlay BB, and Vallance BA. Citrobacter rodentium infection causes both mitochondrial dysfunction and intestinal epithelial barrier disruption in vivo: role of mitochondrial associated protein (Map). *Cellular microbiology.* 2006;8(10):1669-86.

131. Dickman KG, Hempson SJ, Anderson J, Lippe S, Zhao L, Burakoff R, and Shaw RD. Rotavirus alters paracellular permeability and energy metabolism in Caco-2 cells.

American journal of physiology Gastrointestinal and liver physiology. 2000;279(4):G757-66.

132. Zareie M, Riff J, Donato K, McKay DM, Perdue MH, Soderholm JD, Karmali M, Cohen MB, Hawkins J, and Sherman PM. Novel effects of the prototype translocating Escherichia coli, strain C25 on intestinal epithelial structure and barrier function. *Cellular microbiology.* 2005;7(12):1782-97.

133. Hotz-Behofsits C, Simpson RJ, Walley M, and Bjarnason IT. Role of COX-2 in nonsteroidal anti-inflammatory drug enteropathy in rodents. *Scandinavian journal of gastroenterology.* 2010;45(7-8):822-7.

134. Maity P, Bindu S, Dey S, Goyal M, Alam A, Pal C, Mitra K, and Bandyopadhyay U. Indomethacin, a non-steroidal anti-inflammatory drug, develops gastropathy by inducing reactive oxygen species-mediated mitochondrial pathology and associated apoptosis in gastric mucosa: a novel role of mitochondrial aconitase oxidation. *The Journal of biological chemistry.* 2009;284(5):3058-68.

135. Wallace JL. Prostaglandins, NSAIDs, and gastric mucosal protection: why doesn't the stomach digest itself? *Physiological reviews.* 2008;88(4):1547-65.

136. Somasundaram S, Sigthorsson G, Simpson RJ, Watts J, Jacob M, Tavares IA, Rafi S, Roseth A, Foster R, Price AB, et al. Uncoupling of intestinal mitochondrial oxidative phosphorylation and inhibition of cyclooxygenase are required for the development of NSAID-enteropathy in the rat. *Alimentary pharmacology & therapeutics.* 2000;14(5):639-50.

137. Bjarnason I, Hayllar J, MacPherson AJ, and Russell AS. Side effects of nonsteroidal anti-inflammatory drugs on the small and large intestine in humans. *Gastroenterology.* 1993;104(6):1832-47.

138. Schoultz I, McKay CM, Graepel R, Phan VC, Wang A, Soderholm J, and McKay DM. Indomethacin-induced translocation of bacteria across enteric epithelia is reactive oxygen species-dependent and reduced by vitamin C. *American journal of physiology Gastrointestinal and liver physiology.* 2012;303(5):G536-45.

139. Wallemacq PE, and Reding R. FK506 (tacrolimus), a novel immunosuppressant in organ transplantation: clinical, biomedical, and analytical aspects. *Clinical chemistry.* 1993;39(11 Pt 1):2219-28.

140. Matsuda S, Shibasaki F, Takehana K, Mori H, Nishida E, and Koyasu S. Two distinct action mechanisms of immunophilin-ligand complexes for the blockade of T-cell activation. *EMBO reports.* 2000;1(5):428-34.

141. Madsen KL, Yanchar NL, Sigalet DL, Reigel T, and Fedorak RN. FK506 increases permeability in rat intestine by inhibiting mitochondrial function. *Gastroenterology.* 1995;109(1):107-14.

142. Calne RY, White DJ, Thiru S, Evans DB, McMaster P, Dunn DC, Craddock GN, Pentlow BD, and Rolles K. Cyclosporin A in patients receiving renal allografts from cadaver donors. *Lancet (London, England).* 1978;2(8104-5):1323-7.

143. Kahan BD. Cyclosporine. *The New England journal of medicine.* 1989;321(25):1725-38.

144. Parra T, de Arriba G, Conejo JR, Cantero M, Arribas I, Rodriguez-Puyol D, Rodriguez-Puyol M, and Carballo F. Cyclosporine increases local glomerular synthesis of reactive oxygen species in rats: effect of vitamin E on cyclosporine nephrotoxicity. *Transplantation.* 1998;66(10):1325-9.

145. Perez de Hornedo J, de Arriba G, Calvino M, Benito S, and Parra T. [Cyclosporin A causes oxidative stress and mitochondrial dysfunction in renal tubular cells]. *Nefrologia : publicacion oficial de la Sociedad Espanola Nefrologia.* 2007;27(5):565-73.

146. Karran P, and Attard N. Thiopurines in current medical practice: molecular mechanisms and contributions to therapy-related cancer. *Nature reviews Cancer.* 2008;8(1):24-36.

147. Geller SA, Dubinsky MC, Poordad FF, Vasiliauskas EA, Cohen AH, Abreu MT, Tran T, Martin P, Vierling JM, and Targan SR. Early hepatic nodular hyperplasia and submicroscopic fibrosis associated with 6-thioguanine therapy in inflammatory bowel disease. *The American journal of surgical pathology.* 2004;28(9):1204-11.

148. Ferlitsch A, Teml A, Reinisch W, Ulbrich G, Wrba F, Homoncik M, Gangl A, Peck-Radosavljevic M, and Vogelsang H. 6-thioguanine associated nodular regenerative hyperplasia in patients with inflammatory bowel disease may induce portal hypertension. *The American journal of gastroenterology.* 2007;102(11):2495-503.

149. Daehn I, Brem R, Barkauskaite E, and Karran P. 6-Thioguanine damages mitochondrial DNA and causes mitochondrial dysfunction in human cells. *FEBS letters.* 2011;585(24):3941-6.

150. Farhadi A, Keshavarzian A, Van de Kar LD, Jakate S, Domm A, Zhang L, Shaikh M, Banan A, and Fields JZ. Heightened responses to stressors in patients with inflammatory bowel disease. *The American journal of gastroenterology.* 2005;100(8):1796-804.

151. Soderholm JD, Yang PC, Ceponis P, Vohra A, Riddell R, Sherman PM, and Perdue MH. Chronic stress induces mast cell-dependent bacterial adherence and initiates mucosal inflammation in rat intestine. *Gastroenterology.* 2002;123(4):1099-108.

152. Lewis K, and McKay DM. Metabolic stress evokes decreases in epithelial barrier function. *Annals of the New York Academy of Sciences.* 2009;1165(327-37.

153. D'Haens GR, Geboes K, Peeters M, Baert F, Penninckx F, and Rutgeerts P. Early lesions of recurrent Crohn's disease caused by infusion of intestinal contents in excluded ileum. *Gastroenterology.* 1998;114(2):262-7.

154. Ramachandran A, Patra S, and Balasubramanian KA. Intestinal mitochondrial dysfunction in surgical stress. *The Journal of surgical research.* 2001;99(1):120-8.

155. Harper JA, Dickinson K, and Brand MD. Mitochondrial uncoupling as a target for drug development for the treatment of obesity. *Obesity reviews : an official journal of the International Association for the Study of Obesity.* 2001;2(4):255-65.

156. Lewis K, Caldwell J, Phan V, Prescott D, Nazli A, Wang A, Soderholm JD, Perdue MH, Sherman PM, and McKay DM. Decreased epithelial barrier function evoked by exposure to metabolic stress and nonpathogenic E. coli is enhanced by TNF-alpha. *American journal of physiology Gastrointestinal and liver physiology.* 2008;294(3):G669-78.

157. Lewis K, Lutgendorff F, Phan V, Soderholm JD, Sherman PM, and McKay DM. Enhanced translocation of bacteria across metabolically stressed epithelia is reduced by butyrate. *Inflammatory bowel diseases.* 2010;16(7):1138-48.

158. Nazli A, Wang A, Steen O, Prescott D, Lu J, Perdue MH, Soderholm JD, Sherman PM, and McKay DM. Enterocyte cytoskeleton changes are crucial for enhanced translocation of nonpathogenic Escherichia coli across metabolically stressed gut epithelia. *Infection and immunity.* 2006;74(1):192-201.

159. Williams A, Flavell RA, and Eisenbarth SC. The role of NOD-like Receptors in shaping adaptive immunity. *Current opinion in immunology.* 2010;22(1):34-40.

160. Biswas A, Petnicki-Ocwieja T, and Kobayashi KS. Nod2: a key regulator linking microbiota to intestinal mucosal immunity. *Journal of molecular medicine (Berlin, Germany).* 2012;90(1):15-24.

161. Athman R, and Philpott D. Innate immunity via Toll-like receptors and Nod proteins. *Current opinion in microbiology.* 2004;7(1):25-32.

162. Cardenas C, Miller RA, Smith I, Bui T, Molgo J, Muller M, Vais H, Cheung KH, Yang J, Parker I, et al. Essential regulation of cell bioenergetics by constitutive InsP3 receptor Ca2+ transfer to mitochondria. *Cell.* 2010;142(2):270-83.

163. Coll RC, and O'Neill LA. New insights into the regulation of signalling by toll-like receptors and nod-like receptors. *Journal of innate immunity.* 2010;2(5):406-21.

164. Franchi L, Warner N, Viani K, and Nunez G. Function of Nod-like receptors in microbial recognition and host defense. *Immunological reviews.* 2009;227(1):106-28.

165. Kufer TA, Banks DJ, and Philpott DJ. Innate immune sensing of microbes by Nod proteins. *Annals of the New York Academy of Sciences.* 2006;1072(19-27.

166. Van Limbergen J, Radford-Smith G, and Satsangi J. Advances in IBD genetics. *Nature reviews Gastroenterology & hepatology.* 2014;11(6):372-85.

167. Peters LA, Perrigoue J, Mortha A, Iuga A, Song WM, Neiman EM, Llewellyn SR, Di Narzo A, Kidd BA, Telesco SE, et al. A functional genomics predictive network model identifies regulators of inflammatory bowel disease. *Nature genetics.* 2017.

168. Spehlmann ME, Begun AZ, Burghardt J, Lepage P, Raedler A, and Schreiber S. Epidemiology of inflammatory bowel disease in a German twin cohort: results of a nationwide study. *Inflammatory bowel diseases.* 2008;14(7):968-76.

169. Yazdanyar S, Kamstrup PR, Tybjaerg-Hansen A, and Nordestgaard BG. Penetrance of NOD2/CARD15 genetic variants in the general population. *CMAJ : Canadian Medical Association journal = journal de l'Association medicale canadienne.* 2010;182(7):661-5.

170. Salim SY, and Soderholm JD. Importance of disrupted intestinal barrier in inflammatory bowel diseases. *Inflammatory bowel diseases.* 2011;17(1):362-81.

171. Muise AM, Walters TD, Glowacka WK, Griffiths AM, Ngan BY, Lan H, Xu W, Silverberg MS, and Rotin D. Polymorphisms in E-cadherin (CDH1) result in a mis-localised cytoplasmic protein that is associated with Crohn's disease. *Gut.* 2009;58(8):1121-7.

172. Sabath E, Negoro H, Beaudry S, Paniagua M, Angelow S, Shah J, Grammatikakis N, Yu AS, and Denker BM. Galpha12 regulates protein interactions within the MDCK cell tight junction and inhibits tight-junction assembly. *Journal of cell science.* 2008;121(Pt 6):814-24.

173. Scharl M, Paul G, Weber A, Jung BC, Docherty MJ, Hausmann M, Rogler G, Barrett KE, and McCole DF. Protection of epithelial barrier function by the Crohn's disease associated gene protein tyrosine phosphatase n2. *Gastroenterology.* 2009;137(6):2030-40.e5.

174. Hassan SW, Doody KM, Hardy S, Uetani N, Cournoyer D, and Tremblay ML. Increased susceptibility to dextran sulfate sodium induced colitis in the T cell protein tyrosine phosphatase heterozygous mouse. *PloS one.* 2010;5(1):e8868.

175. Shaw MH, Kamada N, Warner N, Kim YG, and Nunez G. The ever-expanding function of NOD2: autophagy, viral recognition, and T cell activation. *Trends in immunology.* 2011;32(2):73-9.

176. Rioux JD, Xavier RJ, Taylor KD, Silverberg MS, Goyette P, Huett A, Green T, Kuballa P, Barmada MM, Datta LW, et al. Genome-wide association study identifies new

susceptibility loci for Crohn disease and implicates autophagy in disease pathogenesis. *Nature genetics.* 2007;39(5):596-604.

177. Hampe J, Franke A, Rosenstiel P, Till A, Teuber M, Huse K, Albrecht M, Mayr G, De La Vega FM, Briggs J, et al. A genome-wide association scan of nonsynonymous SNPs identifies a susceptibility variant for Crohn disease in ATG16L1. *Nature genetics.* 2007;39(2):207-11.

178. McCarroll SA, Huett A, Kuballa P, Chilewski SD, Landry A, Goyette P, Zody MC, Hall JL, Brant SR, Cho JH, et al. Deletion polymorphism upstream of IRGM associated with altered IRGM expression and Crohn's disease. *Nature genetics.* 2008;40(9):1107-12.

179. Hugot JP, Chamaillard M, Zouali H, Lesage S, Cezard JP, Belaiche J, Almer S, Tysk C, O'Morain CA, Gassull M, et al. Association of NOD2 leucine-rich repeat variants with susceptibility to Crohn's disease. *Nature.* 2001;411(6837):599-603.

180. Ogura Y, Bonen DK, Inohara N, Nicolae DL, Chen FF, Ramos R, Britton H, Moran T, Karaliuskas R, Duerr RH, et al. A frameshift mutation in NOD2 associated with susceptibility to Crohn's disease. *Nature.* 2001;411(6837):603-6.

181. Lesage S, Zouali H, Cezard JP, Colombel JF, Belaiche J, Almer S, Tysk C, O'Morain C, Gassull M, Binder V, et al. CARD15/NOD2 mutational analysis and genotype-phenotype correlation in 612 patients with inflammatory bowel disease. *American journal of human genetics.* 2002;70(4):845-57.

182. Maekawa S, Ohto U, Shibata T, Miyake K, and Shimizu T. Crystal structure of NOD2 and its implications in human disease. *Nature communications.* 2016;7(11813.

183. Gutierrez O, Pipaon C, Inohara N, Fontalba A, Ogura Y, Prosper F, Nunez G, and Fernandez-Luna JL. Induction of Nod2 in myelomonocytic and intestinal epithelial cells via nuclear factor-kappa B activation. *The Journal of biological chemistry.* 2002;277(44):41701-5.

184. Uehara A, Fujimoto Y, Fukase K, and Takada H. Various human epithelial cells express functional Toll-like receptors, NOD1 and NOD2 to produce anti-microbial peptides, but not proinflammatory cytokines. *Molecular immunology.* 2007;44(12):3100-11.

185. Girardin SE, Boneca IG, Viala J, Chamaillard M, Labigne A, Thomas G, Philpott DJ, and Sansonetti PJ. Nod2 is a general sensor of peptidoglycan through muramyl dipeptide (MDP) detection. *The Journal of biological chemistry.* 2003;278(11):8869-72.

186. Inohara N, Ogura Y, Fontalba A, Gutierrez O, Pons F, Crespo J, Fukase K, Inamura S, Kusumoto S, Hashimoto M, et al. Host recognition of bacterial muramyl dipeptide mediated through NOD2. Implications for Crohn's disease. *The Journal of biological chemistry.* 2003;278(8):5509-12.

187. Tanabe T, Chamaillard M, Ogura Y, Zhu L, Qiu S, Masumoto J, Ghosh P, Moran A, Predergast MM, Tromp G, et al. Regulatory regions and critical residues of NOD2 involved in muramyl dipeptide recognition. *The EMBO journal.* 2004;23(7):1587-97.

188. Hsu LC, Ali SR, McGillivray S, Tseng PH, Mariathasan S, Humke EW, Eckmann L, Powell JJ, Nizet V, Dixit VM, et al. A NOD2-NALP1 complex mediates caspase-1-dependent IL-1beta secretion in response to Bacillus anthracis infection and muramyl dipeptide. *Proceedings of the National Academy of Sciences of the United States of America.* 2008;105(22):7803-8.

189. Inohara N, Koseki T, del Peso L, Hu Y, Yee C, Chen S, Carrio R, Merino J, Liu D, Ni J, et al. Nod1, an Apaf-1-like activator of caspase-9 and nuclear factor-kappaB. *The Journal of biological chemistry.* 1999;274(21):14560-7.

190. Ogura Y, Inohara N, Benito A, Chen FF, Yamaoka S, and Nunez G. Nod2, a Nod1/Apaf-1 family member that is restricted to monocytes and activates NF-kappaB. *The Journal of biological chemistry.* 2001;276(7):4812-8.

191. Inohara N, Koseki T, Lin J, del Peso L, Lucas PC, Chen FF, Ogura Y, and Nunez G. An induced proximity model for NF-kappa B activation in the Nod1/RICK and RIP signaling pathways. *The Journal of biological chemistry.* 2000;275(36):27823-31.

192. Abbott DW, Wilkins A, Asara JM, and Cantley LC. The Crohn's disease protein, NOD2, requires RIP2 in order to induce ubiquitinylation of a novel site on NEMO. *Current biology : CB.* 2004;14(24):2217-27.

193. Park JH, Kim YG, McDonald C, Kanneganti TD, Hasegawa M, Body-Malapel M, Inohara N, and Nunez G. RICK/RIP2 mediates innate immune responses induced through Nod1 and Nod2 but not TLRs. *Journal of immunology (Baltimore, Md : 1950).* 2007;178(4):2380-6.

194. Windheim M, Lang C, Peggie M, Plater LA, and Cohen P. Molecular mechanisms involved in the regulation of cytokine production by muramyl dipeptide. *The Biochemical journal.* 2007;404(2):179-90.

195. Opitz B, Puschel A, Schmeck B, Hocke AC, Rosseau S, Hammerschmidt S, Schumann RR, Suttorp N, and Hippenstiel S. Nucleotide-binding oligomerization domain proteins are innate immune receptors for internalized Streptococcus pneumoniae. *The Journal of biological chemistry.* 2004;279(35):36426-32.

196. Hisamatsu T, Suzuki M, Reinecker HC, Nadeau WJ, McCormick BA, and Podolsky DK. CARD15/NOD2 functions as an antibacterial factor in human intestinal epithelial cells. *Gastroenterology.* 2003;124(4):993-1000.

197. Kufer TA, Kremmer E, Banks DJ, and Philpott DJ. Role for erbin in bacterial activation of Nod2. *Infection and immunity.* 2006;74(6):3115-24.

198. Ferwerda G, Girardin SE, Kullberg BJ, Le Bourhis L, de Jong DJ, Langenberg DM, van Crevel R, Adema GJ, Ottenhoff TH, Van der Meer JW, et al. NOD2 and toll-like receptors are nonredundant recognition systems of Mycobacterium tuberculosis. *PLoS pathogens.* 2005;1(3):279-85.

199. Petnicki-Ocwieja T, Hrncir T, Liu YJ, Biswas A, Hudcovic T, Tlaskalova-Hogenova H, and Kobayashi KS. Nod2 is required for the regulation of commensal microbiota in the intestine. *Proceedings of the National Academy of Sciences of the United States of America.* 2009;106(37):15813-8.

200. Biswas A, Liu YJ, Hao L, Mizoguchi A, Salzman NH, Bevins CL, and Kobayashi KS. Induction and rescue of Nod2-dependent Th1-driven granulomatous inflammation of the ileum. *Proceedings of the National Academy of Sciences of the United States of America.* 2010;107(33):14739-44.

201. Barnich N, Aguirre JE, Reinecker HC, Xavier R, and Podolsky DK. Membrane recruitment of NOD2 in intestinal epithelial cells is essential for nuclear factor-{kappa}B activation in muramyl dipeptide recognition. *The Journal of cell biology.* 2005;170(1):21-6.

202. Philpott DJ, Sorbara MT, Robertson SJ, Croitoru K, and Girardin SE. NOD proteins: regulators of inflammation in health and disease. *Nature reviews Immunology.* 2014;14(1):9-23.

203. Strober W, Murray PJ, Kitani A, and Watanabe T. Signalling pathways and molecular interactions of NOD1 and NOD2. *Nature reviews Immunology.* 2006;6(1):9-20.

204. Couturier-Maillard A, Secher T, Rehman A, Normand S, De Arcangelis A, Haesler R, Huot L, Grandjean T, Bressenot A, Delanoye-Crespin A, et al. NOD2-mediated dysbiosis predisposes mice to transmissible colitis and colorectal cancer. *The Journal of clinical investigation.* 2013;123(2):700-11.

205. Watanabe T, Kitani A, Murray PJ, and Strober W. NOD2 is a negative regulator of Toll-like receptor 2-mediated T helper type 1 responses. *Nature immunology.* 2004;5(8):800-8.

206. Corridoni D, Kodani T, Rodriguez-Palacios A, Pizarro TT, Xin W, Nickerson KP, McDonald C, Ley KF, Abbott DW, and Cominelli F. Dysregulated NOD2 predisposes SAMP1/YitFc mice to chronic intestinal inflammation. *Proceedings of the National Academy of Sciences of the United States of America.* 2013;110(42):16999-7004.

207. Watanabe T, Asano N, Murray PJ, Ozato K, Tailor P, Fuss IJ, Kitani A, and Strober W. Muramyl dipeptide activation of nucleotide-binding oligomerization domain 2 protects mice from experimental colitis. *The Journal of clinical investigation.* 2008;118(2):545-59.

208. Mizushima N, Levine B, Cuervo AM, and Klionsky DJ. Autophagy fights disease through cellular self-digestion. *Nature.* 2008;451(7182):1069-75.

209. Kroemer G, Marino G, and Levine B. Autophagy and the integrated stress response. *Molecular cell.* 2010;40(2):280-93.

210. Deretic V, and Levine B. Autophagy, immunity, and microbial adaptations. *Cell host & microbe.* 2009;5(6):527-49.

211. Cooney R, Baker J, Brain O, Danis B, Pichulik T, Allan P, Ferguson DJ, Campbell BJ, Jewell D, and Simmons A. NOD2 stimulation induces autophagy in dendritic cells influencing bacterial handling and antigen presentation. *Nature medicine.* 2010;16(1):90-7.

212. Homer CR, Richmond AL, Rebert NA, Achkar JP, and McDonald C. ATG16L1 and NOD2 interact in an autophagy-dependent antibacterial pathway implicated in Crohn's disease pathogenesis. *Gastroenterology.* 2010;139(5):1630-41, 41.e1-2.

213. Travassos LH, Carneiro LA, Ramjeet M, Hussey S, Kim YG, Magalhaes JG, Yuan L, Soares F, Chea E, Le Bourhis L, et al. Nod1 and Nod2 direct autophagy by recruiting ATG16L1 to the plasma membrane at the site of bacterial entry. *Nature immunology.* 2010;11(1):55-62.

214. Baeuerle PA, and Baltimore D. NF-kappa B: ten years after. *Cell.* 1996;87(1):13-20.

215. Raman M, Chen W, and Cobb MH. Differential regulation and properties of MAPKs. *Oncogene.* 2007;26(22):3100-12.

216. McCubrey JA, Lahair MM, and Franklin RA. Reactive oxygen species-induced activation of the MAP kinase signaling pathways. *Antioxidants & redox signaling.* 2006;8(9-10):1775-89.

217. Torres M, and Forman HJ. Redox signaling and the MAP kinase pathways. *BioFactors (Oxford, England).* 2003;17(1-4):287-96.

218. Ruffels J, Griffin M, and Dickenson JM. Activation of ERK1/2, JNK and PKB by hydrogen peroxide in human SH-SY5Y neuroblastoma cells: role of ERK1/2 in H2O2-induced cell death. *European journal of pharmacology.* 2004;483(2-3):163-73.

219. Stadler WM. Targeted agents for the treatment of advanced renal cell carcinoma. *Cancer.* 2005;104(11):2323-33.

220. Verbon EH, Post JA, and Boonstra J. The influence of reactive oxygen species on cell cycle progression in mammalian cells. *Gene.* 2012;511(1):1-6.

221. Vatish M, Yamada E, Pessin JE, and Bastie CC. Fyn kinase function in lipid utilization: a new upstream regulator of AMPK activity? *Archives of physiology and biochemistry.* 2009;115(4):191-8.

222. Yeo MG, Oh HJ, Cho HS, Chun JS, Marcantonio EE, and Song WK. Phosphorylation of Ser 21 in Fyn regulates its kinase activity, focal adhesion targeting, and is required for cell migration. *Journal of cellular physiology.* 2011;226(1):236-47.

223. Smyth D, McKay CM, Gulbransen BD, Phan VC, Wang A, and McKay DM. Interferon-gamma signals via an ERK1/2-ARF6 pathway to promote bacterial internalization by gut epithelia. *Cellular microbiology.* 2012;14(8):1257-70.

224. Baggiolini M, and Clark-Lewis I. Interleukin-8, a chemotactic and inflammatory cytokine. *FEBS letters.* 1992;307(1):97-101.

225. Oppenheim JJ, Zachariae CO, Mukaida N, and Matsushima K. Properties of the novel proinflammatory supergene "intercrine" cytokine family. *Annual review of immunology.* 1991;9(617-48.

226. Baggiolini M, Dewald B, and Moser B. Human chemokines: an update. *Annual review of immunology.* 1997;15(675-705.

227. Eckmann L, Kagnoff MF, and Fierer J. Epithelial cells secrete the chemokine interleukin-8 in response to bacterial entry. *Infection and immunity.* 1993;61(11):4569-74.

228. Eckmann L, Jung HC, Schurer-Maly C, Panja A, Morzycka-Wroblewska E, and Kagnoff MF. Differential cytokine expression by human intestinal epithelial cell lines: regulated expression of interleukin 8. *Gastroenterology.* 1993;105(6):1689-97.

229. Izzo RS, Witkon K, Chen AI, Hadjiyane C, Weinstein MI, and Pellecchia C. Interleukin-8 and neutrophil markers in colonic mucosa from patients with ulcerative colitis. *The American journal of gastroenterology.* 1992;87(10):1447-52.

230. Kucharzik T, Hudson JT, 3rd, Lugering A, Abbas JA, Bettini M, Lake JG, Evans ME, Ziegler TR, Merlin D, Madara JL, et al. Acute induction of human IL-8 production by intestinal epithelium triggers neutrophil infiltration without mucosal injury. *Gut.* 2005;54(11):1565-72.

231. Akhtar M, Watson JL, Nazli A, and McKay DM. Bacterial DNA evokes epithelial IL-8 production by a MAPK-dependent, NF-kappaB-independent pathway. *FASEB journal : official publication of the Federation of American Societies for Experimental Biology.* 2003;17(10):1319-21.

232. Venza I, Visalli M, Cucinotta M, Teti D, and Venza M. NOD2 triggers PGE2 synthesis leading to IL-8 activation in Staphylococcus aureus-infected human conjunctival

epithelial cells. *Biochemical and biophysical research communications.* 2013;440(4):551-7.

233. Abreu MT. Toll-like receptor signalling in the intestinal epithelium: how bacterial recognition shapes intestinal function. *Nature reviews Immunology.* 2010;10(2):131-44.

234. Sato T, and Clevers H. Primary mouse small intestinal epithelial cell cultures. *Methods in molecular biology (Clifton, NJ).* 2013;945(319-28.

235. Smyth D, Phan V, Wang A, and McKay DM. Interferon-gamma-induced increases in intestinal epithelial macromolecular permeability requires the Src kinase Fyn. *Laboratory investigation; a journal of technical methods and pathology.* 2011;91(5):764-77.

236. Dharmsathaphorn K, McRoberts JA, Mandel KG, Tisdale LD, and Masui H. A human colonic tumor cell line that maintains vectorial electrolyte transport. *The American journal of physiology.* 1984;246(2 Pt 1):G204-8.

237. Tsuchiya S, Yamabe M, Yamaguchi Y, Kobayashi Y, Konno T, and Tada K. Establishment and characterization of a human acute monocytic leukemia cell line (THP-1). *International journal of cancer.* 1980;26(2):171-6.

238. Chomczynski P, and Sacchi N. The single-step method of RNA isolation by acid guanidinium thiocyanate-phenol-chloroform extraction: twenty-something years on. *Nature protocols.* 2006;1(2):581-5.

239. Schmittgen TD, and Livak KJ. Analyzing real-time PCR data by the comparative C(T) method. *Nature protocols.* 2008;3(6):1101-8.

240. Bradford MM. A rapid and sensitive method for the quantitation of microgram quantities of protein utilizing the principle of protein-dye binding. *Analytical biochemistry.* 1976;72(248-54.

241. Yui S, Nakamura T, Sato T, Nemoto Y, Mizutani T, Zheng X, Ichinose S, Nagaishi T, Okamoto R, Tsuchiya K, et al. Functional engraftment of colon epithelium expanded in vitro from a single adult Lgr5(+) stem cell. *Nature medicine.* 2012;18(4):618-23.

242. Saxena A, Lopes F, Poon KKH, and McKay DM. Absence of the NOD2 protein renders epithelia more susceptible to barrier dysfunction due to mitochondrial dysfunction. *American journal of physiology Gastrointestinal and liver physiology.* 2017;313(1):G26-g38.

243. Jacob M, Bjarnason I, Rafi S, Wrigglesworth J, and Simpson RJ. A study of the effects of indometacin on liver mitochondria from rats, mice and humans. *Alimentary pharmacology & therapeutics.* 2001;15(11):1837-42.

244. Zamora SA, Hilsden RJ, Meddings JB, Butzner JD, Scott RB, and Sutherland LR. Intestinal permeability before and after ibuprofen in families of children with Crohn's disease. *Canadian journal of gastroenterology = Journal canadien de gastroenterologie.* 1999;13(1):31-6.

245. Akira S, Uematsu S, and Takeuchi O. Pathogen recognition and innate immunity. *Cell.* 2006;124(4):783-801.

246. Kawagoe T, Sato S, Matsushita K, Kato H, Matsui K, Kumagai Y, Saitoh T, Kawai T, Takeuchi O, and Akira S. Sequential control of Toll-like receptor-dependent responses by IRAK1 and IRAK2. *Nature immunology.* 2008;9(6):684-91.

247. Hemmi H, Takeuchi O, Kawai T, Kaisho T, Sato S, Sanjo H, Matsumoto M, Hoshino K, Wagner H, Takeda K, et al. A Toll-like receptor recognizes bacterial DNA. *Nature.* 2000;408(6813):740-5.

248. Lim HK, Seppanen M, Hautala T, Ciancanelli MJ, Itan Y, Lafaille FG, Dell W, Lorenzo L, Byun M, Pauwels E, et al. TLR3 deficiency in herpes simplex encephalitis: high allelic heterogeneity and recurrence risk. *Neurology.* 2014;83(21):1888-97.

249. Bernard JJ, Cowing-Zitron C, Nakatsuji T, Muehleisen B, Muto J, Borkowski AW, Martinez L, Greidinger EL, Yu BD, and Gallo RL. Ultraviolet radiation damages self noncoding RNA and is detected by TLR3. *Nature medicine.* 2012;18(8):1286-90.

250. Ewaschuk JB, Backer JL, Churchill TA, Obermeier F, Krause DO, and Madsen KL. Surface expression of Toll-like receptor 9 is upregulated on intestinal epithelial cells in response to pathogenic bacterial DNA. *Infection and immunity.* 2007;75(5):2572-9.

251. Abreu MT, Vora P, Faure E, Thomas LS, Arnold ET, and Arditi M. Decreased expression of Toll-like receptor-4 and MD-2 correlates with intestinal epithelial cell protection against dysregulated proinflammatory gene expression in response to bacterial lipopolysaccharide. *Journal of immunology (Baltimore, Md : 1950).* 2001;167(3):1609-16.

252. Naik S, Kelly EJ, Meijer L, Pettersson S, and Sanderson IR. Absence of Toll-like receptor 4 explains endotoxin hyporesponsiveness in human intestinal epithelium. *Journal of pediatric gastroenterology and nutrition.* 2001;32(4):449-53.

253. Murakami H, and Masui H. Hormonal control of human colon carcinoma cell growth in serum-free medium. *Proceedings of the National Academy of Sciences of the United States of America.* 1980;77(6):3464-8.

254. Navabi N, McGuckin MA, and Linden SK. Gastrointestinal cell lines form polarized epithelia with an adherent mucus layer when cultured in semi-wet interfaces with mechanical stimulation. *PloS one.* 2013;8(7):e68761.

255. Heazlewood CK, Cook MC, Eri R, Price GR, Tauro SB, Taupin D, Thornton DJ, Png CW, Crockford TL, Cornall RJ, et al. Aberrant mucin assembly in mice causes endoplasmic reticulum stress and spontaneous inflammation resembling ulcerative colitis. *PLoS medicine.* 2008;5(3):e54.

256. Corthesy-Theulaz I, Porta N, Pringault E, Racine L, Bogdanova A, Kraehenbuhl JP, Blum AL, and Michetti P. Adhesion of Helicobacter pylori to polarized T84 human intestinal cell monolayers is pH dependent. *Infection and immunity.* 1996;64(9):3827-32.

257. McKay DM, Philpott DJ, and Perdue MH. Review article: In vitro models in inflammatory bowel disease research--a critical review. *Alimentary pharmacology & therapeutics.* 1997;11 Suppl 3(70-80.

258. Hidalgo IJ, Raub TJ, and Borchardt RT. Characterization of the human colon carcinoma cell line (Caco-2) as a model system for intestinal epithelial permeability. *Gastroenterology.* 1989;96(3):736-49.

259. Wilson SS, Tocchi A, Holly MK, Parks WC, and Smith JG. A small intestinal organoid model of non-invasive enteric pathogen-epithelial cell interactions. *Mucosal immunology.* 2015;8(2):352-61.

260. Abraham C, and Cho JH. Functional consequences of NOD2 (CARD15) mutations. *Inflammatory bowel diseases.* 2006;12(7):641-50.

261. Linsinger G, Wilhelm S, Wagner H, and Hacker G. Uncouplers of oxidative phosphorylation can enhance a Fas death signal. *Molecular and cellular biology.* 1999;19(5):3299-311.

262. Bjarnason I, and Takeuchi K. Intestinal permeability in the pathogenesis of NSAID-induced enteropathy. *Journal of gastroenterology.* 2009;44 Suppl 19(23-9.

263. Mahmud T, Rafi SS, Scott DL, Wrigglesworth JM, and Bjarnason I. Nonsteroidal antiinflammatory drugs and uncoupling of mitochondrial oxidative phosphorylation. *Arthritis and rheumatism.* 1996;39(12):1998-2003.

264. Sartor RB. Mechanisms of disease: pathogenesis of Crohn's disease and ulcerative colitis. *Nature clinical practice Gastroenterology & hepatology.* 2006;3(7):390-407.

265. Ott SJ, Musfeldt M, Wenderoth DF, Hampe J, Brant O, Folsch UR, Timmis KN, and Schreiber S. Reduction in diversity of the colonic mucosa associated bacterial microflora in patients with active inflammatory bowel disease. *Gut.* 2004;53(5):685-93.

266. Barnich N, and Darfeuille-Michaud A. Role of bacteria in the etiopathogenesis of inflammatory bowel disease. *World journal of gastroenterology.* 2007;13(42):5571-6.

267. Baumgart M, Dogan B, Rishniw M, Weitzman G, Bosworth B, Yantiss R, Orsi RH, Wiedmann M, McDonough P, Kim SG, et al. Culture independent analysis of ileal mucosa reveals a selective increase in invasive Escherichia coli of novel phylogeny relative to depletion of Clostridiales in Crohn's disease involving the ileum. *The ISME journal.* 2007;1(5):403-18.

268. Seksik P, Rigottier-Gois L, Gramet G, Sutren M, Pochart P, Marteau P, Jian R, and Dore J. Alterations of the dominant faecal bacterial groups in patients with Crohn's disease of the colon. *Gut.* 2003;52(2):237-42.

269. Tabaqchali S, O'Donoghue DP, and Bettelheim KA. Escherichia coli antibodies in patients with inflammatory bowel disease. *Gut.* 1978;19(2):108-13.

270. Arnott ID, Landers CJ, Nimmo EJ, Drummond HE, Smith BK, Targan SR, and Satsangi J. Sero-reactivity to microbial components in Crohn's disease is associated with disease severity and progression, but not NOD2/CARD15 genotype. *The American journal of gastroenterology.* 2004;99(12):2376-84.

271. Darfeuille-Michaud A, Boudeau J, Bulois P, Neut C, Glasser AL, Barnich N, Bringer MA, Swidsinski A, Beaugerie L, and Colombel JF. High prevalence of adherent-invasive Escherichia coli associated with ileal mucosa in Crohn's disease. *Gastroenterology.* 2004;127(2):412-21.

272. Boudeau J, Glasser AL, Masseret E, Joly B, and Darfeuille-Michaud A. Invasive ability of an Escherichia coli strain isolated from the ileal mucosa of a patient with Crohn's disease. *Infection and immunity.* 1999;67(9):4499-509.

273. Maeda S, Hsu LC, Liu H, Bankston LA, Iimura M, Kagnoff MF, Eckmann L, and Karin M. Nod2 mutation in Crohn's disease potentiates NF-kappaB activity and IL-1beta processing. *Science (New York, NY).* 2005;307(5710):734-8.

274. Jing X, Zulfiqar F, Park SY, Nunez G, Dziarski R, and Gupta D. Peptidoglycan recognition protein 3 and Nod2 synergistically protect mice from dextran sodium sulfate-induced colitis. *Journal of immunology (Baltimore, Md : 1950).* 2014;193(6):3055-69.

275. Liu J, Xiang J, Li X, Blankson S, Zhao S, Cai J, Jiang Y, Redmond HP, and Wang JH. NF-kappaB activation is critical for bacterial lipoprotein tolerance-enhanced bactericidal activity in macrophages during microbial infection. *Scientific reports.* 2017;7(40418.

276. Ferwerda G, Kullberg BJ, de Jong DJ, Girardin SE, Langenberg DM, van Crevel R, Ottenhoff TH, Van der Meer JW, and Netea MG. Mycobacterium paratuberculosis is recognized by Toll-like receptors and NOD2. *Journal of leukocyte biology.* 2007;82(4):1011-8.

277. Diebold L, and Chandel NS. Mitochondrial ROS regulation of proliferating cells. *Free radical biology & medicine.* 2016;100(86-93.

278. Keshavarzian A, Sedghi S, Kanofsky J, List T, Robinson C, Ibrahim C, and Winship D. Excessive production of reactive oxygen metabolites by inflamed colon: analysis by chemiluminescence probe. *Gastroenterology.* 1992;103(1):177-85.

279. McKenzie SJ, Baker MS, Buffinton GD, and Doe WF. Evidence of oxidant-induced injury to epithelial cells during inflammatory bowel disease. *The Journal of clinical investigation.* 1996;98(1):136-41.

280. Maloy KJ, and Powrie F. Intestinal homeostasis and its breakdown in inflammatory bowel disease. *Nature.* 2011;474(7351):298-306.

281. Simon HU, Haj-Yehia A, and Levi-Schaffer F. Role of reactive oxygen species (ROS) in apoptosis induction. *Apoptosis : an international journal on programmed cell death.* 2000;5(5):415-8.

282. Ma TY, Hollander D, Freeman D, Nguyen T, and Krugliak P. Oxygen free radical injury of IEC-18 small intestinal epithelial cell monolayers. *Gastroenterology.* 1991;100(6):1533-43.

283. Seeger W, Hansen T, Rossig R, Schmehl T, Schutte H, Kramer HJ, Walmrath D, Weissmann N, Grimminger F, and Suttorp N. Hydrogen peroxide-induced increase in lung endothelial and epithelial permeability--effect of adenylate cyclase stimulation and phosphodiesterase inhibition. *Microvascular research.* 1995;50(1):1-17.

284. Donaldson JG. Multiple roles for Arf6: sorting, structuring, and signaling at the plasma membrane. *The Journal of biological chemistry.* 2003;278(43):41573-6.

285. Matsubayashi Y, Ebisuya M, Honjoh S, and Nishida E. ERK activation propagates in epithelial cell sheets and regulates their migration during wound healing. *Current biology : CB.* 2004;14(8):731-5.

286. Zhang J, Owen CR, Sanders MA, Turner JR, and Basson MD. The motogenic effects of cyclic mechanical strain on intestinal epithelial monolayer wound closure are matrix dependent. *Gastroenterology.* 2006;131(4):1179-89.

287. Juarez E, Carranza C, Hernandez-Sanchez F, Leon-Contreras JC, Hernandez-Pando R, Escobedo D, Torres M, and Sada E. NOD2 enhances the innate response of alveolar macrophages to Mycobacterium tuberculosis in humans. *European journal of immunology.* 2012;42(4):880-9.

288. Mizushima N. Autophagy: process and function. *Genes & development.* 2007;21(22):2861-73.

289. Nakatogawa H, Suzuki K, Kamada Y, and Ohsumi Y. Dynamics and diversity in autophagy mechanisms: lessons from yeast. *Nature reviews Molecular cell biology.* 2009;10(7):458-67.

290. Nakatogawa H, Ichimura Y, and Ohsumi Y. Atg8, a ubiquitin-like protein required for autophagosome formation, mediates membrane tethering and hemifusion. *Cell.* 2007;130(1):165-78.

291. Kimura S, Fujita N, Noda T, and Yoshimori T. Monitoring autophagy in mammalian cultured cells through the dynamics of LC3. *Methods in enzymology.* 2009;452(1-12.

292. Noda T, and Ohsumi Y. Tor, a phosphatidylinositol kinase homologue, controls autophagy in yeast. *The Journal of biological chemistry.* 1998;273(7):3963-6.

293. Oberstein A, Jeffrey PD, and Shi Y. Crystal structure of the Bcl-XL-Beclin 1 peptide complex: Beclin 1 is a novel BH3-only protein. *The Journal of biological chemistry.* 2007;282(17):13123-32.

294. Zalckvar E, Berissi H, Mizrachy L, Idelchuk Y, Koren I, Eisenstein M, Sabanay H, Pinkas-Kramarski R, and Kimchi A. DAP-kinase-mediated phosphorylation on the BH3 domain of beclin 1 promotes dissociation of beclin 1 from Bcl-XL and induction of autophagy. *EMBO reports.* 2009;10(3):285-92.

295. Fournier BM, and Parkos CA. The role of neutrophils during intestinal inflammation. *Mucosal immunology.* 2012;5(4):354-66.

296. Meddings JB, Sutherland LR, and May GR. Intestinal permeability in patients with Crohn's disease. *Gut.* 1994;35(11):1675-6.

297. Guijarro LG, Mate J, Gisbert JP, Perez-Calle JL, Marin-Jimenez I, Arriaza E, Olleros T, Delgado M, Castillejo MS, Prieto-Merino D, et al. N-acetyl-L-cysteine combined with mesalamine in the treatment of ulcerative colitis: randomized, placebo-controlled pilot study. *World journal of gastroenterology.* 2008;14(18):2851-7.

298. Jarnerot G, Strom M, Danielsson A, Kilander A, Loof L, Hultcrantz R, Lofberg R, Floren C, Nilsson A, and Brostrom O. Allopurinol in addition to 5-aminosalicylic acid based drugs for the maintenance treatment of ulcerative colitis. *Alimentary pharmacology & therapeutics.* 2000;14(9):1159-62.

299. Kolacek M, Muchova J, Dvorakova M, Paduchova Z, Zitnanova I, Cierna I, Orszaghova Z, Szekyova D, Jajcaiova-Zednickova N, Kovacs L, et al. Effect of natural polyphenols (Pycnogenol) on oxidative stress markers in children suffering from Crohn's disease--a pilot study. *Free radical research.* 2013;47(8):624-34.

300. Balana ME, Niedergang F, Subtil A, Alcover A, Chavrier P, and Dautry-Varsat A. ARF6 GTPase controls bacterial invasion by actin remodelling. *Journal of cell science.* 2005;118(Pt 10):2201-10.

301. Radhakrishna H, Klausner RD, and Donaldson JG. Aluminum fluoride stimulates surface protrusions in cells overexpressing the ARF6 GTPase. *The Journal of cell biology.* 1996;134(4):935-47.

302. Fernando EH, Dicay M, Stahl M, Gordon MH, Vegso A, Baggio C, Alston L, Lopes F, Baker K, Hirota SA, et al. A simple, cost-effective method for generating murine colonic 3D enteroids and 2D monolayers for studies of primary epithelial cell function. *American journal of physiology Gastrointestinal and liver physiology.* 2017:ajpgi.00152.2017.

303. Liang HL, Sedlic F, Bosnjak Z, and Nilakantan V. SOD1 and MitoTEMPO partially prevent mitochondrial permeability transition pore opening, necrosis, and mitochondrial apoptosis after ATP depletion recovery. *Free radical biology & medicine.* 2010;49(10):1550-60.

304. Krols M, Bultynck G, and Janssens S. ER-Mitochondria contact sites: A new regulator of cellular calcium flux comes into play. *The Journal of cell biology.* 2016;214(4):367-70.

305. Rizzuto R, De Stefani D, Raffaello A, and Mammucari C. Mitochondria as sensors and regulators of calcium signalling. *Nature reviews Molecular cell biology.* 2012;13(9):566-78.

306. Kugathasan S, Collins N, Maresso K, Hoffmann RG, Stephens M, Werlin SL, Rudolph C, and Broeckel U. CARD15 gene mutations and risk for early surgery in pediatric-onset Crohn's disease. *Clinical gastroenterology and hepatology : the official clinical practice journal of the American Gastroenterological Association.* 2004;2(11):1003-9.

Appendix

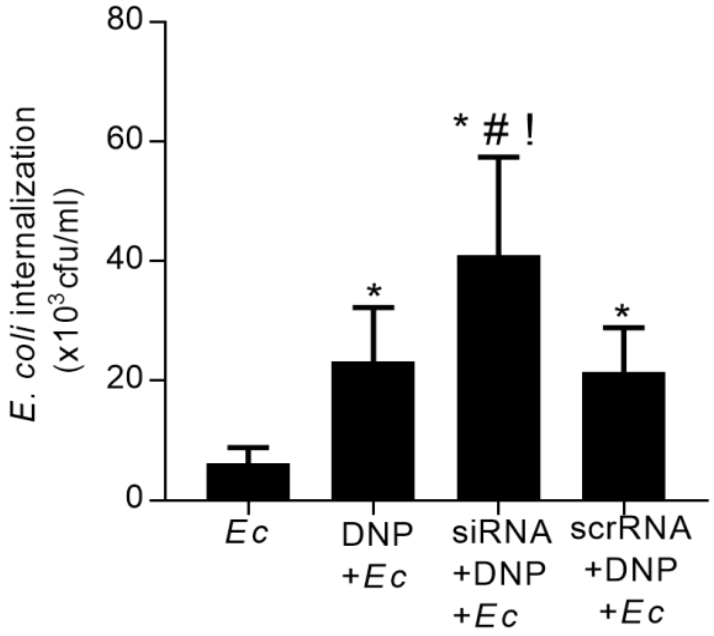

Figure 35: DNP-induced internalization of *E. coli* was increased in T84s in which NOD2 was KD with (f) siRNA (data are mean ± SEM; n=6 from 2 experiments; * p <0.05 from *Ec*, # p <0.05 from the DNP+*Ec*, ! p <0.05 from DNP + *Ec* + Scr (scrambled) RNA (control)).

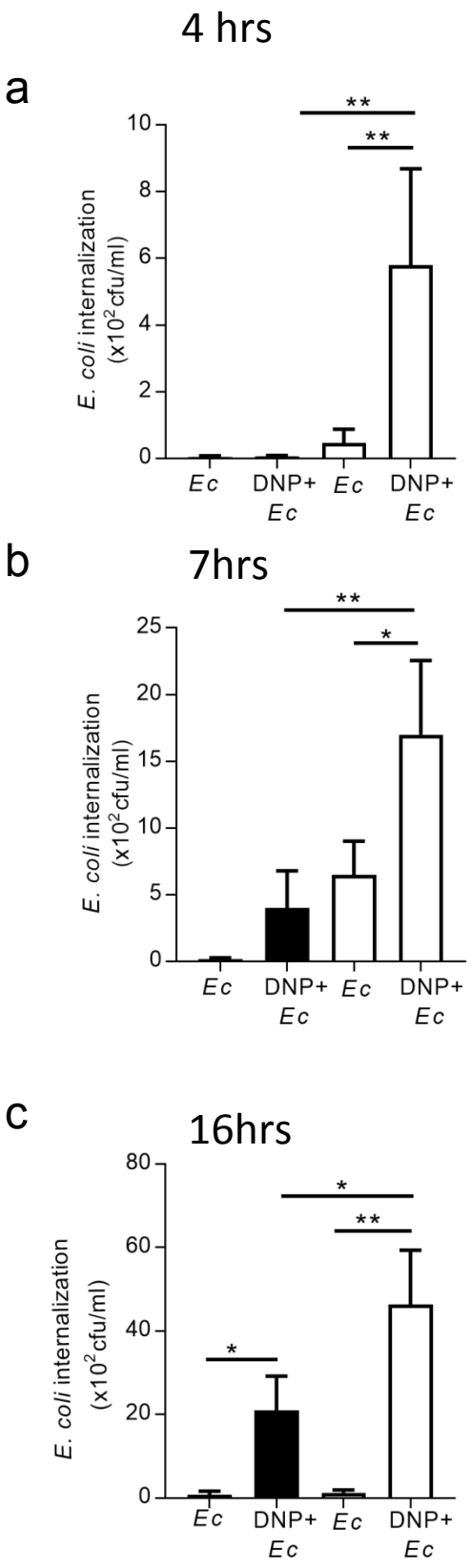
4 hrs
a
**
**
10
8
6
4
2
0
E. coli internalization
(x10² cfu/ml)
Ec
DNP+ Ec
Ec
DNP+ Ec
b
7hrs
**
*
25
20
15
10
5
0
E. coli internalization
(x10² cfu/ml)
Ec
DNP+ Ec
Ec
DNP+ Ec
c
16hrs
*
**
*
80
60
40
20
0
E. coli internalization
(x10² cfu/ml)
Ec
DNP+ Ec
Ec
DNP+ Ec

Figure 36: The increased number of intracellular bacteria in metabolically-stressed epithelia is due to reduced killing. Wild-type (WT) and NOD2 KD T84 epithelial monolayers were treated with dinitrophenol (DNP: 0.1 mM) and *E. coli* HB101 (*Ec*, $1x10^6$ cfu/ml) for (a) 4 hrs, (b) 7 hrs or (c) 16 hrs. Following the defined period of exposure to *E. coli*, extracellular bacteria were killed by gentamycin and the in the case of the 4 hrs and 7 hrs treatments the cells were returned to 37^{o}C for 12 hrs or 9 hrs, respectively, to align with a total 16 hrs experiment as in (c). At this point, cells were rinse, lysed and intracellular viable bacteria counted after growth on LB agar plates (n=3 epithelial preparations from 1 experiment, * p <0.05, ** p <0.001, *** p <0.0001).